

12-2009

Rainsford Island Shoreline Evolution Study (RISES)

Christopher V. Maio

University of Massachusetts Boston

Follow this and additional works at: http://scholarworks.umb.edu/masters_theses



Part of the [Environmental Sciences Commons](#), and the [Oceanography Commons](#)

Recommended Citation

Maio, Christopher V., "Rainsford Island Shoreline Evolution Study (RISES)" (2009). *Graduate Masters Theses*. Paper 86.

This Open Access Thesis is brought to you for free and open access by the Doctoral Dissertations and Masters Theses at ScholarWorks at UMass Boston. It has been accepted for inclusion in Graduate Masters Theses by an authorized administrator of ScholarWorks at UMass Boston. For more information, please contact library.uasc@umb.edu.

RAINSFORD ISLAND SHORELINE EVOLUTION STUDY (RISES)

A Thesis Presented

by

CHRISTOPHER V. MAIO

Submitted to the Office of Graduate Studies,
University of Massachusetts Boston,
in partial fulfillment of the requirements for the degree of

MASTER OF SCIENCE

December 2009

Environmental, Earth, and Ocean Science Program

© 2009 by Christopher V. Maio
All rights reserved

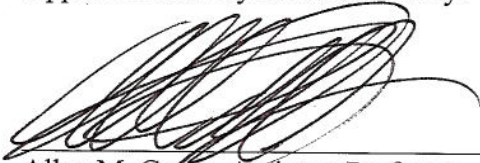
RAINSFORD ISLAND SHORELINE EVOLUTION STUDY (RISES)

A Thesis Presented

by

CHRISTOPHER V. MAIO

Approved as to style and content by:



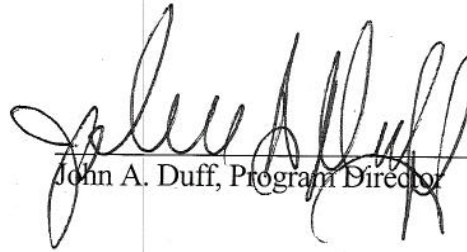
Allen M. Gentz, Assistant Professor
Chairperson of Committee



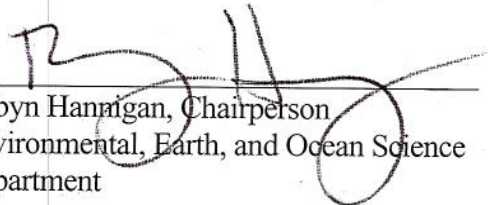
Curtis R. Olsen, Professor
Member



David E. Tenenbaum, Assistant Professor
Member



John A. Duff, Program Director



Robyn Hanigan, Chairperson
Environmental, Earth, and Ocean Science
Department

ABSTRACT

RAINSFORD ISLAND SHORELINE EVOLUTION STUDY (RISES)

December 2009

Christopher V. Maio, B.S. University of Massachusetts Boston
M.S., University of Massachusetts Boston

Directed by Assistant Professor Allen M. Gontz

RISES conducted a shoreline change study in order to accurately map, quantify, and predict trends in shoreline evolution on Rainsford Island occurring from 1890-2008. It employed geographic information systems (GIS) and analytical statistical techniques to identify coastal hazard zones vulnerable to coastal erosion, rising sea-levels, and storm surges. The 11-acre Rainsford Island, located in Boston Harbor, Massachusetts, consists of two eroded drumlins connected by a low-lying spit. Settled by Europeans in 1636, the Island was later used as the Harbor's main quarantine station. Previous archeological surveys have identified numerous historically sensitive sites dating to before the Revolutionary War period, including a large cemetery.

Multiple data sources were integrated within a GIS, including historical maps, aerial photographs, and Light Detection and Ranging (LIDAR) data. The United States Geological Survey's (USGS) Digital Shoreline Analysis System (DSAS) was utilized to determine rate-of-change statistics and distances. A comparison analysis was carried out between datasets to determine the change in area above the high water line (HWL).

RISES used two proxies to delineate shoreline positions and one to delineate vegetated areas. The main shoreline indicator was the visually discernable high water line (HWL). A tidal datum/LIDAR derived mean high water (MHW) shoreline was also developed. Lastly, the visually discernable vegetation line was used to delineate vegetated areas.

The results show that 14% of the Island has been eroded during the study period with the largest losses coming between 1970 and 1992. There has been 60 m of accretion, at a rate of 0.83 m/y, within the West Cove. The spit connecting the two drumlins has migrated southeast by 17 m at a rate of 0.33 m/y resulting in erosion along its northern side and accretion along its southern side. The southeast beach on the northern drumlin eroded 43 m at a rate of 0.59 m/y. All other areas of the Island remained stable. Predictive modeling indicates that 26% of the Island would become inundated with 1-m of sea-level-rise including the area containing the cemetery. The northern beaches and the cemetery area on the southern drumlin have been identified as coastal hazard zones.

DEDICATION

I would like to dedicate this work to all the people that have provided me with the opportunity to succeed at my goals and supported me along the way.

To my beautiful wife Sarah,

and my loving parents,

Jane and Vincent Maio.

&

To my Committee:

Allen Gontz, Curtis Olsen, and David Tenenbaum

Thank You

TABLE OF CONTENTS

DEDICATION	vi
LIST OF FIGURES.....	x
LIST OF TABLES	xv
LIST OF ABBREVIATIONS	xvi
CHAPTER	Page
1. INTRODUCTION.....	1
1.1. Background	1
1.2. Study Intention	6
1.3. Study Site.....	9
1.4. Geologic Framework	10
1.5. Prehistoric Landuse.....	17
1.6. Historic Landuse	20
2. METHODS.....	28
2.1. Introduction	28
2.2. Data Sources.....	35
2.2.1. Historical Aerial Photographs.....	35
2.2.2. Digital Orthophotographs and USGS Historical Map	36
2.2.3. LIDAR Data.....	37
2.3. Data Integration and Management	38
2.3.1. Data Management: Unrectified Aerial Photographs	39
2.3.2. Data Management: Digital Orthophotographs..	40
2.3.3. Data Management: LIDAR Data.....	42
2.4. Geographic Information System Procedures	42
2.4.1. Shoreline Delineation and Digitization	42
2.4.2. Creating the 2002 Mean High Water Shoreline	49
2.4.3. Creating the Mean High Water Offset-Corrected Shoreline	52
2.5. Data Analysis	52
2.5.1. Comparison Analysis	52
2.5.2. Digital Shoreline Analysis System	55

CHAPTER	Page
2.5.3. Digital Shoreline Analysis System Statistics	59
2.5.4. Flood Hazard Predictive Mapping.....	61
3. RESULTS.....	63
3.1. DSAS Analysis.....	63
3.1.1. North Mixed Sediment Beach (NMSB).....	65
3.1.2. Southeast Sand Beach (SESB).....	70
3.1.3. Northwest Boulder Beach (NWBB).....	73
3.1.4. Seawall (SW).....	76
3.1.5. Southeast Boulder Beach (SEBB).....	79
3.1.6. West Cove (WC).....	82
3.1.7. Southwest Sand Beach (SWSB).....	84
3.2. Comparison Analysis.....	87
3.2.1. Shoreline Data Compared to 2008 Basefile.....	87
3.2.2. Data Comparison to the Mean High Water Offset-Corrected Shoreline	90
3.2.3. Vegetation Comparison to 2008 Basefile.....	92
3.2.4. Shoreline Comparison Analysis Between Datasets.....	92
3.2.5. Vegetation Comparison Analysis Between Datasets.....	96
3.3. Mean High Water Visual Analysis	96
3.3.1. Mean High Water Shoreline and the 1890 Historical Map.....	98
3.3.2. Mean High Water Shoreline and the 1904 Historical Map.....	100
3.3.3. Mean High Water Shoreline and the 1944 Aerial Photograph.....	102
3.4. Flood Hazard Predictive Maps	104
3.4.1. 1-Meter Flood Hazard Map	104
3.4.2. 2-Meter Flood Hazard Map	106
3.4.3. 3-Meter Flood Hazard Map	107
4. DISCUSSION.....	110
4.1. Data Integration.....	110
4.2. Digital Shoreline Analysis System (DSAS)	113
4.4. Areas of Significant Change.....	118
4.4.1. Southeast Boulder Beach (SEBB)	118
4.4.2. Migration of low-lying spit	120
4.4.3. West Cove (WC).....	121

CHAPTER	Page
4.5. Coastal Hazard Zones on Rainsford Island.....	123
4.5.1. Designation of Coastal Hazard Zones	123
4.5.2. North Beaches.....	123
4.5.3. Cemetery	125
4.5.4. Southeast Boulder Beach (SEBB)	125
4.6. Future Work	126
5. CONCLUSIONS.....	130
5.1. Itemized Conclusions.....	130
 APPENDIX	
A. IMAGE DATA: SOURCES AND INFORMATION	134
B. BOSTON HARBOR TIDAL DATUM.....	137
C. NATIONAL GEODETIC SURVEY ELEVATION DATA	138
D. DIGITAL SHORELINE ANALYSIS SYSTEM (DSAS) TRANSECT RESULTS	139
REFERENCE LIST.....	140

LIST OF FIGURES

Figure	Page
1.1. Rainsford Island is located within Quincy Bay, Boston Harbor, Massachusetts	11
1.2. LIDAR derived 1-meter contour map with elevation profile	12
1.3. Drumlin profile showing section and plan views	14
1.4. Holocene sea-level curve showing three distinct periods of the Harbor’s geomorphic evolution	15
1.5. Simplistic reconstruction of Holocene sea-level rise in Boston Harbor.....	18
1.6. Rainsford Island historical timeline spanning 373 years.....	21
1.7. Circa 1840’s painting of Rainsford Island by Robert Salmon.....	23
1.8. Historic 1904 map of Rainsford Island with digitized version	25
2.1. MassGIS LIDAR derived DEM shown with tidal datum MHW elevation	33
2.2. 1992 MassGIS composite orthophotograph shown with rectangular “Area of Interest” (AOI).....	41
2.3. The high water line (HWL) identified by red arrows, is shown digitized.....	44
2.4. 1944 shoreline files	45
2.5. The vegetation line as a proxy to delineate and digitize vegetated areas of Rainsford Island	47
2.6. 1944 vegetation files	48
2.7. 1952 aerial photograph with MHW shoreline shown in red	51
2.8. Map of Rainsford Island showing shoreline change occurring between 1944 and 2008.....	54

Figure	Page
2.9. Appended shoreline data shown with baseline.....	57
2.10. Appended vegetation data shown with baseline.....	58
2.11. 1-Meter Flood Hazard Map.....	62
3.1. Linear regression rates for shoreline analysis	64
3.2. Beach location map showing eight areas of Rainsford Island	66
3.3. Shoreline transect (T_s) location map	67
3.4. Linear regression analysis of T_s 74 along the NMSB for the 1890 dataset.....	68
3.5. Linear regression analysis of T_s 74 along the NMSB for the 1944 dataset.....	68
3.6. Linear regression analysis of T_s 232 along the NMSB for the 1890 dataset.....	69
3.7. Linear regression analysis of T_s 232 along the NMSB for the 1944 dataset.....	69
3.8. Vegetation transect (T_v) location map.....	71
3.9. Linear regression analysis of T_v 176 along the NMSB for the 1944 dataset.....	72
3.10. Linear regression analysis of T_s 202 along the SESB for the 1890 dataset.....	72
3.11. Linear regression analysis of T_s 202 along the SESB for the 1944 dataset.....	73
3.12. Linear regression analysis of T_s 83 along the NWBB for the 1890 dataset.....	75
3.13. Linear regression analysis of T_s 83 along the NWBB for the 1944 dataset.....	75

Figure	Page
3.14. Linear regression analysis of T_v 27 along the NWBB for the 1944 dataset.....	76
3.15. Linear regression analysis of T_s 97 along the SW for the 1944 dataset.....	78
3.16. Linear regression analysis of T_s 122 along the SW for the 1944 dataset.....	78
3.17. Linear regression analysis of T_v 43 along the SW for the 1944 dataset.....	79
3.18. Linear regression analysis of T_s 178 along the SEBB for the 1890 dataset.....	80
3.19. Linear regression analysis of T_s 178 along the SEBB for the 1944 dataset.....	81
3.20. Linear regression analysis of T_v 83 along the SEBB for the 1944 dataset.....	81
3.21. Linear regression analysis of T_s 194 along the WC for the 1890 dataset.....	83
3.22. Linear regression analysis of T_s 194 along the WC for the 1944 dataset.....	83
3.23. Linear regression analysis of T_v 99 along the WC for the 1944 dataset.....	84
3.24. Linear regression analysis of T_s 47 along the SWSB for the 1890 dataset.....	85
3.25. Linear regression analysis of T_s 47 along the SWSB for the 1944 dataset.....	85
3.26. Linear regression analysis of T_v 141 along the SWSB for the 1944 dataset.....	86
3.27. Map of Rainsford Island showing shoreline change occurring between 1944 and 2008.....	88

Figure	Page
3.28. Bar graph showing results of 2008 basefile comparison.	89
3.29. Bar graph showing results of MHW offset shoreline basefile comparison.....	91
3.30. Bar graph showing results of vegetation comparison using 2008 basefile	93
3.31. Bar graph showing results of shoreline comparisons between datasets	94
3.32. Map of Rainsford Island showing shoreline change occurring between 1970 and 1992.....	95
3.33. Bar graph showing results of vegetation comparisons between datasets	97
3.34. Historical USGS quadrangle map of Rainsford Island with MHW shoreline	99
3.35. Historical 1904 georeferenced map of Rainsford Island with MHW shoreline	101
3.36. 1944 aerial photograph with MHW shoreline.....	103
3.37. 1-Meter Flood Hazard Map.....	106
3.38. 2-Meter Flood Hazard Map.....	107
3.39. 3-Meter Flood Hazard Map.....	109
4.1. Dynamic nature of historical shoreline positions	117
4.2. Areas of significant change	119
4.3. Dynamic shoreline trends along the SEBB.....	120
4.4. Area below MHW elevation within the WC	122
4.5. Coastal Hazard Zone Map	124

Figure	Page
4.6. Ground penetrating radar (GPR) survey of Rainsford Island Cemetery	127
4.7. Shoreline change analysis employing two LIDAR datasets	128

LIST OF TABLES

Table	Page
3.1. Results from the shoreline comparison analysis using the 2008 basefile	89
3.2. Results from the shoreline comparison analysis using the Mean High Water Offset-Corrected Shoreline basefile.....	91
3.3. The results from the vegetation comparison analysis using the 2008 basefile	93
3.4. Results from the shoreline comparisons between datasets	94
3.5. Results from the vegetation comparisons between datasets	97
4.1. Comparison rate-of-change statistics	115

LIST OF ABBREVIATIONS

ABBREVIATION	NAME
AOI	Area of Interest
BLC	Boston Landmarks Commission
BR	Bedrock
cm	Centimeter
CO-OPS	Center for Operational Oceanographic Products and Services
C-CAP	Coastal Change Analysis Program
CCOM.....	Center of Coastal and Ocean Mapping
DATIS	Digital Airborne Topographic Imaging System
DEM	Digital Elevation Model
DSAS	Digital Shoreline Analysis System
EPR	End Point Rate
FEMA.....	Federal Emergency Management Agency
GCP	Ground Control Point
GIS	Geographic Information System
GIT	Geographic Information Technology
GPR	Ground Penetrating Radar
HWL	High Water Line
IPCC	Intergovernmental Panel on Climate Change
km	Kilometers
LIDAR.....	Light Detection and Ranging
LR	Linear Regression
LRR	Linear Regression Rate
LMS	Least Median of Squares
MassGIS.....	Massachusetts Office of Geographic and Environmental Information
m	Meter

ABBREVIATION	NAME
mm	Millimeters
MHW	Mean High Water
MLLW	Mean Lower Low Water
MrSID	Multiresolution Seamless Database
NAVD	North American Vertical Datum of 1988
NOAA	National Oceanic and Atmospheric Administration
NMSB	North Mixed Sediment Beach
NOS	National Ocean Services
NSM	Net Shoreline Movement
NWBB	Northwest Boulder Beach
ppb	Parts Per Billion
SCE	Shoreline Change Envelope
SESB	Southeast Sand Beach
SLR	Sea-Level Rise
SW	Seawall
SWBB	Southwest Boulder Beach
SWSB	Southwest Sand Beach
RISES	Rainsford Island Shoreline Evolution Study
T _s	Shoreline Transect
T _v	Vegline Transect
TIFF	Tagged Image File Format
USGS	United States Geological Society
WC	West Cove
y	Years
ybp	Years Before Present

CHAPTER 1

INTRODUCTION

1.1 Background

One of the planet's greatest natural treasures is its vast network of coastal systems. These areas are the interface between the terrestrial and marine environments and furnish some of the most ecologically productive areas in the world, playing a "paramount role" in maintaining the sustainability of the global environment (Zeidler, 1998). There are over 1.6 million kilometers of shorelines globally containing approximately 41% of the world's population within the coastal limit of 100 km (Martinez et al., 2007). Coastal areas also provide enormous economic benefits through the abundant goods and services they provide to human civilization (Martinez et al., 2007). Costanza et al. (1997) calculated that 77% of global ecosystem goods and services can be attributed to coastal ecosystems. Coastlines also contain some of the most valuable real estate in the world with 21 of the world's 33 megacities found along the shores (Costanza et al., 1997).

Valuable natural and socioeconomic coastal resources include commercial fisheries (e.g., Teh et al., 2005), minerals and oil resources, and protected ports for marine commerce (e.g., Martinez et al., 2007). The coastal zone also provides enormous benefits through natural

services, which are difficult to quantify but are “invaluable to human society and to life on Earth” (Martinez et al., 2007). Natural services provided by coastal systems include the filtration of polluted water supplies by coastal wetlands, infrastructure protection through the buffering capacity of barrier beaches and wetlands during extreme storm events, and the storing and cycling of nutrients (Ledoux and Turner, 2002; Woodward and Wui, 2002). Coastal systems also provide the fertile nursery grounds for much of the world’s commercial fish stocks as well as abundant areas for recreation and tourism (Van Der Meulen et al., 2004).

These dynamic coastal systems and the enormous ecological and socioeconomic benefits they provide are under threat from a predicted rise in sea-level and increased occurrence and intensity of storm surges associated with current trends in global climate change (IPCC, 2007). The planet has been experiencing a natural trend of warming and sea-level rise (SLR) during the Holocene Transgression beginning approximately 12,000 years ago (Oldale and Coleman, 1993). However, the United Nations Intergovernmental Panel on Climate Change (IPCC) (2007), states that recent increases in warming during the past 50 years are “very likely” due to the dramatic increases in greenhouse gas emissions. The panel reports a 70% increase in anthropogenic greenhouse gasses being released into the atmosphere from 1970-2005. In 2005, carbon dioxide concentrations in the atmosphere have increased from the pre-industrial values of 270 parts per billion (ppb), to 379 ppb, which far exceed concentrations occurring during the past 650,000 years (IPCC, 2007).

Future impacts of climate change will undoubtedly have widespread impacts on the global environment and sea-level fluctuations, but how will these predictions play out in the Boston Metropolitan Area? There are many factors that contribute to local sea-level

fluctuations in Boston Harbor. Land surface changes, including isostatic rebound and subsidence resulting from the advancements and retreat of glaciers, and changes to regional oceanographic conditions directly impact local sea-levels (Clark et al., 1998). In addition to these local and regional contributions, global sea-level fluctuations must also be accounted for when determining local or relative sea-levels. There are numerous factors controlling global sea-level, also referred to as eustatic sea-level. These include the thermal expansion or contraction of the world's oceans, which is predominately dependent on atmospheric temperatures (e.g., Church et al., 1991), changing volumes of meltwater flow into ocean basins (e.g., Arendt et al., 2002), tectonic dynamics which alter ocean basin size, and global ocean circulation dynamics (e.g., Yin, et al., 2009). Relative sea-level, therefore, refers to the combined contributions of these regional and global factors. Based on local tide gauges Donnelly (2006), places the rate of SLR in Boston Harbor between 1922 and 2002 at 2.8 mm per year. This figure is much lower than the recent IPCC (2007) predictions indicating recent increases in the rate of SLR.

As a result of recent anthropogenic warming, the IPCC (2007) predicted an increased rate of SLR due to the thermal expansion of the oceans and the melting of ice sheets in polar regions. The IPCC (2007) predictions are based on different SLR scenarios varying from 15 cm to 150 cm per century depending on the amount of emissions reductions put in place by the global community (Penland and Ramsey, 1990; Shinkle and Dokka, 2004). Under the higher emissions scenarios, the rate of SLR would be greater than at any time during the past 4000 years (IPCC, 2007) and would undoubtedly have enormous impacts on the Massachusetts coastline (Kirschen et al., 2008). The IPCC (2007) report states that there

would be “major changes to coastlines and inundation of low-lying areas...” The shoreline response to current SLR is already being seen globally. Galgano et al. (2004) reports that presently over 70% of the shorelines around the world are retreating landward and, on the eastern U.S. coast, nearly 86% of barrier beaches have experienced erosion during the past century.

These statistics are very important to those living in coastal communities grappling with how to deal with the rapid increase in erosion occurring on shorelines. For example, in Chatham, Massachusetts, a small coastal town on Cape Cod, a large storm during the summer of 2007 breached the barrier beach that had long buffered the embayment from erosion. As a result of the new breach, the mainland has been left highly vulnerable to future storms and the town has been struggling with how to manage their coastal zone. The increasing occurrence of extreme erosional events, such as in Chatham, presents enormous challenges to coastal managers and policy makers.

A recent report written by Yin et al. (2009) projects that, due to human-induced climate change, the heavily populated northeastern coast of the United States will experience a considerably faster and larger rate of relative SLR compared to the global mean. These model predictions, based on the 2007 IPCC Fourth Assessment Report, are attributed to a possible weakening of the North Atlantic thermohaline circulation. If the North Atlantic thermohaline circulation were to slow down or stop, as a result of increased freshwater input, the present steep dynamic sea surface height, which slopes upward from the coastline having its highest elevation within the approximate center of the gulf stream current, would relax and level out causing an increase in relative sea-levels along the northeast coast of the United States (Yin, et

al., 2009). This leaves numerous densely populated and developed areas, such as New York and Boston, highly vulnerable to coastal flooding and extreme erosional events.

Kirshen et al. (2008) showed that the predicted increases in SLR under the Fourth Assessment highest emissions scenario would result in increased reoccurrence and height of future 100-year flood events in the Boston Harbor area. The 100-year flood event refers to the flood height, which on average will be met or exceeded every hundred years or that has a 1% chance of occurring each year (Pugh, 1987). “By 2050 the elevation of the 2005 100-year event may be equaled or exceeded every 30 years at all sites” (Kirshen et al., 2008). Kirshen et al., (2008), also reports that under the higher emission scenarios, Boston may experience the current 100-year flood at a “considerably higher frequency of every 8 years or less.”

An increased rate of relative SLR along the Massachusetts coast will, undoubtedly, have enormous environmental and socioeconomic impacts. These include the loss of recreational beaches due to extreme erosional events, inundation of low-lying developed areas, the submergence and loss of sensitive historical and cultural sites, and the increased height and penetration of storm surges. In the past, coastal flooding in Massachusetts has resulted in enormous costs (Cooper et al., 2005). Kirshen et al. (2004) put the cost of coastal damages from the February “Blizzard of 1978” at \$550 million, with emergency costs of \$95 million, mainly within the Boston Metropolitan area. In another report, Cooper et al. (2005) states that the “Halloween Nor’easter of 1991”, more recently known as the “Perfect Storm,” inflicted over \$1.5 billion in damages.

In order to provide the information needed to coastal managers and policy makers to enhance their ability to develop sound coastal zone management strategies, there is a strong

need for shoreline change analysis studies along the Massachusetts coastline. Shoreline change analysis uses advanced geographic information systems (GIS) and analytical statistical techniques to better understand and quantify the coastal geomorphic trends that have occurred in the past and that may occur in the future. These investigations are a key component to developing effective coastal zone management policies needed to address future shoreline changes associated with climate change (e.g., Dobson et al., 2003; Scavia et al., 2002). The Rainsford Island Shoreline Evolution Study (RISES) has addressed this need in the Boston Harbor area, and will enhance the ability of local coastal managers and policy makers to confront the future challenges associated with climate change.

1.2 Study Intention

The landform that now makes up Rainsford Island has been shaped and molded by dramatic environmental change for thousands of years and provides coastal scientists with an ideal natural laboratory in which to analyze historical shoreline change. RISES sought to enhance the integration and development of new methods in order to accurately map, quantify, and predict trends in shoreline evolution on Rainsford Island occurring from 1890-2008. It also employed advanced GIS and analytical statistical techniques to identify coastal hazard zones that are particularly vulnerable to coastal flooding.

This investigation was carried out through the use of multiple data sources and techniques including historical maps and air photos, high resolution digital orthophoto imagery, light detection and ranging (LIDAR) data, and the utilization of GIS and statistical analysis software. These technological advancements have dramatically improved the ability

of coastal investigators to more accurately quantify shoreline rates-of-change and accretion and erosion trends.

Boak and Turner (2005) point out that the shoreline change analysis is of “fundamental importance” to numerous investigations carried out by coastal scientists, engineers, and managers. Accurately determining the long term trends, rates-of-change, and varying positions of the shoreline is crucial for a variety of coastal investigations (Zeidler, 1997; Zuzek et al., 2003). Coastal managers and engineers depend on accurate information for a number of purposes, including the delineation of flood and hazard zones, developing effective coastal zone management plans, erosion and accretion studies, predictive modeling, and the proper installation of coastal defense and shipping structures (Moore et al., 2006; Liu, 2007; Zeidler, 1997; Zuzek et al., 2003). Due to the importance of robust and accurate shoreline change analysis, these studies are no longer considered merely an academic exercise, but a key objective of many coastal planning and management programs (Moore et al., 2006).

The goal of most recent shoreline change studies is to use the available data sources to identify where a shoreline has been in the past, where it is presently, and where it may be in the future (Boak and Turner, 2005). In order to achieve this goal, an actual “line” representing the “true” shoreline needs to be identified and defined within the data sources (Boak and Turner, 2005). This “line,” or indicator feature, can then be used as a reference point and analysis can then be carried out within a GIS. The process of shoreline change analysis is made difficult by the fact that shorelines are very dynamic and rapidly respond to natural and anthropogenic forcing mechanisms.

As a result of the dynamic nature of the shoreline, the very feature which the investigator is attempting to identify, is in a state of constant geomorphic change. Major factors which influence the coastline include seasonal fluctuations in wind and wave energies, extreme storm events, changes to relative sea-level, and a broad range of coastal development projects (Moore et al., 2006). Combined, these numerous natural and anthropogenic forcing mechanisms contribute to shoreline evolution and lend to the difficulty in these investigations.

Numerous methods and data sources have been employed for the complicated endeavor of historical shoreline change analysis (Moore et al., 2006). Older methods relied primarily on shoreline tracing of historical maps and low resolution aerial photography and traditional field based surveys. New methods incorporate modern advancements in technology, including high resolution digital imagery obtained from a variety of airborne remote sensing platforms, topographic LIDAR surveys, and automated image processing techniques.

Over the past decade, the methods employed in shoreline change analysis have been dramatically improved due to the ability to integrate data sets of differing spatial and temporal resolutions together within a geographic information system (GIS). Powerful mapping software has recently been developed, which has significantly improved these studies. These include ESRI's ArcMap, Leica Geosystem's ERDAS Imagine, and the Digital Shoreline Analysis System (DSAS), an extension for ArcMap developed by the United States Geological Survey (USGS). Combined, these programs offer an array of tools to assist in shoreline change analysis which have all been effectively employed within RISES. In addition, analytical statistical techniques, including end point rate (EPR), net shoreline

movement (NSM), and linear regression rate (LRR), have also been employed. These statistical techniques have been employed in past studies and proven to be a reliable method for analyzing shoreline variability and in eliminating potential uncertainties inherent in these studies (Maiti and Bhattacharya, 2009).

One of the most promising technological developments in shoreline change analysis is the use of LIDAR data (Robertson et al., 2004). The increasing availability of LIDAR data over the past decade is revolutionizing the geospatial analysis of coastal features, and as its availability and temporal range increases, it will undoubtedly provide the foundation for many future shoreline change studies. LIDAR data is obtained from an aircraft mounted instrument and provides the capability of producing high resolution digital elevation models (DEMs), which may effectively be utilized for geospatial and statistical analysis.

LIDAR is based on a relatively simple concept of measuring the time it takes a laser pulse to leave an instrument, reflect off a surface, and return after reflection (Cracknell, 1999). By measuring the roundtrip travel time of the laser pulse, highly dense and accurate elevation measurements can be obtained and used to build high-resolution DEM's (Liu, 2007; Robertson, et al., 2004). RISES integrated high resolution LIDAR derived DEMs, obtained through the Massachusetts Office of Geographic and Environmental Information (MassGIS), which dramatically improved this investigation.

1.3 Study Site

The approximate center of the 11-acre Rainsford Island is located at 42°18'43.10"N, and 70°57'15.3"W, and is located within Quincy Bay, Boston Harbor, Massachusetts, between

the larger Long and Peddocks Islands (Figure 1.1). The Island is made up of two heavily eroded drumlins connected by a low elevation sand and gravel spit. The north drumlin reaches a height of 16.7 m and is armored on its northeastern shore by a seawall erected in 1836 (Claesson and Carella, 2002). The north drumlin on its longest axis is approximately 400 m with a maximum width of 170 m. The smaller south drumlin measures approximately 270 m by 100 m along its longest axis and has been reduced through erosional processes to a flat plain of 6 m with a sandy cove anchored by two bedrock outcrop. (Figure 1.2).

1.4 Geologic Framework

In order to map and quantify the recent geomorphic evolution of Rainsford Island, it is first necessary to look at the framework geology of the Boston Harbor area. An understanding of how this larger area was shaped by geologic processes laid the groundwork for RISES and enhanced the ability to map and predict future coastal trends.

The geologic foundation for Boston Harbor consists of bedrock dating to the Precambrian and Paleozoic age known as Cambridge Argillite (Kaye and Barchoorn, 1964). Cambridge Argillite of the Boston Bay Group dates to Proterozoic Z to Early Cambrian of a maximum age of 520 million years (Goldsmith, 1991). During the numerous glacial advancements during the Pleistocene Period, the preexisting bedrock foundation was abraded and scoured into an irregular surface on which glacial drift was later deposited (Rendigs and Oldale, 1990). The older glacial drift is referred to as “drumlin till,” and is predominately composed of compact cobbles, boulders, and finer sediments scoured from the area during the period of the Wisconsin Glacial (Aubrey, 1994; Knebel et al., 1993; Oldale and Coleman,

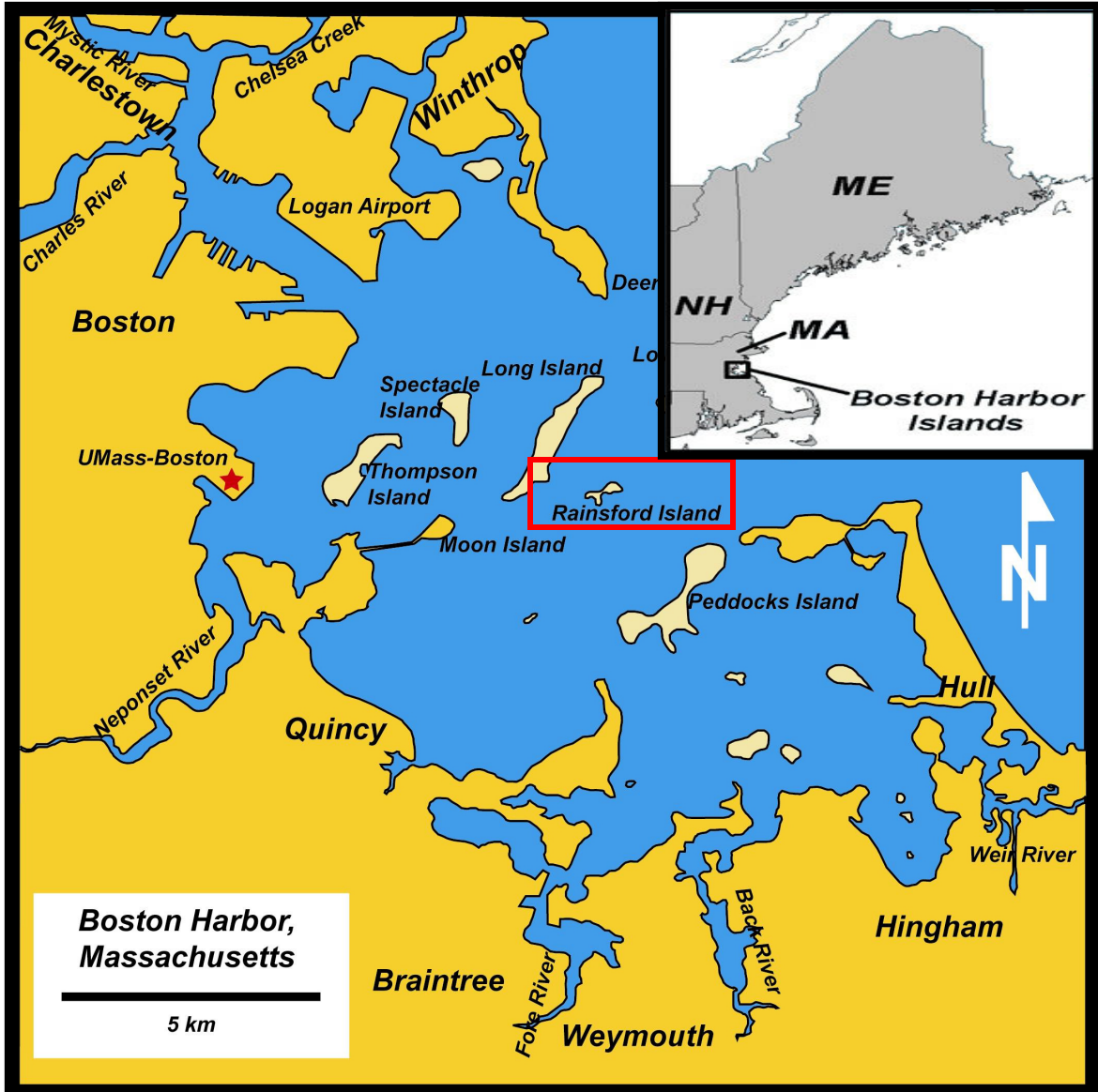


Figure 1.1. Rainsford Island is located within Quincy Bay, Boston Harbor, Massachusetts. The Island is positioned between the larger Long and Peddocks Islands. Rainsford Island is currently managed by the City of Boston and is included in the Boston Harbor National Recreation Area. A red star identifies The University of Massachusetts, Boston.

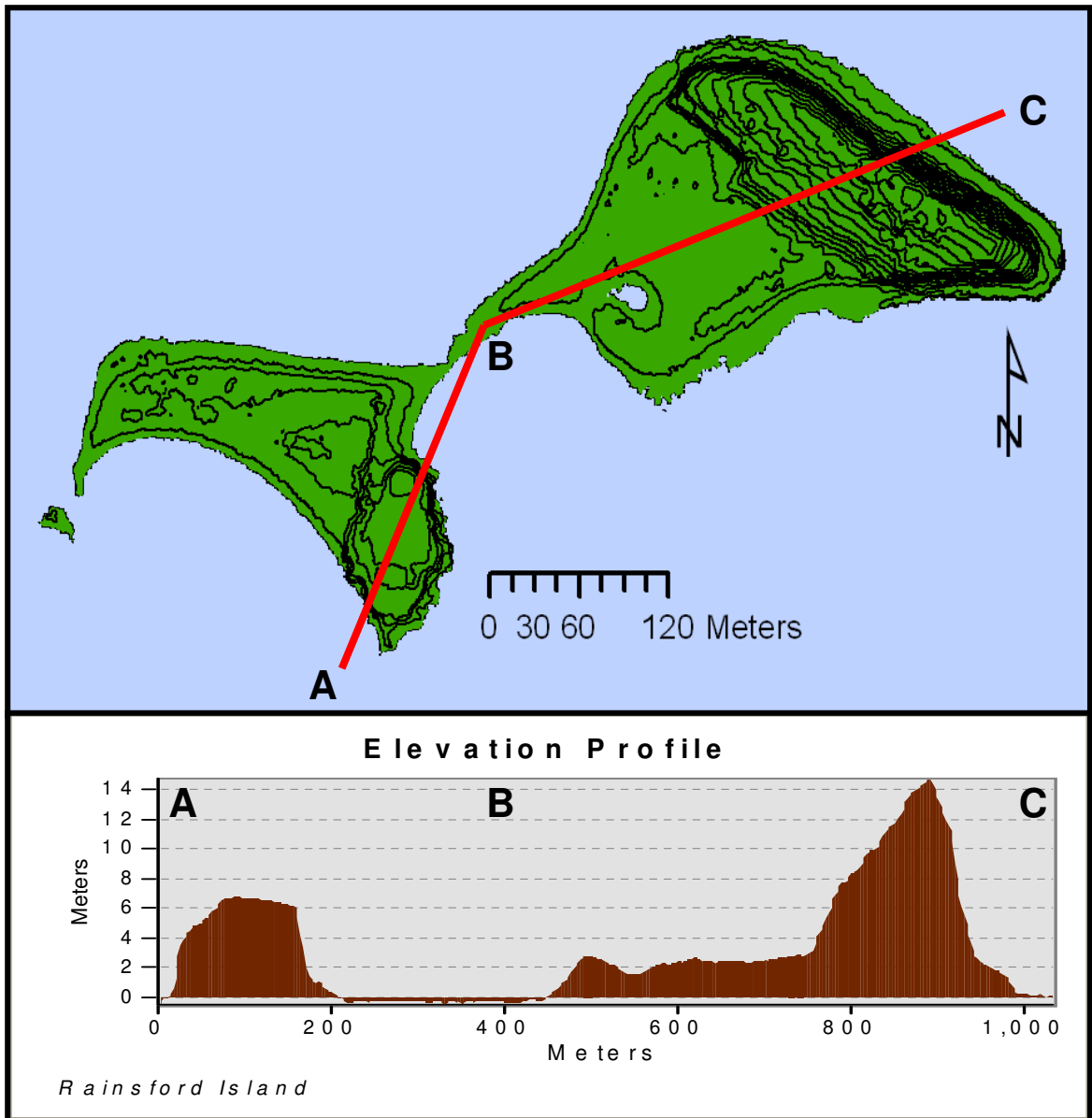


Figure 1.2. LIDAR-derived 1-m contour map with elevation profile. The vertical profile shown below was taken along the cross section shown with the redline proceeding from A to B to C. The heavily eroded north and south drumlins are connected by a low elevation sand and gravel spit. The north drumlin reaches a maximum height of 16.7 m while the south has been eroded to a flat plain with a maximum relief of 6 m. The north portion of the Island displays classic drumlin morphology that has been modified by erosion with high steep bluffs gently sloping downward towards the direction of ice flow.

1992). This drumlin till forms the backbone of the landforms that today make up the Boston Harbor Islands.

Drumlins, geologic features formed during glacial advancements, are oval half-ellipsoid shaped hills which have a distinct teardrop shape (Figure 1.3). Many of the Boston Harbor Islands are the eroded remnants of drumlins. These elongated features have their longest axis parallel to the direction of ice flow and provide geologists with directional signposts for past glacial advancements. The drumlin formations within the Boston Harbor trend northwest/southeast indicating that the glaciers likely advanced from the northwest during the Wisconsin Glacial (Himmelstross et al., 2006).

Many of the geological processes, which formed the present topography of Boston Harbor, occurred primarily during three distinct periods of recent geologic history. These three periods; Ice Contact during the Late Pleistocene, Holocene Regression, and Holocene Transgression, are defined by fluctuations to sea-level along the Massachusetts coastline. These periods were documented in the sea-level curve created by Oldale et al. (1993) (Figure 1.4).

Ice Contact, the earliest of these periods, occurred when Boston was under the glacial ice of the Laurentide Ice Sheet, approximately 118k -18k years before present (ybp). During Ice Contact, the Earth's crust in the area was heavily depressed due to the tremendous weight of the ice. Global sea-levels were 120 m below present levels during the last glacial maximum, as significant amounts of water was locked up in the enormous ice sheets

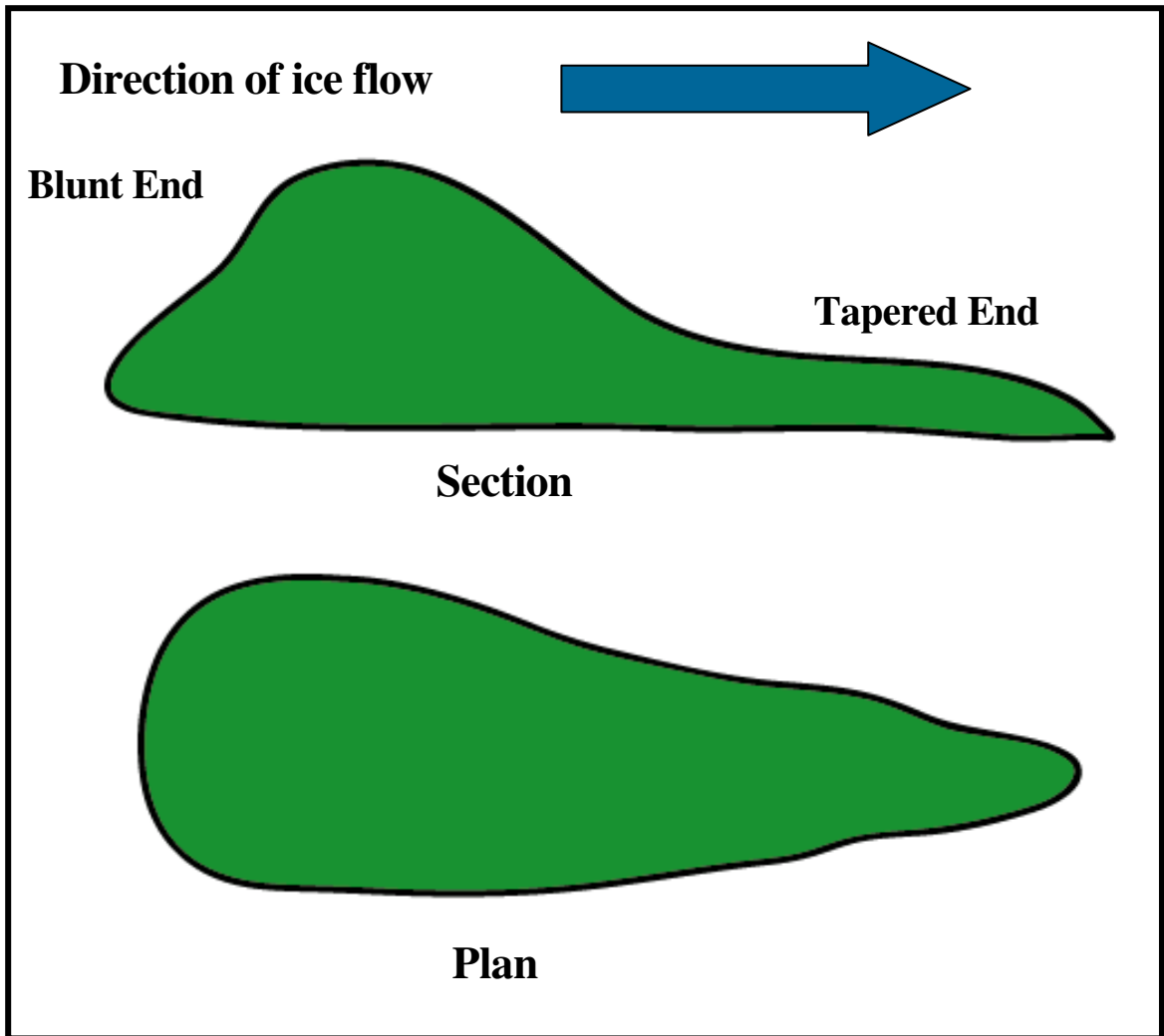


Figure 1.3. Drumlin profile showing section and plan views. Characteristically, drumlins have a high and steep blunt end which tapers off towards the direction of ice flow indicated by the blue arrow. The plan view shows the common “teardrop” shape of these geologic features. Rainsford Island consists of two drumlins connected by a low elevation sand and gravel spit.

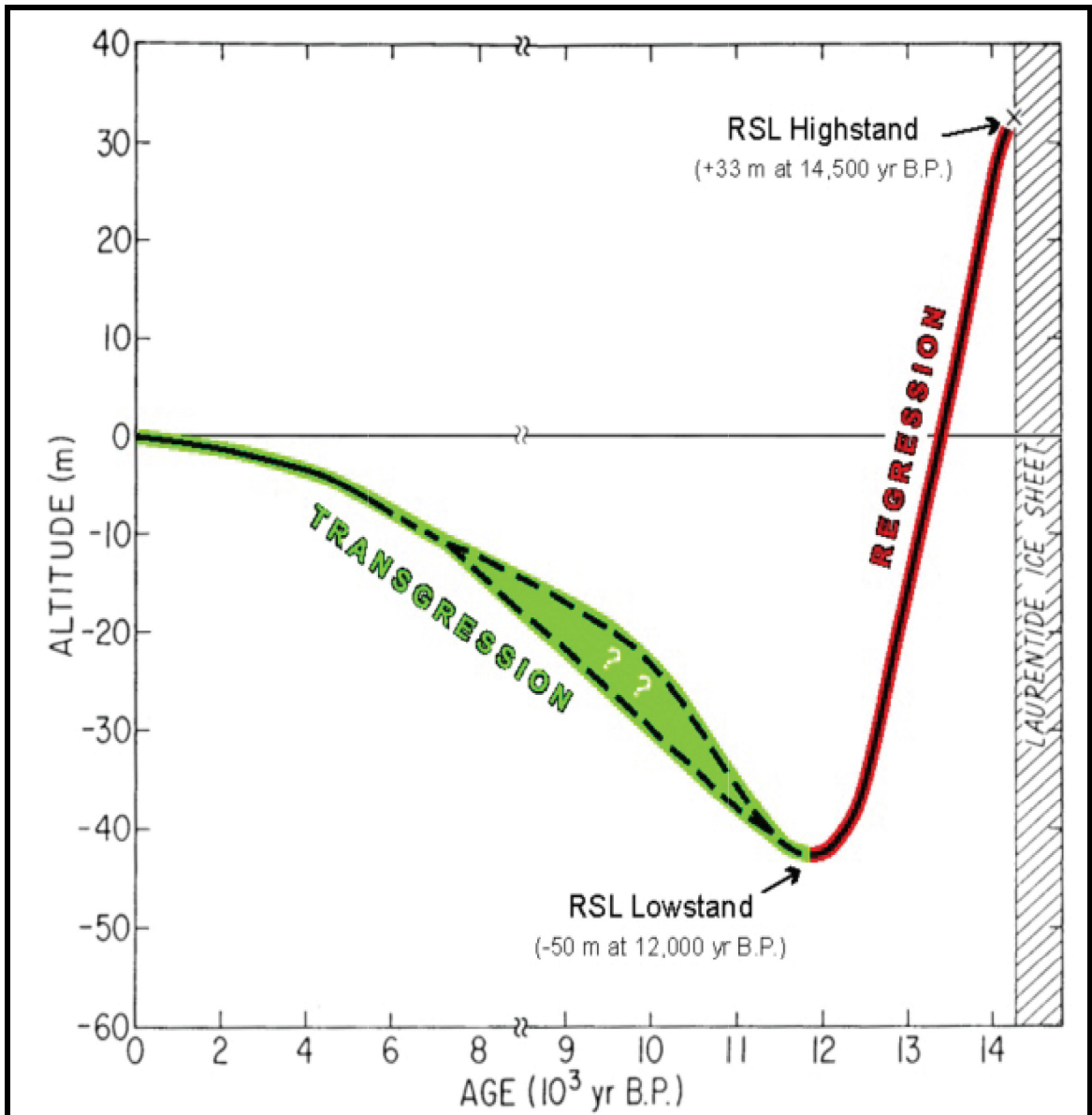


Figure 1.4. Holocene sea-level curve showing three distinct periods of the Harbor's geomorphic evolution. Oldale et al. (1993) report that during the period of Ice Contact occurring prior to 14k ybp there was over a mile of ice over Boston Harbor and sea levels were much higher than today. During the Holocene Regression between 14k ybp and 12k ybp, sea-levels were rapidly dropping due to the isostatic rebound of the surrounding topography. The Holocene Transgression beginning approximately 12k ybp and continuing to present, is marked by rapid SLR and the rapid landward retreat of the shoreline (After, Oldale, et al., 1993).

(Fairbanks, 1989). While the area was covered by ice, many of the drumlins that make up the area's topography were formed by glacial processes.

The backbone of the Harbor Islands consists of one or more of these partially drowned drumlins connected by low elevation sand and or gravel spits (Himmelstross et al., 2006). Characteristically, the glacial or upstream sides of drumlins are high and steep, while the lee side gradually slopes down towards the direction of ice flow. Though heavily eroded, many of the Harbor's islands still have this characteristic surface topography with high bluffs on their northwestern shores sloping down toward the southeast. Their characteristic shape within Boston Harbor is primarily due to local erosional processes. Together, the Harbor Islands make up a drumlin archipelago, which is a unique geologic feature not seen anywhere else in the United States (Himmelstross et al., 2006).

During the early Holocene Regression, immediately after the Laurentide Ice sheet began retreating northward, proximal deposits of gravel, sand, and till, as well as a thick layer of glaciomarine muds were deposited over the top of the earlier formed drumlins (Rendigs and Oldale, 1990). As local sea-level during this time was almost 18 m above present day, many of these deposits occurred directly into the sea (Newman et al., 1990).

After the rapid retreat of the ice sheet, during the Holocene Regression, the Earth's crust quickly rebounded after being relieved of the enormous weight of the continental glaciers (Aubrey, 1994). As the land uplifted, relative sea-levels dropped dramatically until reaching their low stand between 10,000-11,000 ybp at approximately 50 m below present day sea-level (Oldale et al., 1983; Oldale, 1985). At the end of the Holocene Regression, it is

estimated that the Boston Harbor shoreline was located roughly eight kilometers seaward of the present day mouth (Aubrey, 1994) (Figure 1.5).

The final period of the Harbor's geomorphic evolution occurred during the Holocene Transgression marked by SLR and a rapid retreat of the shoreline. During this period, sea-levels rose over 40 m. The most rapid rise in relative sea-level during the Holocene Transgression occurred between 9,000 –5,000 ybp as global eustatic SLR caused by increased volumes of meltwater flowing into the oceans quickly outpaced the decreasing rate of isostatic rebound (Emery and Aubrey, 1991) (Figure 1.5). This resulted in the resubmergence of the Boston Harbor basin and the development of numerous embayments and peninsulas (Aubrey, 1994).

As Boston Harbor became increasingly inundated by SLR, the drumlin hills that once overlooked the broad coastal plain became islands and were separated from the mainland (Himmelstross et al., 2006). A more gradual, but steady rise in relative sea-level after 5,000 ybp resulted in a reworking of the existing deposits by increased wave and current erosion (Aubrey, 1994). These reworked glaciomarine sediments and till would later become overlain by fine deposits of estuarine silts, clays, and organic sediments deposited after the establishment of sheltered estuarine systems within the Harbor (Rendigs and Oldale, 1990).

1.5 Prehistoric Landuse

Boston Harbor has a rich and dynamic cultural past stretching back thousands of years. Many of the Harbor Islands have been systematically surveyed for archeological resources with approximately 60 sites being identified as of 1999 (Luedtke, 2000). As sea

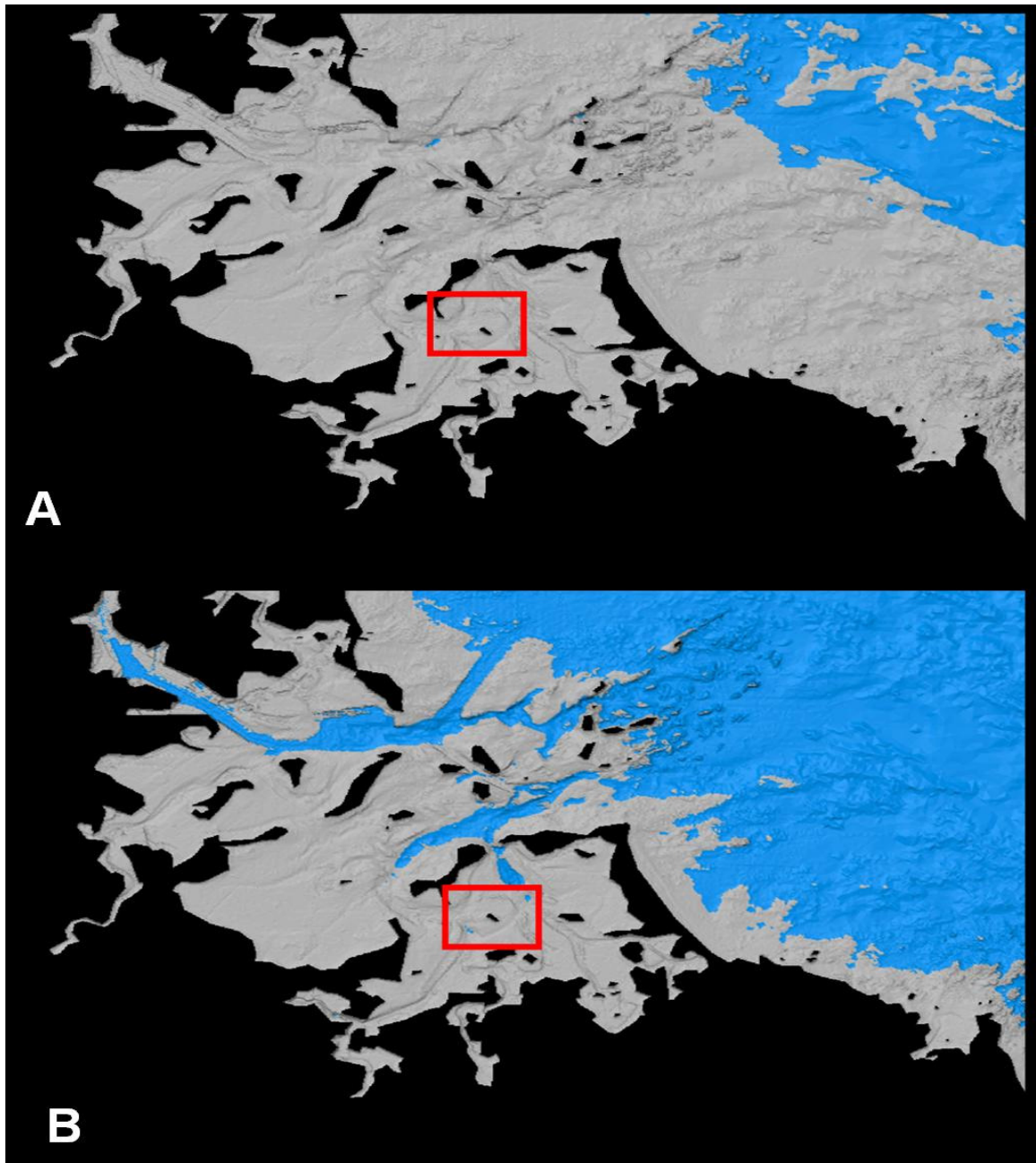


Figure 1.5. Simplistic reconstruction of Holocene sea-level rise in Boston Harbor. Rapid sea-level rise occurred between (A) 9000 ybp and (B) 6000 ybp. Rainsford Island, shown within the red box, remained landlocked until after 5000 ybp. This reconstruction was based on present day bathymetry. As a result dredged areas are highlighted and paleo rivers channels are absent (After, Aubrey, 1994).

levels rose dramatically during the Holocene Transgression, ecological habitats changed considerably and numerous terrestrial and marine plants and animals were displaced (Bell, 2009). These dramatic environmental changes were witnessed by the area's human populations (Bell, 2009). Although there are no documented prehistoric archeological sites on Rainsford Island, on nearby Long Island a single isolated bifurcate projectile spear point was found dating to the early Archaic Period approximately 11,000-8,900 ybp (Luedtke, 1984). The rapid inundation of the broad coastal plain during the early Transgression likely submerged much of the evidence for early prehistoric habitation within the Harbor (Aubrey, 1994). Further investigation of ancient archeological sites, likely located on the now submerged prehistoric shores of the Harbor's estuaries and river mouths would be necessary to find further evidence of the ancient inhabitants.

The majority of documented sites on the Harbor Islands date to the Middle or Late Woodland periods approximately 450-1300 ybp (Luedtke, 2000). One of the largest of these sites was located on Spectacle Island which is approximately 1 km northwest of Rainsford Island. A large site on Spectacle Island (Site 19-SU-38) is similar to other Woodland sites within the Harbor. The site contained two large shell middens and an assortment of bone tools and ceramics (Simon, 2000). The abundance of documented Woodland period sites within the Harbor is likely due to the fact that relative sea-level was rising much more gradually during this time and coastal systems within the Harbor at this point in time had become well established, providing abundant marine resources that could be exploited by the local Native populations (Luedtke, 2000).

Despite the fact that no prehistoric sites have been uncovered on Rainsford Island, it does not mean that they do not exist. Qualitative environmental criteria and anecdotal accounts suggest that Rainsford Island does contain prehistoric sites, though many may be buried beneath historically reclaimed lands (Berkland, 2009). Only a small percentage of the Island has been tested archeologically, leaving much of the Island unsurveyed. Due to these factors, the 2002 Rainsford Island Archeological Survey concluded that the Island was an area of high prehistoric sensitivity (Claesson and Carella, 2002).

Environmental conditions during the Holocene period show Rainsford Island would have been well suited for human habitation. Prior to 6000 ybp, the area that now makes up Rainsford Island was a hill attached to the mainland overlooking embayments and estuarine river channels (Figure 1.5) (Aubrey, 1994). Once the low-lying areas of the Harbor became submerged and the Island was formed, it was still accessible to the mainland and had reliable freshwater sources (Berkland, 2009).

1.6 Historic Landuse

Rainsford Island has numerous historically significant sites which provide a rich chronology of cultural and environmental developments during the past 370 years (Figure 1.6). Throughout its history, Rainsford Island has been transformed by human intervention and development. Although many of the individuals that played a roll in its history have long passed, the physical imprints they left behind continue to influence the Island's shoreline evolution. For example, a seawall built over a hundred and fifty years ago continues to serve its purpose buffering much of the Island's high northern bluffs from erosion. Much of the

RAINSFORD ISLAND HISTORICAL TIMELINE

1636 - 2009

- 1636 Edward Raynsford purchases Island from the Mass Bay Colony
- 1737 Island taken over by Province of Massachusetts and used as quarantine hospital
- 1775 First documented small pox vaccination administered by acting physician Dr. John Jeffries
- 1797 Stone and timber wharf built on southeast boulder beach
- 1832 Stone Hospital or “Greek Temple” built as new quarantine hospital
- 1835 Violent storm completely destroys seawall protecting northeastern bluff
- 1836 City of Boston builds large granite seawall along northeastern bluff
- 1895 House of Reformation established to house Boston’s troubled youth
- 1898 The “Portland Gale” partially destroys the main wharf and numerous buildings and other infrastructure
- 1920 Due to a lack of funds during the onset of the Great Depression, the Island is abandoned and buildings fall into disrepair
- 1950 Island retained by the City of Boston and used for recreation
- 1996 Boston Harbor National Recreation Area established including Rainsford Island
- 2001 Rainsford Island Archeological Survey conducted
- 2009 Island Managed by City of Boston and currently off limits to the general public

Figure 1.6. Rainsford Island historical timeline spanning 373 years. (Claesson and Carella, 2002).

historical information in the following section and utilized in the production of Figure 1.6 was taken from the 2002 Rainsford Island Archaeological Reconnaissance and Management Plan, which is considered the predominate source on the history of Rainsford Island (Claesson and Carella, 2002).

The first European inhabitant to occupy the Island was Edward Raynsford when he purchased the Island from the Mass Bay Colony in 1636 (Claesson and Carella, 2002). Records show that for the next hundred years it was used as a fishing station and cattle pasture (Claesson and Carella, 2002). In 1737, the Island was taken over by the Province of Massachusetts and used as a quarantine hospital for incoming ships, Boston residents, and returning war veterans (Claesson and Carella, 2002). The first documented small pox vaccination was given on the Island by its acting physician, Dr. John Jeffries, who, in 1775, inoculated his own son with cow pox (Claesson and Carella, 2002). In 1797, a large stone and timber wharf was built on the southeast side of the Island, providing access to its facilities (Berkland, 2009).

The Stone Hospital or “Greek Temple”, depicted in the following painting by Robert Salmon, ca 1840, was built in 1832 and was likely designed by the famous American architect, Isaiah Rogers, who had also designed the Tremont Hotel in Boston and the Treasury Building in Washington, D.C. (Figure 1.7) (Claesson and Carella, 2002). The large granite foundation for this elaborate structure can still be seen on the Island today.

During the Island’s documented history, several large storms caused significant damages to the Island’s shoreline and infrastructure. In 1835, the Island’s seawall, which had protected its northeastern bluff, was completely destroyed by a violent storm. During the



Figure 1.7. Circa 1840's painting of Rainsford Island by Robert Salmon. Though highly stylized, this painting provides a window into what life may have been like around Rainsford Island in the early 1800's. The elaborate Stone Hospital also referred to as the "Greek Temple," which acted as the Island's main quarantine facilities, was likely designed by the famous American architect Isaiah Rogers (Claesson and Carella, 2002).

same year, the Massachusetts General Court appropriated funding to “defray the expenses of protecting Rainsford Island from the ravages of the sea” and, in 1836, the City of Boston built a larger granite seawall along the northern and eastern shores (Claesson and Carella, 2002). Though the seawall has been eroded considerably, it continues to play a roll in the Island’s shoreline evolution by protecting its high bluffs from erosion. Other large storms, including the “Portland Gale” of 1898, the “1938 Hurricane,” and the “The Blizzard of 78,” dramatically altered the Island’s shoreline, though there is little documentation of the changes.

During the remaining years of the 19th century, the facilities on Rainsford Island continued to be utilized as the City’s main quarantine station, though towards the end of the century it doubled as an alms house for returning Civil War veterans as well as a summer hospital for small children (Claesson and Carella, 2002). During the 180 years that the Island’s medical facilities were in use, many of its inhabitants were laid to rest in the Rainsford Island Cemetery located on the low-lying area of the south drumlin (Figure 1.8). It is believed that 1000’s were buried here during the Island’s history (Berkland, 2009).

During the 1890’s, The House of Reformation was built to house and employ the troubled youth of Boston (Claesson and Carella, 2002). This three story brick structure, as well as some smaller adjacent buildings, including a stable and school house, were used for the Island’s print, shoe, and garment shops. The boys were also employed in farming and the raising of livestock (Claesson and Carella, 2002). In a twist of irony, half of the north wing of The House of Reformation was mostly destroyed when seven of its occupants set it on fire

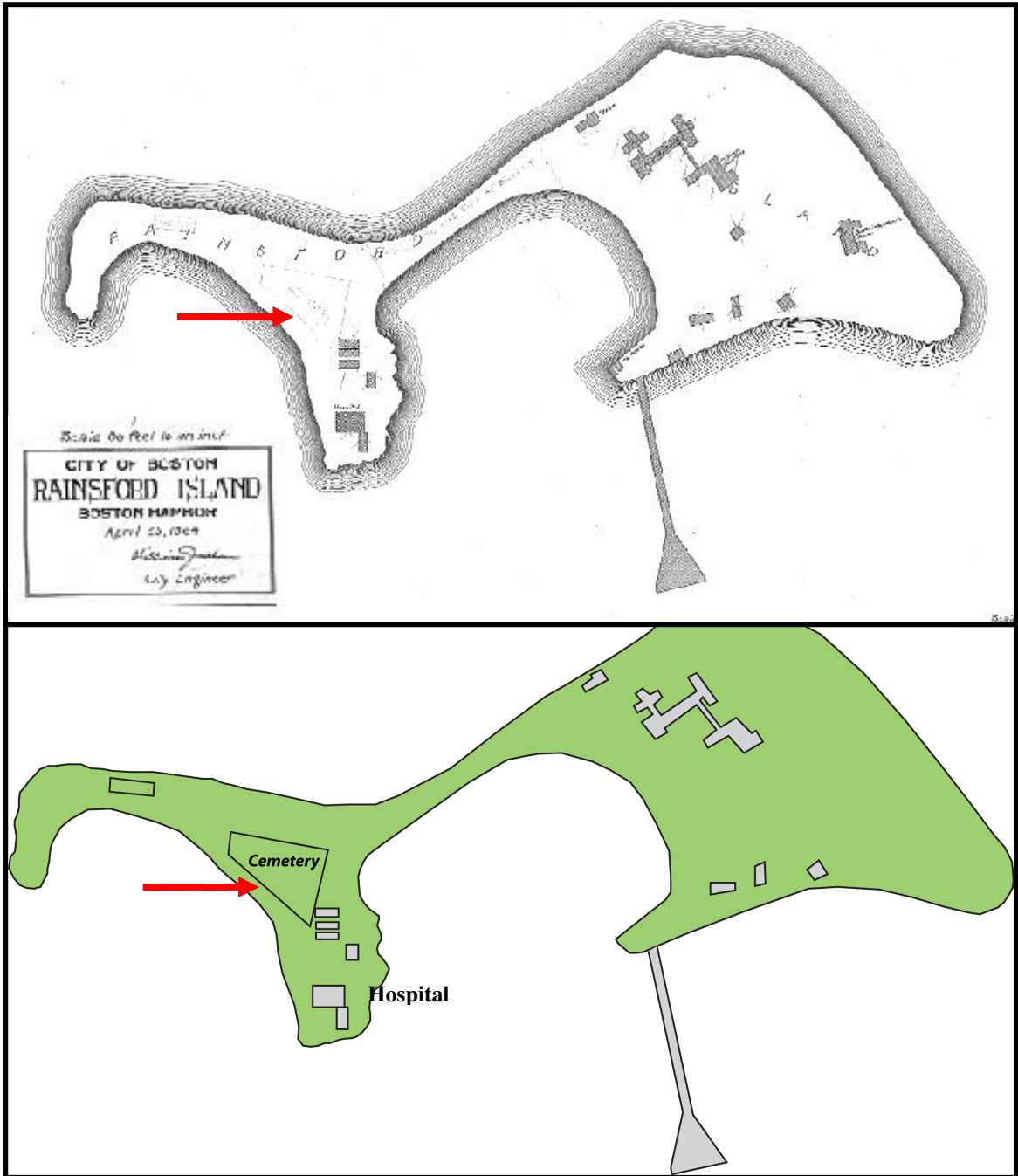


Figure 1.8. Historic 1904 map of Rainsford Island with digitized version. The map shows the location of the Island's historic infrastructure during the late 1800's, including the large wharf, hospital facilities, reform school, stable, and cemetery. Little of the infrastructure still exists, as numerous fires and large storms have taken their toll. The 1898 "Portland Gale" referred to as a "Great Storm" in historical documents destroyed the main wharf and many of the buildings (Claesson and Carella, 2002).

(Claesson and Carella, 2002). Other adjacent buildings would later meet the same fate.

Around the same time period, in 1898, the “Portland Gale”, referred to in historical records as a, “great storm,” partially destroyed the large stone and timber wharf, numerous buildings, and other infrastructure on the Island (Claesson and Carella, 2002).

After the turn of the century, there were some additional improvements made to the existing facilities on the Island but with the onset of the Great Depression, many of the buildings soon became dilapidated. Due to a lack of funds and the poor condition of many of the buildings, the Island was officially abandoned in the early 1920’s. In 1948, the Mayor of Boston announced the city’s intention of selling the Island, but his plan never came to fruition. For the next 40 years the Island was retained by the City of Boston and used for recreational purposes by the area’s residents (Claesson and Carella, 2002).

In 1996, the Boston Harbor Islands National Recreation Area was established by congressional mandate and included Rainsford Island. The recreation area was created in order to protect the Harbor Islands and their associated resources and improve public knowledge and access. The recreational area offers a diverse array of natural, geologic, cultural, and historic features which provide a rich timeline of environmental and cultural developments along the U.S. East Coast. These attractions are made even more significant due to their close proximity to the City of Boston. Although Rainsford Island is included in the recreation area, it has remained under the management of the City of Boston.

In 2001, the extensive Rainsford Island Archeological Survey, carried out by the Institute of Maritime History, with support of the Center of Coastal and Ocean Mapping (CCOM), and sponsored by the Boston Landmarks Commission (BLC), brought attention to

the Island. As managers of the Island at the time, the BLC used this survey to develop a long range management plan for the Island's cultural and natural resources, resulting in the 2002 Rainsford Island Archaeological Reconnaissance and Management Plan (Claesson and Carella, 2002).

Presently, Rainsford Island is under the management of the City of Boston and, as mentioned, is part of the Boston Harbor Islands National Recreation Area. The Island is currently off limits to the general public and has been set aside for educational and research projects. Despite this, the Island is still heavily used during the summer months by campers and boaters. Over the past decade, large amounts of rubbish and recreational debris have been left behind, littering the Island and its numerous sensitive historical and potential prehistoric sites. This was highlighted on the front page of the February 27, 2009 issue of the Boston Globe titled "Nature, abuse imperil a harbor island heritage Centuries-old hospital graveyard falls prey to the elements, squatters" (MacQuarrie, 2009).

CHAPTER 2

METHODS

2.1 Introduction

Calculating shoreline change over time requires two main components: 1) the selection and definition of an indicator feature to use as a proxy to delineate the shoreline, and 2) the detection and digitization of the indicator feature using available data sources (Boak and Turner, 2005). Utilizing and developing methods which can be effectively employed to accurately identify these components, is therefore, crucial for accurate analysis. Despite the new breakthroughs in remote sensing technology and computer mapping techniques, all but the most recent shoreline change studies still rely heavily on manual visual identification and definition of an indicator feature (List and Farris, 1999).

This subjective detection method of delineation relies heavily on the skills, judgment, and experience of the individual interpreter. Due to the subjective nature of this approach, there are potential uncertainties and errors inherent with shoreline change analysis. As a result, the spatial error in determining the historical positions of shorelines may be greater than the actual rate of change the investigator is seeking to quantify (Boak and Turner, 2005). These uncertainties could potentially severely hamper sound coastal management decision

making and must, therefore, be recognized and minimized if possible in order to produce a more accurate analysis (McBride et al., 2002).

Shoreline indicators usually fall into one of two categories: 1) Visually discernable indicators are coastal features that can be manually identified on aerial photographs and in the field, such as the high water line (HWL), the vegetation line, and the storm debris line. 2) Elevation-based indicators can be derived from the intersection of a coastal profile with a specific elevation taken from a statistically derived tidal datum such as the mean high water (MHW) elevation. MHW is a value derived from the average of all high tides occurring during the selected tidal datum epoch, which in this case is 19 years.

Boak and Turner (2005) did an extensive review of the numerous indicators used to delineate shorelines and found 28 different indicator features applied within the literature. They point out that the numerous definitions of the term “shoreline” are as variable and dynamic as the coastal feature itself (Boak and Turner, 2005). For example, the HWL has a wide array of definitions, including the wet-dry boundary on the beach, the storm debris line, or the furthest extent of the last high tide (Farrel et al., 1999; McBride et al., 1991; Gorman, et al., 1998). Because there are so many definitions for the same feature, it is important to clearly define the indicator as it will be utilized in a particular study in order to ensure a consistent, accurate, and repeatable interpretation of the actual shoreline.

The accurate, consistent, and repeatable identification of the selected indicator feature within the available data sources is another potential source of uncertainty and error. The approach is dependent on both the ability and skill of the interpreter and the quality of data sources. An effective use of shoreline change analysis is highly dependent on the quality of

the available data sources. In order to analyze shoreline change over the longest time period possible, many different data sources are often integrated in a single shoreline change study (Boak and Turner, 2005). Many of these data sources are often of different spatial and temporal resolutions, making their integration difficult.

RISES sought to conduct a study covering the longest time scale possible and, therefore, needed to utilize most available data sources, despite the potential uncertainties that this introduced. As a result, there was a wide variance in the spatial and temporal resolutions of the images used in this study. For example, the spatial resolution and image quality of the aerial photographs used in the study varied widely, with large temporal gaps between datasets, sometimes spanning 20 years. This hampered the ability to link specific storm events to dramatic changes of shoreline evolution. In addition, the study integrated a USGS historical map dating to the 1890's with modern datasets such as aerial photographs and LIDAR data. In order to minimize some of the uncertainties introduced by using varied data sources, RISES eliminated two of the aerial photographs initially obtained due to their poor spatial resolution and quality.

RISES used two proxies to delineate shoreline positions and one to delineate the vegetated areas of the Island. The main indicator used as the proxy to delineate the Rainsford Island shoreline was the visually discernable HWL. This proxy was applied to all of the aerial images used in this study. In addition to using the HWL, a tidal datum/LIDAR data derived MHW shoreline was also created. The objectively created MHW shoreline was integrated with the other data sources for analysis. Lastly, the visually discernable vegetation line was used as a proxy to delineate the vegetated areas of the island.

The HWL was defined, in this study, as the markings left on the beach face by the furthest extent of the last high tide. This feature is physically represented within the available data by both the most seaward line of seaweed and debris (wrack line), and the wet-dry boundary on the beach face. These two features were often spatially synonymous within the data and, for the purposes of this study, were collectively referred to as the HWL.

There are numerous justifications for choosing the HWL as the indicator to delineate positions of the Rainsford Island shoreline. The HWL is by far the most common indicator used in shoreline change analysis and is the official shoreline on historical maps and charts. As use of the HWL as an indicator spans a longer temporal scale than many other indicators, its use allows for comparisons on a centurial time scale between modern and historical shorelines (Leatherman, 2003). For these reasons, the HWL is an appropriate indicator to use for historical shoreline change analysis (McBride et al., 2002) and was, therefore, employed within this investigation.

Most studies define the HWL strictly as the wet-dry boundary on the beach face (Anders and Byrnes, 1991; Leatherman and Eskandary, 1999; Zhang et al., 2002). This definition is most effectively applied to low sloping sandy beaches where the wet-dry interface stays visible throughout the tidal cycle. The coastal geomorphology of Rainsford Island's beaches prevented the exclusive use of this definition for the HWL. The medium to high energy beaches that fringe the Island consist of a mix of sand, gravel, and cobbles, which vary in slope from 7° – 15°. Due to the relatively steep slope and high porosity of the beach substrate, a wet-dry line was difficult to consistently identify within the images. It likely became indiscernible shortly after the high tide. In addition, some of the aerial photographs

used in the study were taken during high tide, making it impossible to identify the wet-dry boundary in some areas. It was therefore necessary to rely more heavily on the most seaward wrackline as the main indicator feature, only falling back on the wet-dry line when necessary or when the wrack was not visually discernable. The HWL is identified as the most seaward line of seaweed and other debris left on the beach face by the last high tide.

The MHW elevation obtained from the integration of the LIDAR-derived DEM and NOAA's Boston Harbor tidal datum was used as a proxy to objectively create a MHW shoreline. Statistically derived tidal datums act as a benchmark height to measure local water levels and are based on long running tide gauge records. The MHW is the average of all high tides occurring during the 19 year tidal datum epoch. Parker (2003) concluded that using the shoreline defined by the MHW elevation value as an indicator is suitable for delineating shorelines, as it takes into account all high tides occurring over many years. The MHW is also considered the "legal" shoreline by many government agencies including the U.S. Army Corp of Engineers (USACE) and the Federal Emergency Management Agency (FEMA) (Parker, 2003).

The MHW shoreline can be accurately and consistently derived from high resolution LIDAR data (Harris, et al., 2005). Creating the MHW shoreline was achieved by linking the 2002 MassGIS LIDAR DEM with NOAA's statistically derived tidal datum (Figure 2.1). Liu (2007) discussed that one of the most significant benefits to using LIDAR is the ability to link the data with a statistically derived tidal datum. This linkage provides coastal investigators with the ability to objectively create a shoreline based on statistically derived tidal elevation values, alleviating all uncertainties inherent in traditional shoreline change studies. Unlike a

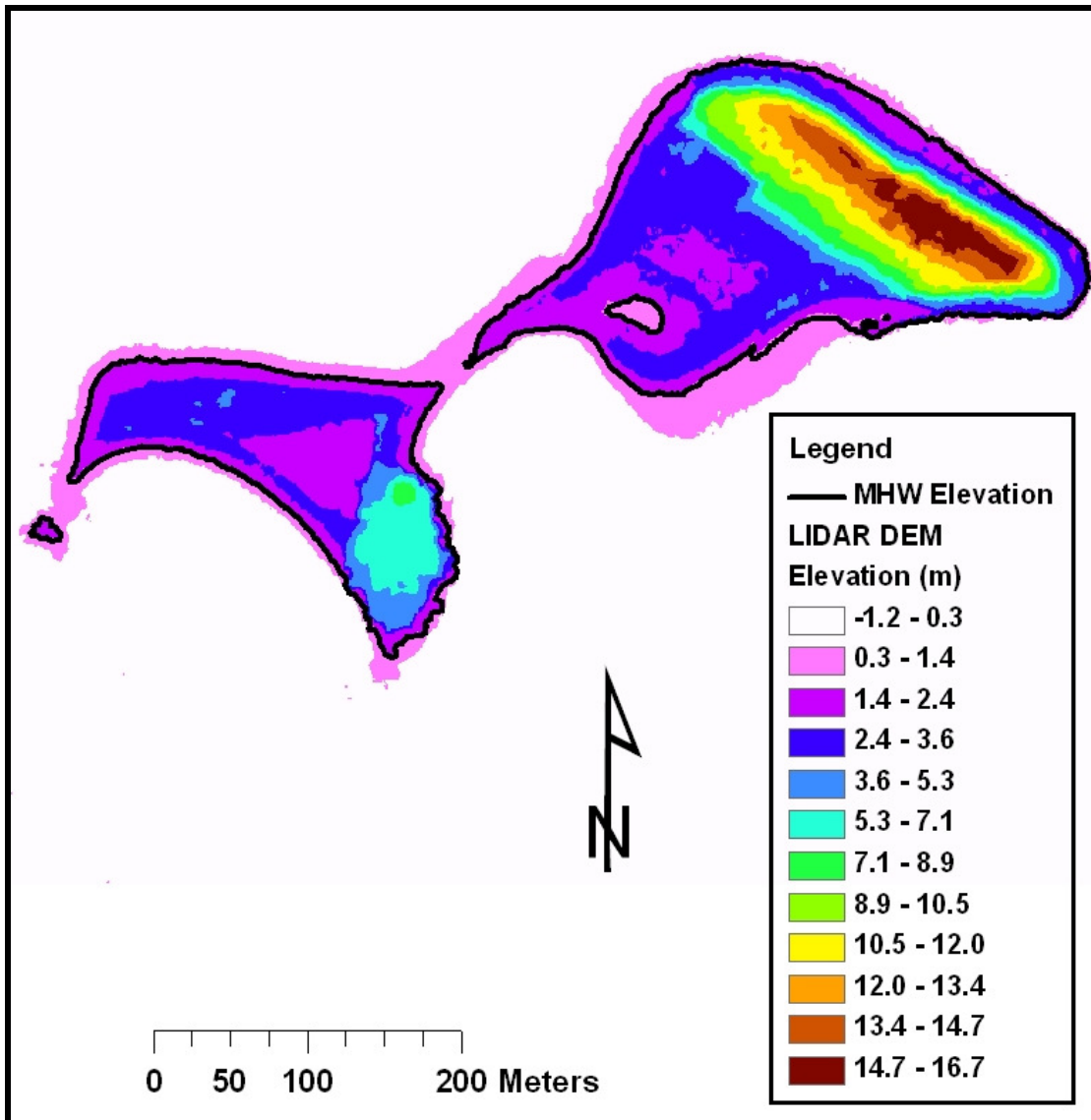


Figure 2.1. MassGIS LIDAR derived DEM shown with tidal datum MHW elevation. The MHW elevation value shown in black was obtained from NOAA's Boston Harbor tidal datum. The integration of the two data sources enabled for the production of the MHW shoreline, predictive maps, and the DSAS baselines.

visually discernible proxy, such as the HWL, the datum-derived shoreline only varies due to morphologic changes, keeping fine spatial details of coastal change (Moore et al., 2006). The methods used to create the MHW shoreline and its integration with the other data sources will be discussed in Section 2.4.2.

RISES also used the vegetation line as a visual indicator in which to delineate and quantify the change to the vegetated areas of the Island. The vegetation line is an easily distinguishable coastal feature represented on the image data by a dramatic tonal difference between the light colored non-vegetated beach areas and the darker colored vegetative areas. This feature was easily identified on all of the aerial photographs used in this study, but could not be identified on the USGS historical map nor on the LIDAR DEM, as these lacked vegetation features.

The applicability of this data may be limited in some cases, as coastal geomorphic changes cannot always be correlated to changes in vegetation and vice versa. For example, a loss in vegetation during a particular year may be predominately a result of poor growing conditions rather than any geomorphic shifts that may have occurred. On the other hand, a loss in vegetation may be evidence for a large storm surge resulting in the loss and/or burial of vegetation. Despite the difficulty in directly correlating vegetation change to shoreline change, the confidence and accuracy in delineating this clearly discernable feature throughout the image data made it a very useful tool in which to analyze the historical evolution of Rainsford Island's environments.

2.2 Data Sources

The shoreline change analysis of Rainsford Island was carried out through the use of multiple data sources including historical maps and aerial photographs, high resolution orthophotos, 2002 MassGIS LIDAR data, and NOAA's tidal datum for the Boston Harbor area. The data available for this study, beginning with the 1890 USGS 15-Minute Quadrangle map, and ending with the 2008 MassGIS orthophoto, covers over a century of time. The data sources ranged dramatically in their temporal and spatial scales. Because of this, sufficient accuracy in the delineation of the Rainsford Island shoreline could only be achieved if the actual rate-of-change was greater than the uncertainties in using the centurial scale data (Harris, et al., 2005).

In most cases, comparing shoreline positions between similar data sources over longer temporal periods provides a greater degree of accuracy than when shorter time periods are compared (Robertson, et al., 2004). For example, the comparison between the 1944 and 2008 shorelines delivered the most accurate data for mapping and quantifying the geomorphic evolution of Rainsford Island. All of the data used for the shoreline and vegetation change analysis were converted to a 1-meter per pixel spatial resolution. This resulted in the higher resolution images being downsized while the lower resolution images were upsized. These conversions set the error potential of +/- 1 meter and standardized all image data.

2.2.1 Historical Aerial Photographs

Aerial photographs have been incorporated into shoreline change studies for decades and provide good spatial coverage of coastal areas (Dolan et al., 1983). Though their temporal

range is often limited and sporadic, they are by far the most common data source for the identification of historical shorelines (Boak and Turner, 2005). RISES incorporated four unrectified aerial photographs within the investigation (Appendix A).

Aerial photographic surveys began along the Massachusetts coastline in the late 1930's (Himmelstoss, 2009). Two of the historical aerial photographs (1952 and 1970) used in this study were identified on aerial photographic index maps of Boston Harbor stored at the Massachusetts State Archives, which holds many of the area's original historical aerial photographs. Once the specific grid numbers containing Rainsford Island were obtained, the higher resolution individual grid photographs were requested from the Massachusetts Office of Cultural Resources, Division of Planning. The individual grid section photographs were provided on a CD by the Division's Archivist as digitized unrectified JPEG files.

The historical 1944 unrectified aerial photograph and the high resolution 2002 unrectified aerial photograph were obtained on a CD as GeoTIFF files from the Principle Investigator of the 2001-2002 Rainsford Island Archeological Survey (Claesson and Carella, 2002). A GeoTiff file combines georeferencing information with a Tagged Image File Format (TIFF) and is a standard way of distributing image data. The 1944 image proved to be a crucial dataset for this investigation as it marked the earliest high quality aerial photograph used in the study.

2.2.2 Digital Orthophotographs and USGS Historical Map

An orthophotograph is an aerial photograph that has been geometrically corrected, or "orthorectified," making it spatially equivalent to a map. The four medium and high

resolution digital orthophotos utilized in this project (1992, 1994, 2005, and 2008) were obtained through the Massachusetts Office of Geographic and Environmental Information (MassGIS) (Appendix A). The orthophotos containing the area of Rainsford Island were identified using the MassGIS Orthoimage Index as tiles 245894 and 249894. Although the island is relatively small, both files were needed to capture the entire area. The orthophotos were downloaded as multiresolution seamless database (MrSID) files, a format used to encode georeferenced raster graphics. The files were stored within separate folders named with the image's year. The USGS historical map used in this study was also identified, downloaded as a MrSID file, and stored through the same process (Appendix A).

2.2.3 LIDAR Data

The LIDAR data used in this project was acquired by 3Di Technologies, Inc., now Spectrum Mapping LLC, and titled "MassGIS LIDAR." The data acquisition began on April 7, 2002 and ran to June 25, 2002. The data was obtained from a Cessna 206 fixed wing aircraft using 3Di's Digital Airborne Topographic Imaging System II (DATIS II) (MassGIS, 2003). After acquisition, the data was put through a number of post processing steps by Spectrum Mapping LLC, and was delivered to MassGIS as bare earth tiles corresponding with the MassGIS Orthoimage Index. These files were then converted to GeoTiff DEMs and projected into the Massachusetts Mainland State Plane, NAD83 coordinate system (MassGIS, 2003).

Though the acquisition of LIDAR data has increased dramatically over the past decade, its temporal and spatial availability is still very limited. This is a problem in shoreline

change analysis which often seeks to investigate coastal geomorphic changes occurring over the longest time periods possible. Many coastal areas still lack adequate LIDAR coverage, and those that have been surveyed usually only have one or two datasets spanning a time period of less than 10 years. For example, the MassGIS LIDAR data used in this study is the only available dataset for Boston Harbor. Despite these limitations, LIDAR data and the objectively based shorelines derived from linking it with local tidal datums has a very promising future. As its availability and temporal range increases, it will undoubtedly provide the foundation for future shoreline change studies.

2.3 Data Integration and Management

The ability to integrate maps and analyze multiple data sources at varying temporal and spatial scales within a GIS was an integral part of this investigation. All data processing and GIS tasks were carried out on a Dell Optiplex GX 620 Intel(R) Pentium 4, equipped with a 3.20 GHz CPU and 2.00 GB of RAM. The system was operated and supported by Microsoft Windows XP, Professional Version 2002, with Service Pack 3. The ArcGIS version 9.2 software package, designed by ESRI Inc., has enormous capabilities to integrate and analyze a variety of types of spatial data. Leica Geosystems, ERDAS Imagine, a remote sensing and photogrammetric processing software package, was utilized for the geoprocessing of all image data.

2.3.1 Data Management: Unrectified Aerial Photographs

The 1944, 1952, 1970, and 2002 unrectified aerial photographs were geoprocessed using ERDAS Imagine software. These images required the application of geometric corrections before they could be integrated and utilized within the GIS (Boak and Turner, 2005). The first step in geoprocessing was to georeference the aerial photographs to the same coordinate system and resolution as the source data. The term georeferencing refers to the process of modifying the spatial registration of an image to match a standard geographic coordinate system, and, in doing so, reduce any geometric and location distortions that were present. These distortions are inherent within all aerial photographs due to the curvature of the earth and the optical characteristics of the photographic equipment used.

In order to georeference aerial photographs using ERDAS Imagine, it is necessary to identify ground control points (GCPs) on both the source data and on the image being referenced. The 2005 MassGIS orthophoto, registered to the Massachusetts State Plane Mainland NAD1983 Meters coordinate system with a 1-meter per pixel resolution, was used as the source data for this process. GCPs are used within ERDAS Imagine to compute rectification transformation coefficients for use with bilinear interpolation resampling algorithms. The selection and repeatability of the GCPs and rectification algorithms are key to successful and accurate geoprocessing (Dobson, et al., 1995). On Rainsford Island there are several static features in the landscape spanning the temporal range of the data sets. These features were used as GCPs and identified on both the 2005 MassGIS orthophoto and on the five other unrectified images. These included the concrete and granite foundation corners of the pig livery and quarantine hospital, sections of the large granite sea-wall along the northeast

shore, and several bedrock outcrops on the south drumlin. Combined, over ten GCP's were identified within both the source data and the unrectified target image. By referencing these locations between the source data and the target image, a new geometrically corrected and georeferenced image was created. This process was carried out for each of the five unrectified images which brought them all into the same coordinate system and resolution.

The data was processed further within ERDAS Imagine through the Subset Data function. The Subset function allows the user to extract the necessary data for the area of interest while eliminating the extraneous surrounding data. To use an analogy, the Subset function acts as a cookie cutter that removes the extra dough around the desired cookie's shape. In the case of Rainsford Island, the desired shape only included the terrestrial and nearshore areas of the Island. A rectangular "area of interest" (AOI) file, measuring approximately 835 m by 617 m, with an area of 0.51 km², was created in order to reduce the extraneous data (Figure 2.2). The AOI file was named "RI_AOI", and was later utilized to subset the other datasets used in this study. Once the four unrectified aerial photographs were geoprocessed, they were available for analysis within the GIS.

2.3.2 Data Management: Digital Orthophotographs

Image data obtained from MassGIS for use in this study was registered to the NAD1983 datum, Massachusetts State Plane Mainland zone coordinate system as MrSID files. Because of this, the time consuming process of georectification was unnecessary with the MassGIS data and historical map. All other data sources used in this project were brought into this same coordinate system for efficient processing and analysis in the GIS. After the



Figure 2.2. 1992 MassGIS composite orthophotograph shown with rectangular “Area of Interest” (AOI). The Rainsford Island AOI measures 835 m by 617 m and was created within ERDAS Imagine to subset extraneous data allowing for more efficient processing and analysis. The same AOI was also used to subset and reduce other image data utilized within this study. The figure also shows why it was necessary to mosaic many of the MassGIS orthophotographs together. The Island, though relatively small, was often divided into two separate files which can be seen by the tonal difference between the left and right side of this image.

orthophotos were downloaded, the next step was to mosaic the two separate files together into a single image file. This was carried out using the Mosaic Image function within ERDAS Imagine. Once combined, the newly created image file was named with the appropriate year and stored in that year's folder. The next step in data management was to subset the combined images using the same process as described above for the unrectified aerial photographs in Section 2.3.1.

2.3.3 Data Management: LIDAR Data

The LIDAR data that covered the Rainsford Island area was identified as GeoTiff Files 245894 and 249894 using the MassGIS Orthoimage Index. The files were downloaded from the MassGIS website and brought into ERDAS Imagine for geoprocessing. Using the same procedures as those applied to the orthophotos, the two separate raster files were mosaiced together and subset using the previously created AOI file. After the LIDAR data was mosaiced and subsetting, it was loaded into ArcMap as a GeoTIFF DEM and named "RI_LIDAR." This file was then used as the DEM source file for a number of spatial analysis operations explained in detail in the following sections.

2.4 Geographic Information System Procedures

2.4.1 Shoreline Delineation and Digitization

The process of delineating and digitizing the shoreline of Rainsford Island was carried out using ArcGIS software components, including ArcMap, ArcToolbox, and ArcCatalog.

ArcCatalog was used to create new polygon shapefiles registered to the same coordinate system as the other datasets. The new shapefile was then named with the appropriate year and geometry. Using the 1944 shoreline as an example, the new file was named, “1944_polygon.”

The shoreline feature was then digitized using the Editor tools. The first step was to add both the 1944 geoprocessed image and the newly created 1944_polygon shape file to the Data Frame. The Editor Tool was then used to create a new feature placing the “1944_polygon” in the Target window. The 1944 image was then zoomed in on until the HWL indicator feature was most discernable. The shoreline was then digitized by placing vertices with the cursor over the HWL continuing around the entire Island, until the new polygon feature was completed (Figure 2.3). The area of the newly created polygon represented all the area of Rainsford Island above the HWL (Figure 2.4). The newly created polygon feature was then saved and placed in a separate “polygon_shorelines” folder for future use and analysis.

As previously discussed, the process of manually delineating visual proxy-based shorelines is highly subjective with inherent uncertainties in the process. When delineating the Rainsford Island shoreline, some of these uncertainties arose and needed to be addressed. The greatest source of potential uncertainty in this process was when the HWL was not visually discernable along certain stretches of the Island’s shore. In some cases, the wrackline was visible, while in others, the wet dry line was evident, and, in still other cases, neither was present for several meters of the shore. This occurred throughout the study area and it was, therefore, necessary to interpolate between identifiable indicator features. This process inevitably introduced some spatial uncertainties to the interpolated areas of the shoreline. The

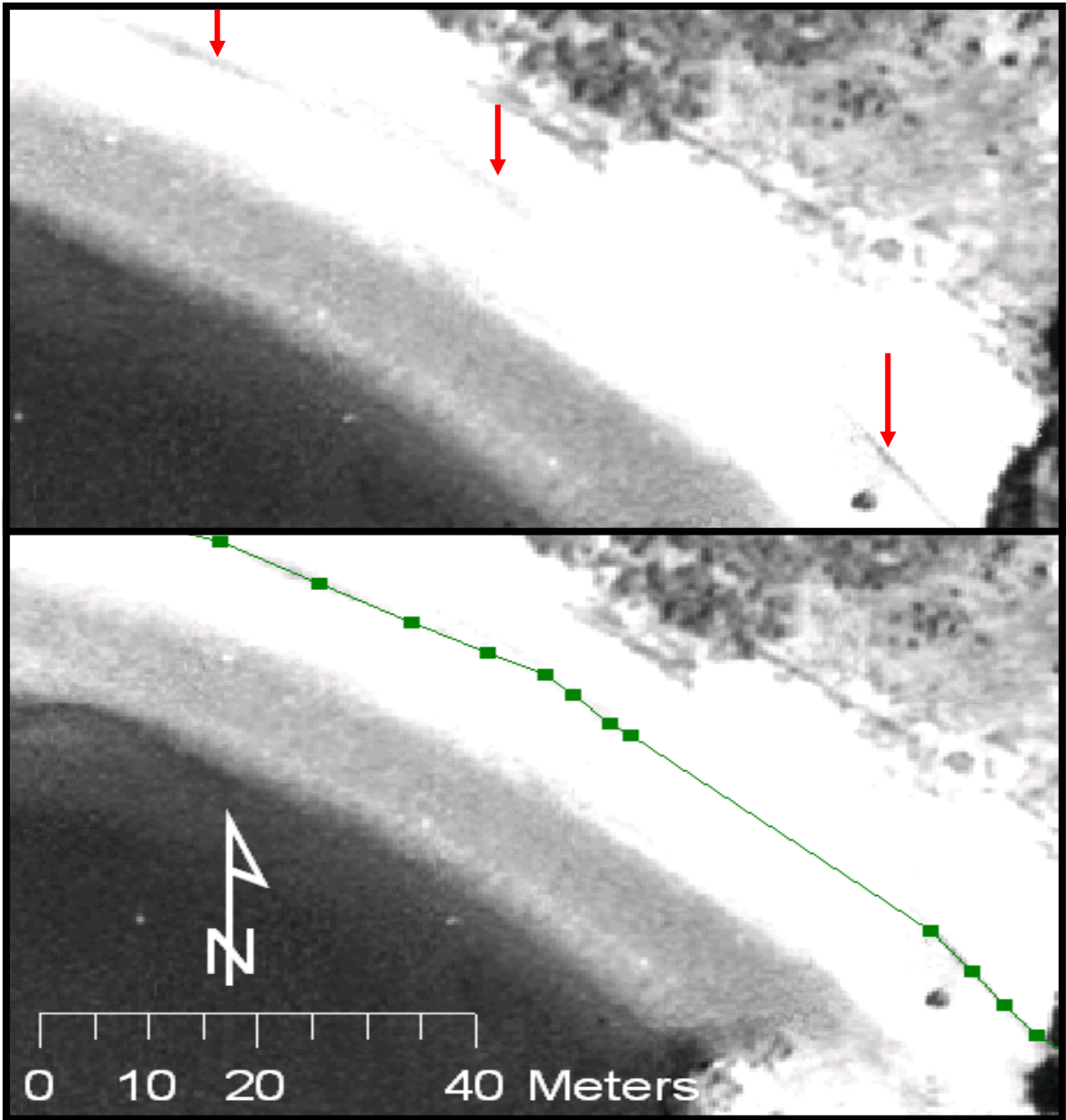


Figure 2.3. The high water line (HWL), identified by red arrows, is shown digitized. The HWL was used as the proxy to delineate and digitize the shoreline on Rainsford Island. The HWL was defined in this study as the most seaward debris or wrack line.

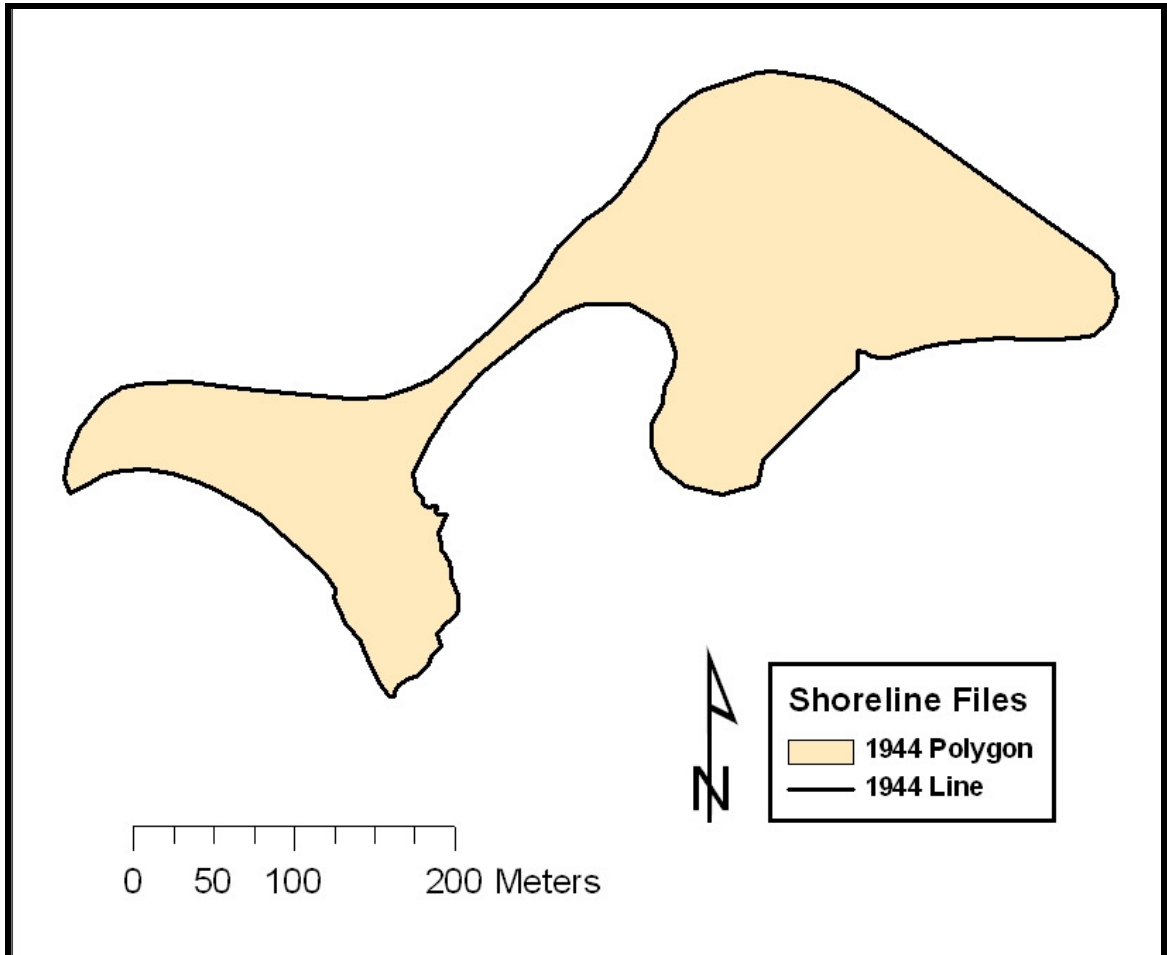


Figure 2.4. 1944 shoreline files. The polygon file is shown in beige and the line file is shown in black. The polygon files were employed in the Comparison Analysis providing an area in m^2 in which to compare to the other data. The polyline files were appended together and employed in the DSAS analysis.

1994 image was particularly difficult to accurately identify the HWL as the areas of the beach were bright white with little to no contrast. Whether this was due to excessive sunlight and reflection when the photograph was taken, or due to a processing distortion is unknown, but as it was impossible to accurately identify the HWL on this dataset, it was eliminated from the shoreline change analysis aspect of the study. However, because the vegetation line was clearly discernable, the image was utilized for vegetation analysis.

After the shorelines were digitized as polygons, ArcToolbox was used to convert the polygon files to polyline files, which is necessary for their analysis within the DSAS ArcMap extension (see Section 2.5.4). The conversion was made using the Polygon to Line tool. Within the Polygon to Line window, the 1944_polygon file was designated as the Input Feature, while the Output Feature Class was named, "1944_polyline," and saved to a new folder titled "polyline_shorelines" and stored for future use and analysis. All other polygon files were converted, named, and stored using the same methods. The vegetation line was digitized through the same process, though named differently (Figure 2.5). Again using the 1944 image as an example, the new polygon file was named, "1944_veg" while the polyline file was named, "1944_vegline." As there is no vegetation on the low elevation sandy spit that connects the north and south drumlins of Rainsford Island, there are two separate polygon features within each file representing the vegetated areas of the two drumlins (Figure 2.6).

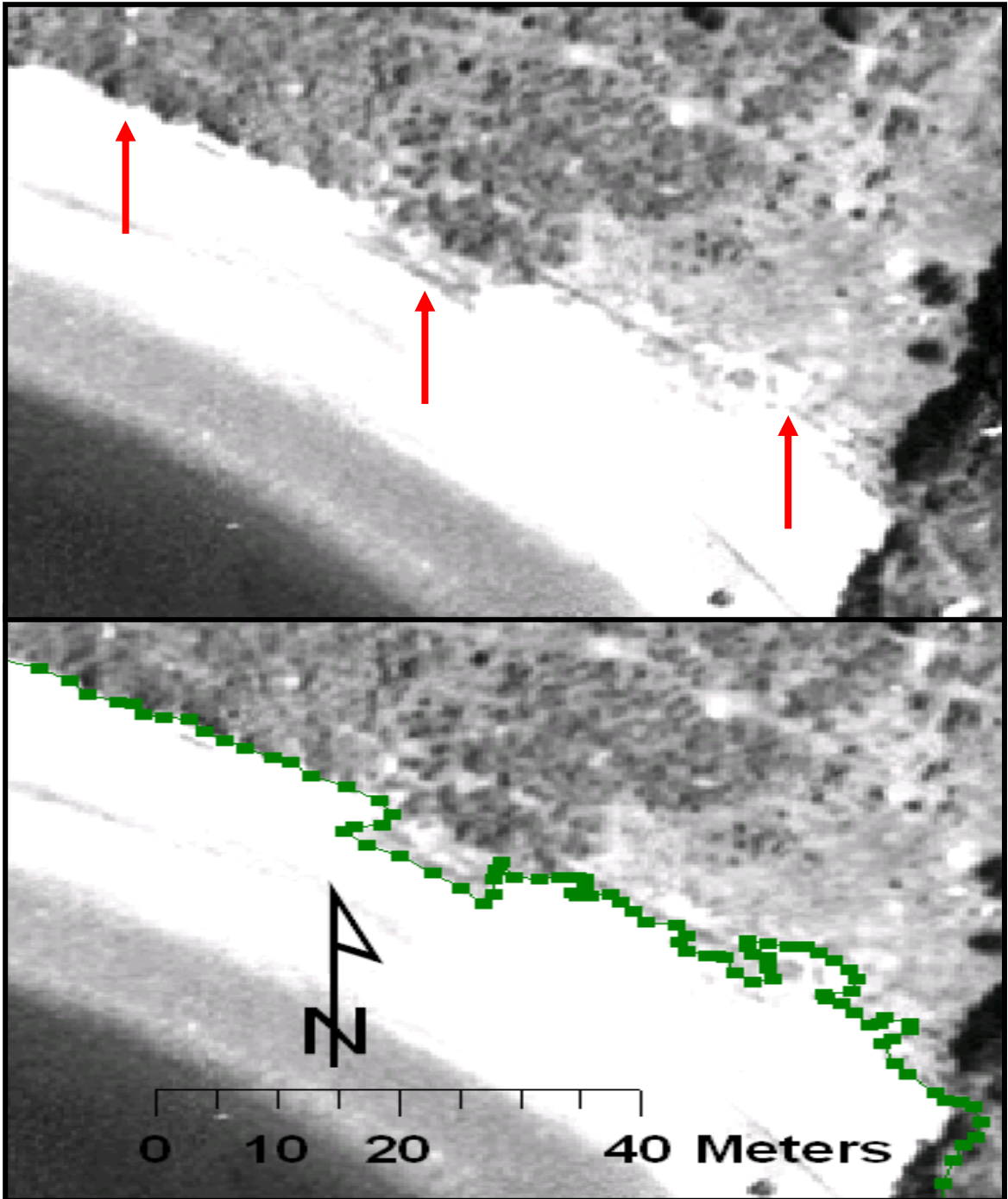


Figure 2.5. The vegetation line as proxy to delineate and digitize vegetated areas of Rainsford Island. The indicator feature identified by the red arrows, is defined as the tonal difference between the white beach face and the darker vegetated area. This feature was digitized in ArcMap as shown in the lower image.

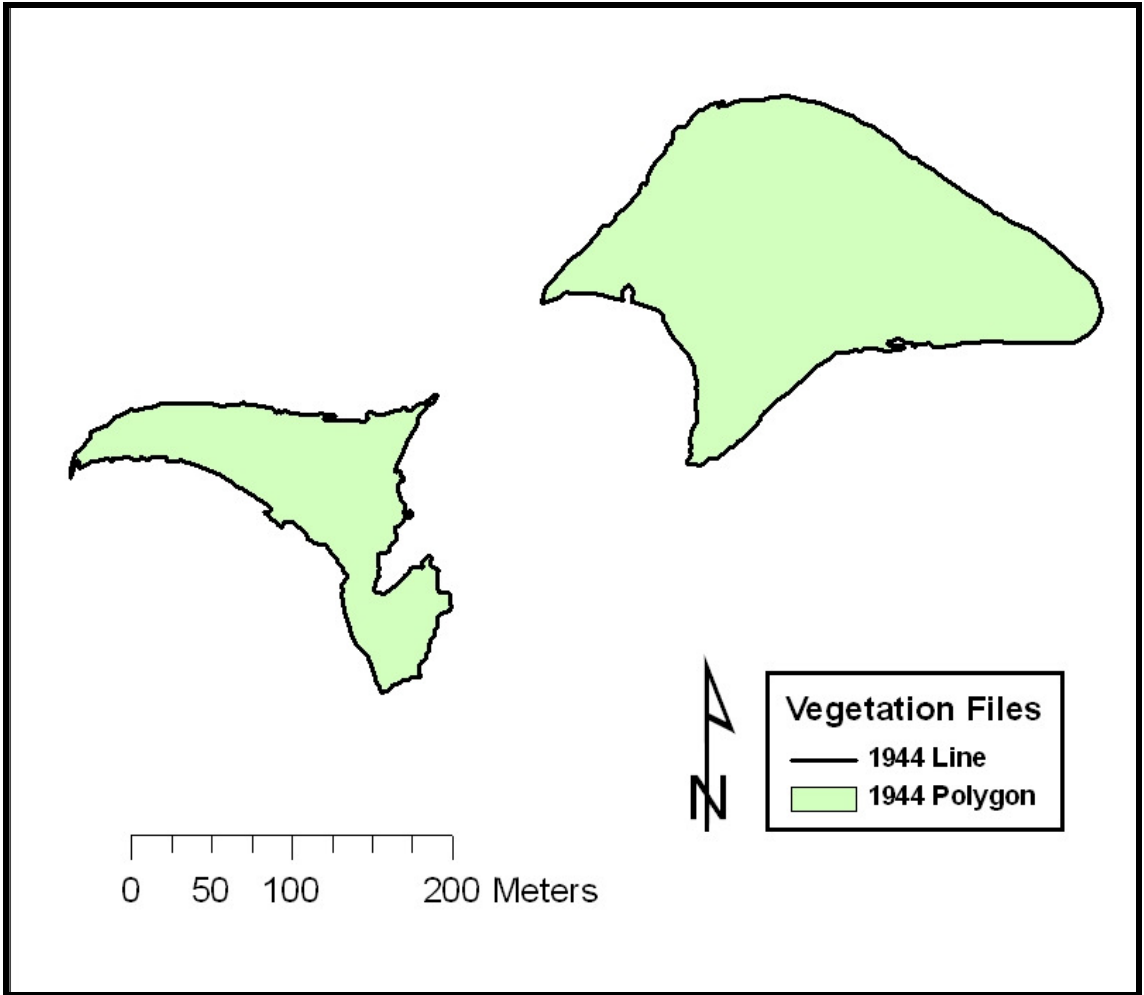


Figure 2.6. 1944 vegetation files. The polygon files are shown in green and the line file is shown in black. The polygon files were employed in the Comparison Analysis and provided the vegetated areas in m^2 . The polyline files were used in the DSAS analysis. As there was no vegetation on the sand and gravel spit connecting the two drumlins, each file had two separate features representing the vegetated areas of the two drumlins.

2.4.2 Creating the 2002 Mean High Water Shoreline

The first step in creating a tidal datum derived shoreline was to integrate the RI_LIDAR DEM with the Boston Harbor tidal datum. The National Oceanic and Atmospheric Administration /National Ocean Service (NOAA/NOS) Center for Operational Oceanographic Products and Services (CO-OPS) Tides and Currents web page (http://tidesandcurrents.noaa.gov/data_menu.shtml?stn=8443970%20Boston,%20MA&) provides an accurate statistically derived tidal datum for the Boston Harbor area, using data obtained from its tidal station # 8443970, located on the south side of the U.S. Coast Guard Building adjacent to Northern Avenue Bridge, within Boston, MA (Appendix B) (NOAA, 2007).

In order to merge the two datasets, it was necessary to relate them to one another, as they have different reference points upon which their elevation values are based. The MassGIS LIDAR data is referenced to the North American Vertical Datum of 1988 (NAVD) Epoch 1983-2001, while NOAA's tidal datums are referenced to Mean Lower Low Water (MLLW), which is the average of the lowest tides occurring during the tidal datum epoch and given the value of zero. Additional information needed to make this calculation was obtained from the National Geodetic Survey and used in conjunction with the NOAA tidal datum elevations (Appendix C).

As the MHW elevation was employed in this study rather than the MLLW, it was necessary to translate the MHW value from the tidal datum to meters relative to NAVD. NAVD is 2.754 m above the tidal datum and MHW is 4.071 m above it. In order to translate the MHW to meters relative to NAVD, it is necessary to subtract the NAVD's 2.754 m, from

the MHW's value of 4.071 m. This results in a difference of 1.319 m, the MHW elevation relative to NAVD. This value could then be effectively utilized within ArcMap to objectively create a MHW shoreline.

Once the relative MHW elevation value (1.319 m) was obtained, the next step in creating the MHW shoreline was to incorporate this value with the RI_LIDAR DEM in ArcMap. This was carried out using the Contour List tool within ArcToolbox. Within the Contour List tool, the RI_LIDAR file was entered as the input raster and 1.319 m was entered as the contour value. This resulted in an output shape file of a single contour line representing the MHW elevation.

The goal in this process was to create an objective tidal datum-derived shoreline comparable to the visual proxy-based shorelines. Further editing was necessary to reduce the MHW contour's excessively noisy and saw-tooth appearance compared with the smoother HWL shorelines. This discrepancy was a result of the differences between the high resolution LIDAR data (10-cm per pixel) and the lower resolution (1 m per pixel) image data. For this process, the Generalization tools were used within ArcToolbox, including Simplify Line and Smooth Line.

The MHW contour was first simplified and then smoothed using a 1 m maximum allowable offset and point remove and peak algorithms respectively. The file was saved in a folder as "MHW_shoreline" and was utilized for analysis throughout the study. The MHW shoreline was then used to visually assess coastal trends occurring on decadal time scales by integrating it with the historical maps and aerial photographs (Figure 2.7). The MHW

shoreline and LIDAR-derived DEM was also used to create coastal flood maps used to identify areas vulnerable to coastal flooding resulting from rising sea-levels and storm surges.

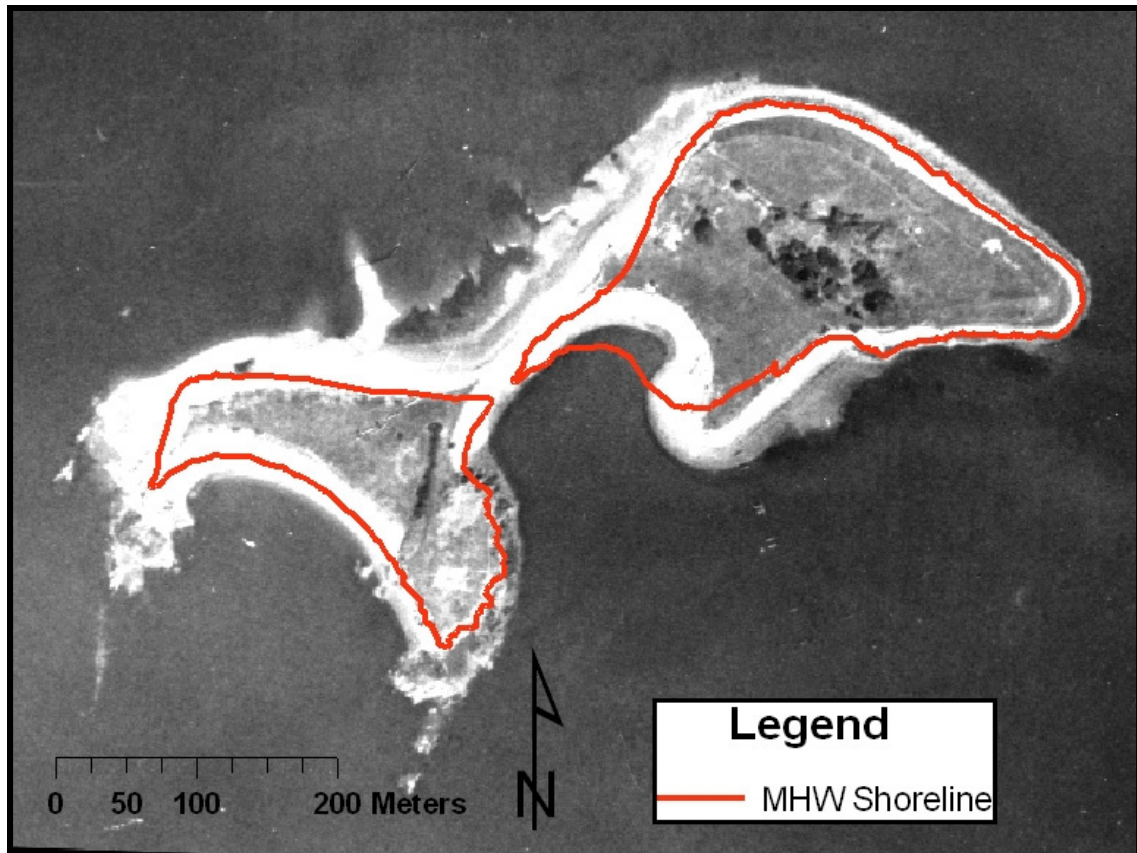


Figure 2.7. 1952 aerial photograph with MHW shoreline shown in red.

2.4.3 Creating the Mean High Water Offset-Corrected Shoreline

Prior to integrating the MHW shoreline with the other data sets for the comparison analysis (Section 2.5.1), it was necessary to quantify the positional differences between it and the 2002 HWL shoreline. Quantifying the offset between the two shorelines allows for the creation of a MHW offset-corrected shoreline that can more accurately be integrated with the manually created HWL shorelines. As both the LIDAR data and the aerial photograph were obtained in the spring of 2002, it enabled for the accurate analysis of their difference.

Determining the average difference between the MHW shoreline and the 2002 HWL shoreline was carried out within DSAS. Once the average difference was obtained, a new offset-corrected shoreline was created by shifting the edited MHW shoreline 1.2 m seaward, which was the average difference between the two shorelines determined within DSAS. The offset-corrected shoreline was converted into a polygon shapefile and named "MHW_offset." It was then integrated with the HWL shorelines in the comparison analysis.

2.5 Data Analysis

2.5.1 Comparison Analysis

For this study, a number of shoreline change maps were created to describe the geomorphic evolution of the Rainsford Island shoreline. One method used to quantify the geomorphic changes occurring on the Island was a comparison analysis of the total areas of loss (erosion), gain (accretion), and stability between the datasets. This was carried out within ArcMap using the previously created polygon shoreline files.

The comparison analysis entailed three sets of comparisons for shoreline analysis and two sets for vegline analysis. The first set quantified the difference between an earlier dataset and the next available dataset; i.e. 1890 compared to 1944, and 1944 compared to 1952, and so on through to 2008. The next comparison set looked at the differences between each data source and the most recent 2008 dataset; i.e. 1890 compared to 2008 and 1944 compared to 2008, and so on. The third set of comparisons was carried out on only the shoreline data using the previously created (Section 2.4.3) MHW offset-corrected shoreline as the base file, i.e. 1944 compared to MHW offset and 1952 compared to the MHW offset. A comparison analysis of the vegetated areas on the Island was also carried out using the 1944 though 2008 image data with the 2008 dataset as the basefile.

The comparison analysis was carried out using the Union function in ArcToolbox. Using the comparison between the 1944 shoreline and the 2008 shoreline as an example, the two polygon shoreline files were entered as the Input Features and the Output Feature Class was named “union_1944_2008” and directed into a new folder titled, “shoreline_comparisons.” The single output shapefile combined both the 1944 shoreline and the 2008 shoreline and divided the Island into three separate polygon areas, representing the areas of erosion, accretion, and stability (Figure 2.8). The area in m² of these polygon features was then obtained using the Measure Tool. The values were exported to Microsoft Excel for further analysis. This process was repeated for each of the comparison sets.

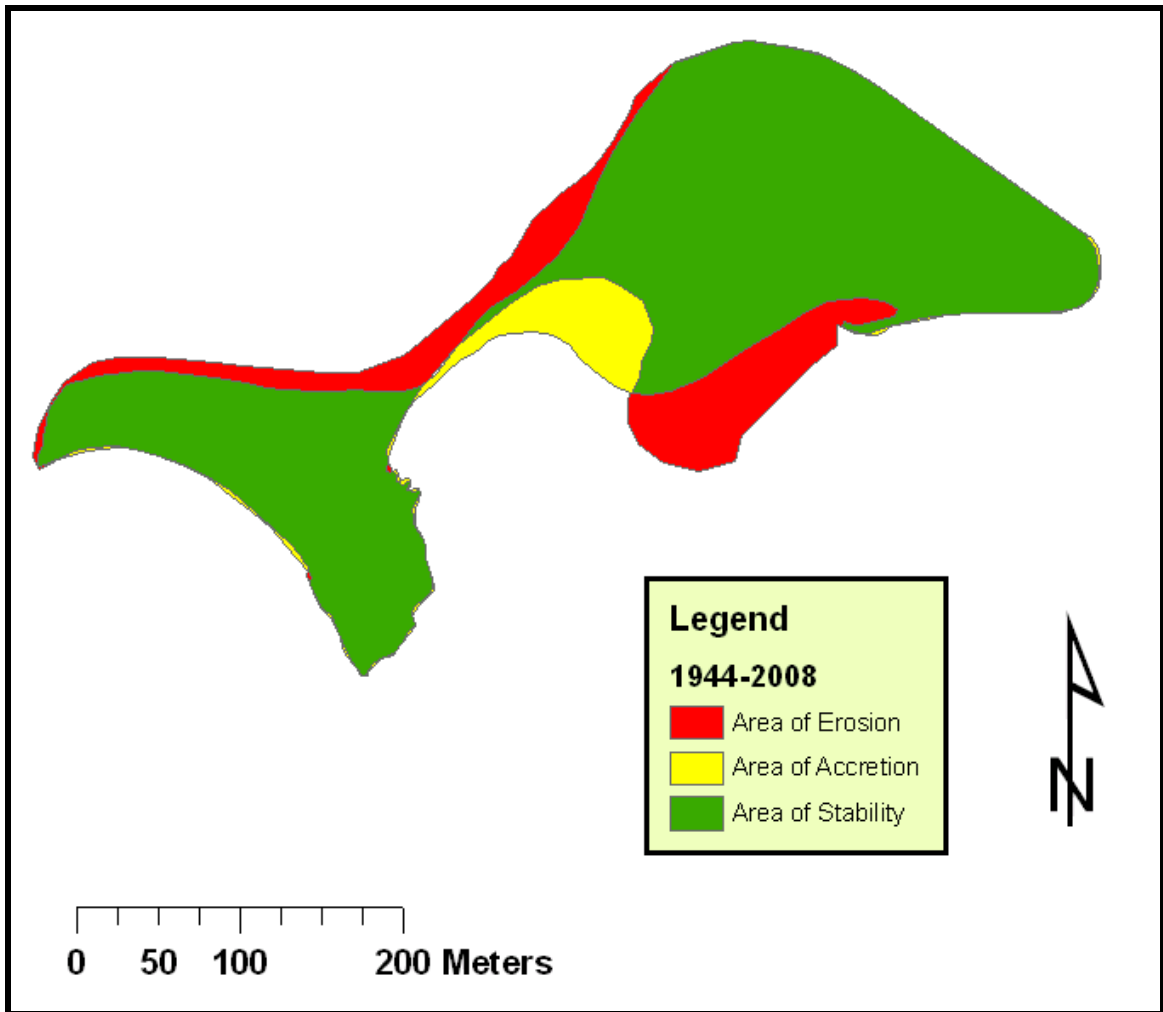


Figure 2.8. Map of Rainsford Island showing shoreline change occurring between 1944 and 2008. The area of erosion is shown in red, area of accretion shown in yellow, and area of stability in green.

2.5.2 Digital Shoreline Analysis System

The Digital Shoreline Analysis System (DSAS), version 4.0, is an extension developed by the USGS for use with ESRI's ArcGIS software (Thieler, et al., 2008). DSAS was designed to enhance the ability of coastal researchers to conduct historic shoreline change studies using multiple historical shoreline positions (Himmelstoss, 2009). RISES utilized this software to calculate the change in shoreline and vegetation positions through time and for obtaining calculations needed to create the MHW offset-corrected shoreline (Section 2.4.3). The DSAS extension generates orthogonal transects from a user generated baseline and determines the rate-of-change and associated statistics between the baseline and the multiple historic shoreline or vegetation line positions within ArcMap (Himmelstoss, 2009).

There were several steps necessary in order to prepare shoreline and vegetation data prior to utilizing the DSAS extension. A detailed 'User Guide & Tutorial' created by the USGS was used as a guide for the necessary tasks (Thieler, et al., 2008). These preparation steps included creating a personal geodatabase, creating a baseline, appending shoreline data, setting the shoreline field requirements, and setting the default parameters. As the creation of the baseline and some of the default parameter settings are the only aspect of these preparation tasks unique to this study, a brief description will be given.

All transects begin at the baseline, making it of fundamental importance to creating accurate rate calculations within DSAS (Himmelstoss, 2009). The baseline can either be created onshore or offshore of the data depending on the study site. In the case of Rainsford Island, it was necessary to create a baseline offshore, as the large variability in shoreline positions did not allow for an onshore baseline. The baseline was created by buffering the

MHW shoreline 55 m seaward. This process was carried out using the Buffer tool within the Analysis Tools of ArcToolbox. This large buffer was necessary in order to create a baseline further seaward than all shoreline positions as this is necessary for analysis within DSAS. The baseline was then manually edited in ArcMap to ensure the proper alignment of transects. Best results are obtained when they cross shorelines at a perpendicular angle (Thieler, et al., 2008). The baseline file was named “baseline_55m.”

The baseline for the vegetation analysis was created using similar procedures, buffering the MHW shoreline 10 m seaward. As there is no vegetation covering the low elevation gravel spit that connects the north and south drumlins, two separate baseline features were created during the editing session. The baseline file was named “baseline_veg.”

Another step to prepare the data for use in the DSAS extension was to append the shoreline and vegetation data, so that a single file was developed for each data type. The Append tool in ArcToolbox was used to combine the individual shoreline polyline data files into one file (Figure 2.9). Two separate append files were created for this analysis. One included the image data sets covering the entire study period (USGS Map, 1944, 1952, 1970, 1992, 2002, 2005, and 2008), and was named “append_1890_2008” and referred to as the 1890 dataset. The other left out the historical map including only the data derived from aerial photographs and was named “append_1944_2008” and was referred to as the 1944 dataset. All of the vegetation polyline files were appended together into one file and named “append_vegline” (Figure 2.10). Rate-change-statistics were separately generated for each of the three appended files.

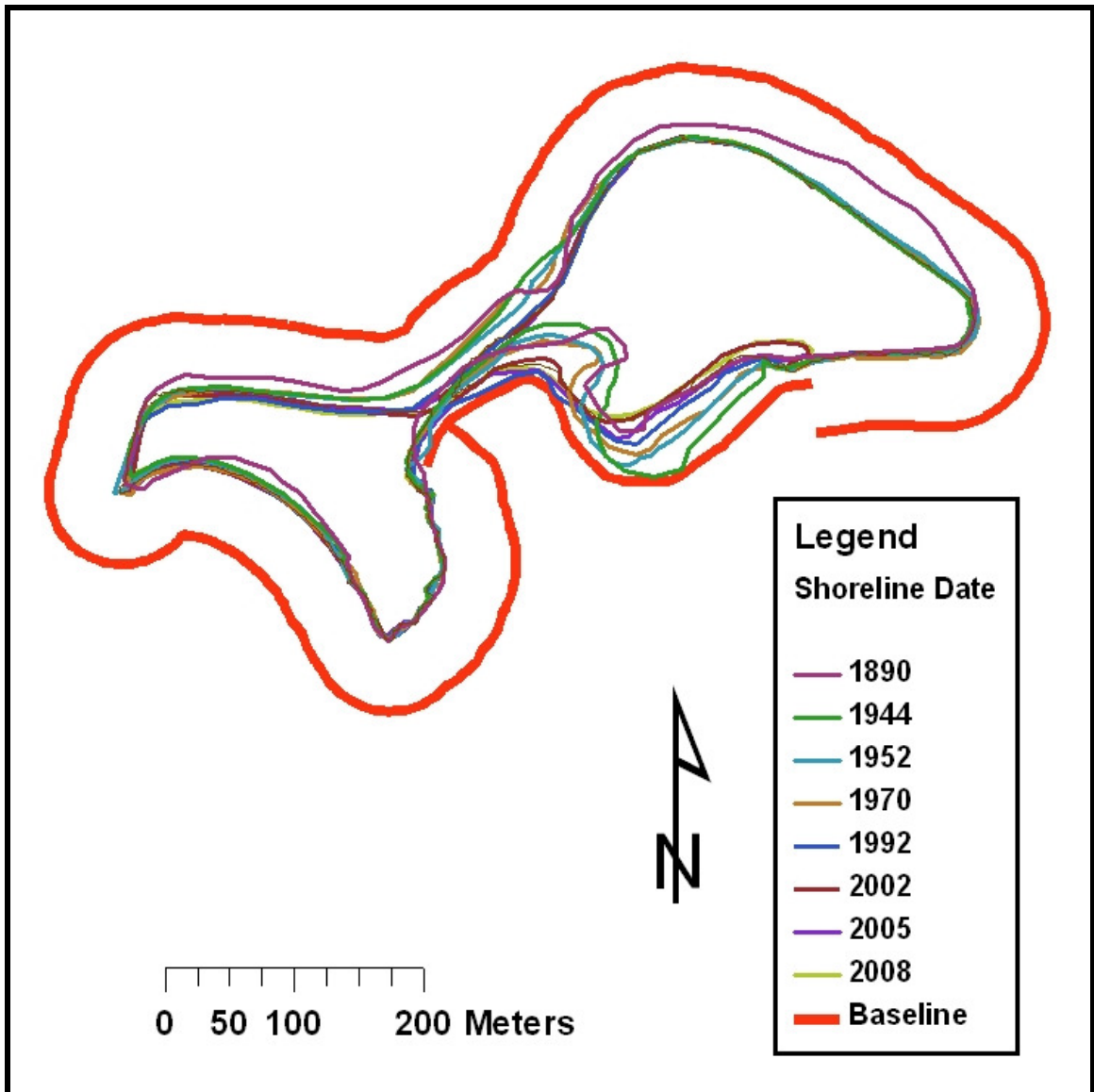


Figure 2.9. Appended shoreline data shown with baseline. Appending or joining the individual shoreline positions into a single file and creating a baseline were necessary steps for analysis within the USGS Digital Shoreline Analysis System (DSAS). The offshore baseline shown in red was created by buffering the 2002 MHW shoreline by 55 meters seaward and then manually editing it to ensure the proper alignment of transects. A likely cartographic error along the north western side of the Island on the USGS historical map can be seen from the far seaward position of its delineated shoreline shown in purple.

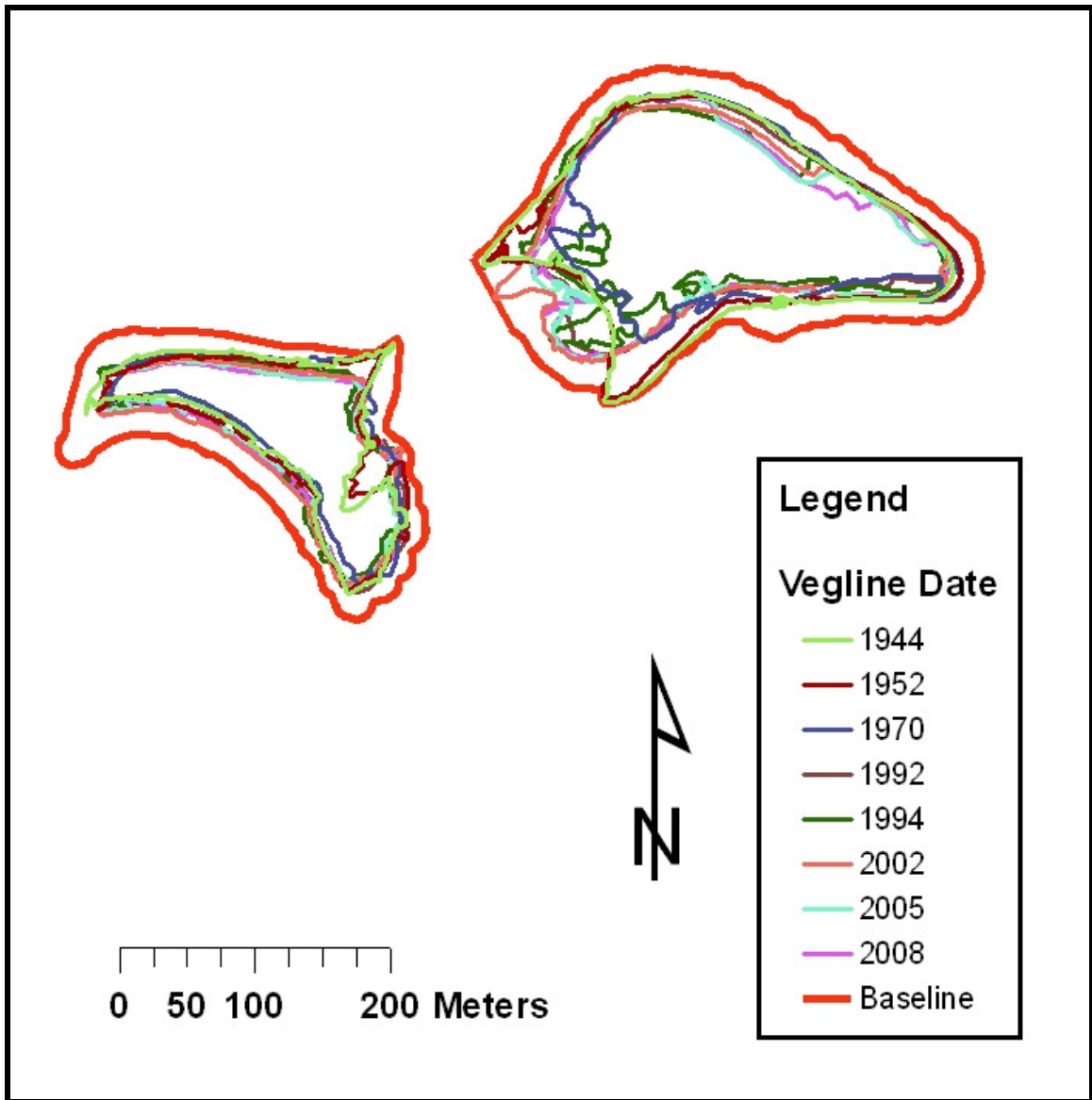


Figure 2.10. Appended vegetation data shown with baseline. Appending or joining the individual vegline positions into a single file and creating a baseline were necessary steps for analysis within the USGS Digital Shoreline Analysis System (DSAS). The offshore baseline shown in red was created by buffering the 2002 MHW shoreline by 20 meters and then manually editing it to encircle the two separate drumlins and ensure the proper alignment of transects.

Transects were 100 m in length and spaced at 10 m apart. Transects were cast using a smoothed baseline, with a smoothing distance of 10 m. The shoreline calculation settings used the closest intersect option with the default data uncertainty setting of +/- 4.4 m with an extended output. There were a total of 234 transects cast in the shoreline analysis and 178 cast in the vegetation analysis. Transects used in the shoreline analysis were referred to as “T_s” and transects used for vegetation analysis as “T_v.” Individual transects were chosen to represent the different areas of the Island based on two criteria. The first criteria was that transects were approximately centered within the geomorphic zone in which they were chosen to represent. The second criteria was that transects crossed the majority of shorelines perpendicularly. In some cases, more than one transect was chosen to represent a particular area as a single transect could not fulfill both criteria.

2.5.3. Digital Shoreline Analysis System Statistics

RISES used the DSAS extension to calculate numerous statistics for each transect based on the differences in measurements between shore and vegetation line positions through time. Statistics were calculated using a 90% confidence interval and include Net Shoreline Movement (NSM), Shoreline Change Envelope (SCE), End Point Rate (EPR), Linear Regression Rate (LRR), Least Median of Squares (LMS), and the R-squared of Linear Regression (R^2). All rates were reported in meters of change per year (m/y) along each transect, with negative values corresponding to areas of erosion.

NSM is the distance between the oldest and youngest shorelines and is useful to assess, in general terms, if a shoreline is eroding or accreting. The SCE is the largest distance

the shoreline position moved during the study period regardless of which was younger or older. The EPR is derived by dividing the NSM by the number of years between the oldest and youngest shorelines. The LRR is determined by fitting the least-squares regression line to the vertices of shorelines and an individual transect. The slope of the regression line provides the LRR (Himmelstoss, 2009). The LMS is a robust regression estimator that minimizes the impact of outlier data and was also employed in this study (Himmelstoss, 2009). The R^2 was used to determine the quality of the statistics gained by the linear regression (LR) calculations.

DSAS automatically generates a table containing the output of the statistical analyses, which can be viewed within ArcMap. The tables were exported to Microsoft Excel for further analysis and visualization. The statistics could also be viewed spatially within ArcMap by joining the statistics table with the transect feature class and choosing which statistic would be displayed (Thieler, et al., 2008).

RISES relied heavily on the LR analysis for computing the change through time of the vegetation and shoreline positions. Douglas and Crowell (2000), report that the LR method of statistical analysis is one of the most effective statistical approaches to shoreline change analysis, as it minimizes potential random errors and short term variability. The LRR analysis also includes all of the available data and is an accepted method for calculating long-term rates of change in shoreline change analysis (Crowell and Leatherman, 1999).

One of the problems in using the LR method is that it is susceptible to outlier effects, which may occur within shoreline change analysis due to the differing spatial and temporal resolution of the numerous data sources employed. The LR method also may underestimate the rate-of-change relative to other methods (Genz et al., 2007). To alleviate some of these

concerns, the LMS method was utilized when R^2 values were less than 0.50, as this lower correlation value may indicate the influence of an outlier. In these cases the LMS provided a more accurate rate-of-change statistic.

2.5.4. Flood Hazard Predictive Mapping

In this study, three flood hazard maps were produced, depicting the areas that may be submerged in response to a 1-m, 2-m, and 3-m rise in SLR or storm surge elevation. These maps were produced within ArcMap using the Spatial Analyst tools. Using the Reclassify tool, the Natural Breaks method with three classes was entered in the Classification window. The three classes were based on the NAVD relative MHW elevation value of 1.319 m. For example, on the map showing the possible shoreline response to a 1-m rise in sea-level, three classes were set. Those below 1.319 m (MHW), representing the presently submerged areas, those between 1.319 m and 2.319 m representing the newly inundated areas after the 1-m rise in sea-level, and those above 2.319 m representing the unaffected terrestrial lands of the island (Figure 2.11). The same methods were employed to create the 2-m and 3-m flood hazard maps with classes based on the appropriate elevation values.

These three maps were relatively easy to produce and provided an effective tool to depict areas that may be vulnerable to flooding in response to static SLR or storm surges. The maps are based on a static sea-level model which does not take into account erosion or accretion, thus limiting their ability to depict shoreline response. They nonetheless offer an effective tool for visually identifying coastal hazard zones that are potentially vulnerable to coastal flooding.

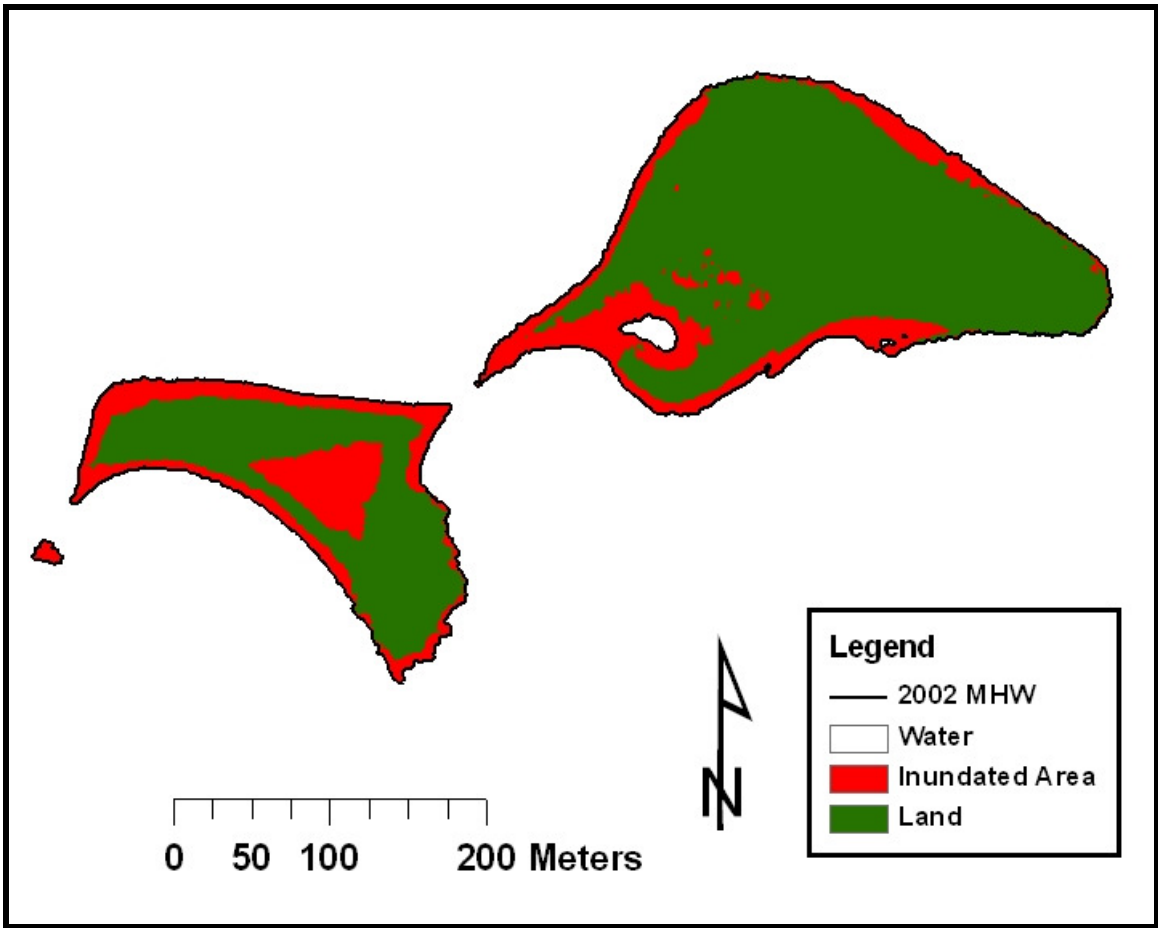


Figure 2.11. 1-Meter Flood Hazard Map. Inundated areas are shown in red and the MHW shoreline is represented by the black line.

CHAPTER 3

RESULTS

3.1 DSAS Analysis

The USGS DSAS extension created for use in ArcMap has enhanced the ability of coastal scientists to obtain robust statistically-based results describing the changing positions of shorelines. The results obtained from the employment of the DSAS extension provided accurate statistically based information which will enhance the ability of local coastal planning and policy makers to make sound coastal zone management decisions based on accepted scientific protocols. All DSAS results used in this study were determined at a 90% confidence interval with a +/- 1 m spatial error.

LR rates for each of the 232 shoreline transects were used to visualize the results in ArcMap (Figure 3.1). This allowed for the effective assessment of Island areas that had experienced rapid coastal change indicated by higher LR rates with negative values corresponding to erosion and positive values to accretion. Through this display, the “hotspot” areas of rapid erosion or accretion could quickly be identified.

To simplify results, Rainsford Island was divided into eight geomorphic zones. These zones are based on the general characteristics of each area. The areas include: the North

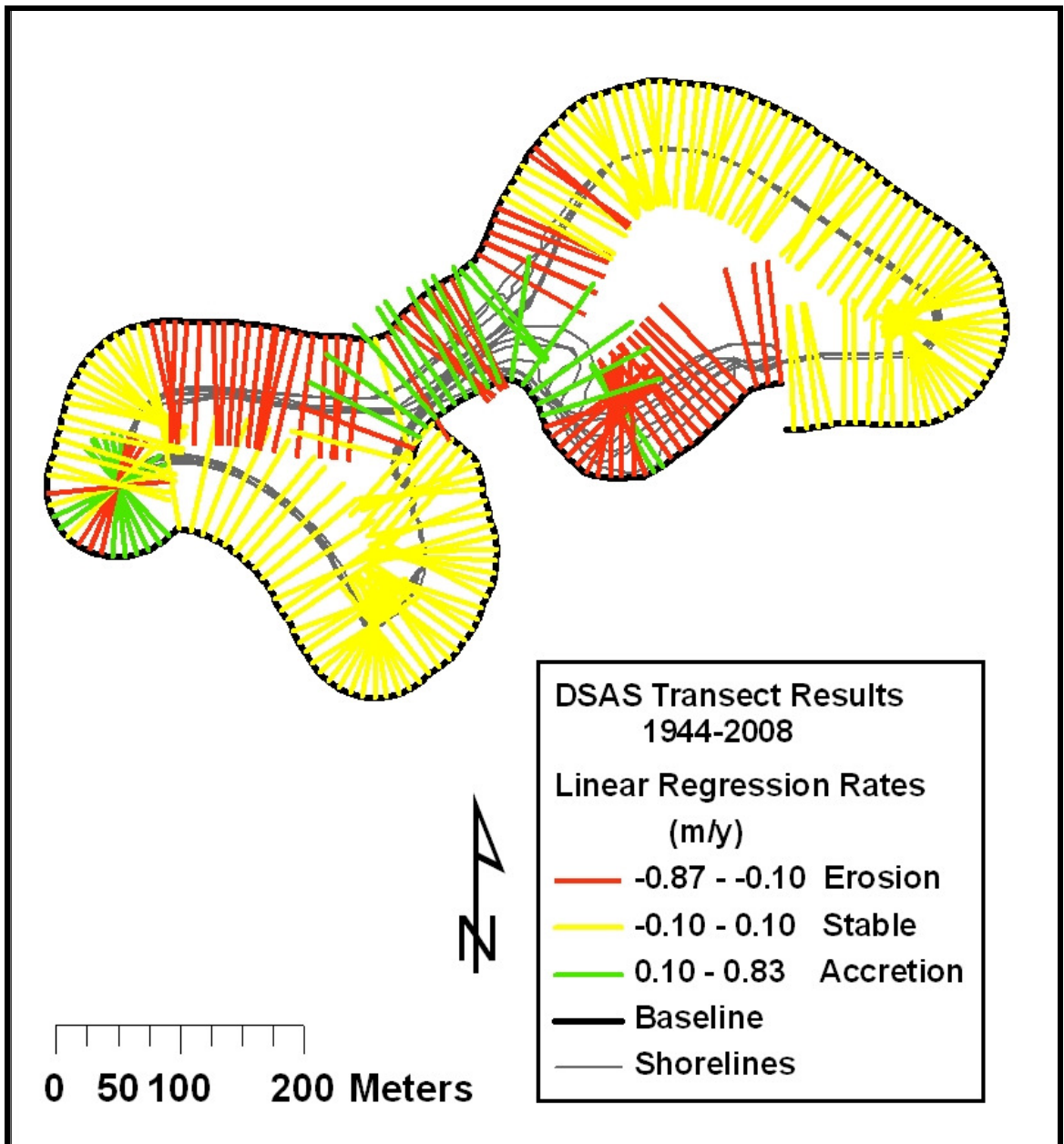


Figure 3.1. Linear regression rates for shoreline analysis.

Mixed Sediment Beach (NMSB); the Southeast Sand Beach (SESB); the Northwest Boulder Beach (NWBB); the Seawall (SW); the Southeast Boulder Beach (SEBB); the West Cove (WC); the Southwest Boulder Beach (SWBB); and the Bedrock (BR) (Figure 3.2). One or two transects were chosen to represent each of these areas based on their centered position within the zone and the angle to which they crossed the shorelines. Statistics were obtained from each of the selected shoreline (T_s) and vegetation (T_v) transects (Appendix D). Although analysis was conducted in the BR zone, the results indicated this area remained stable throughout the study period and they were, therefore, not included in the results.

3.1.1 North Mixed Sediment Beach (NMSB)

The shoreline results for the NMSB were obtained from the analysis of T_s 74 and T_s 232 (Figure 3.3). The 1890 data set for T_s 74 provided a LRR of -0.18 m/y, with an R^2 value of 0.91 (Figure 3.4). The shoreline retreated landward 22 m during this period. The analysis of the 1944 dataset showed similar results, with a LRR of -0.19 m/y, and an R^2 value of 0.82 (Figure 3.5). During this period, the shoreline retreated landward 12 m. Between 1944 and 1970 there was no change in shoreline position. The largest change came between 1970 and 1990 when the shoreline retreated landward 10 m.

The analysis of T_s 232 with the 1890 dataset provided a LRR of -0.13 m/y, with an R^2 value of 0.90 (Figure 3.6). The shoreline retreated landward 18 m in this area. The analysis of the 1944 dataset along T_s 232 provided a LRR of only -0.1 m/y with an R^2 value of 0.69 (Figure 3.7). The shoreline retreated landward 8 m, which is less than that which was found

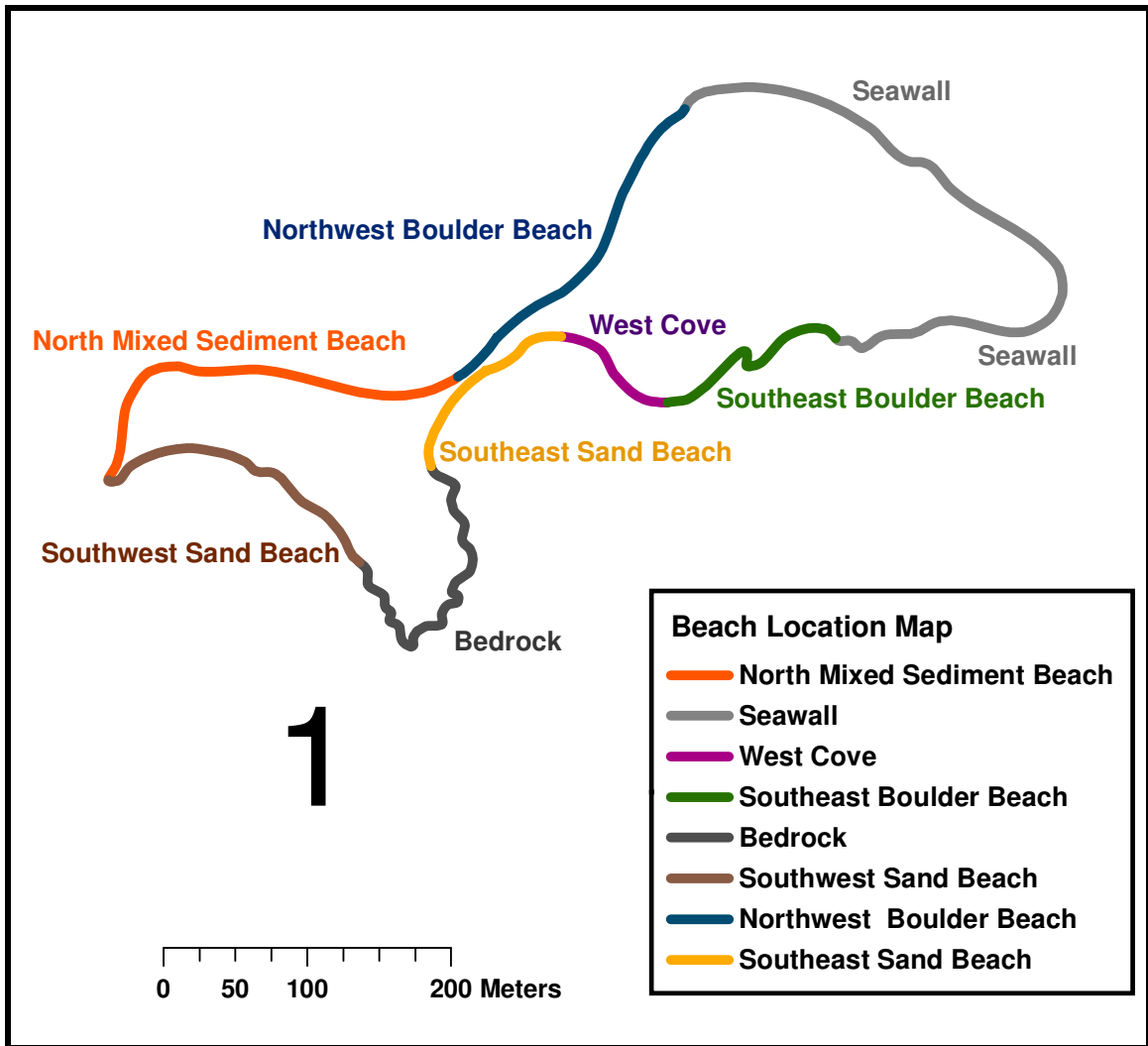


Figure 3.2. Beach location map showing eight areas of Rainsford Island. The SW fringes the north, northeast, east, and southeast bluffs of the north drumlin. The NWBB encompasses the north side of the spit connecting the two drumlins, as well as the boulder beach along the northwest shore of the north drumlin. The NMSB covers the northern beach of the south drumlin, which is a mix of sand, gravel, cobbles, and some small boulders. The SWSB, on the south drumlin, is a steep sand beach anchored by two bedrock outcrops. The BR area was located on the southern tip of the south drumlin, where large bedrock outcrops drop off to the waterline.

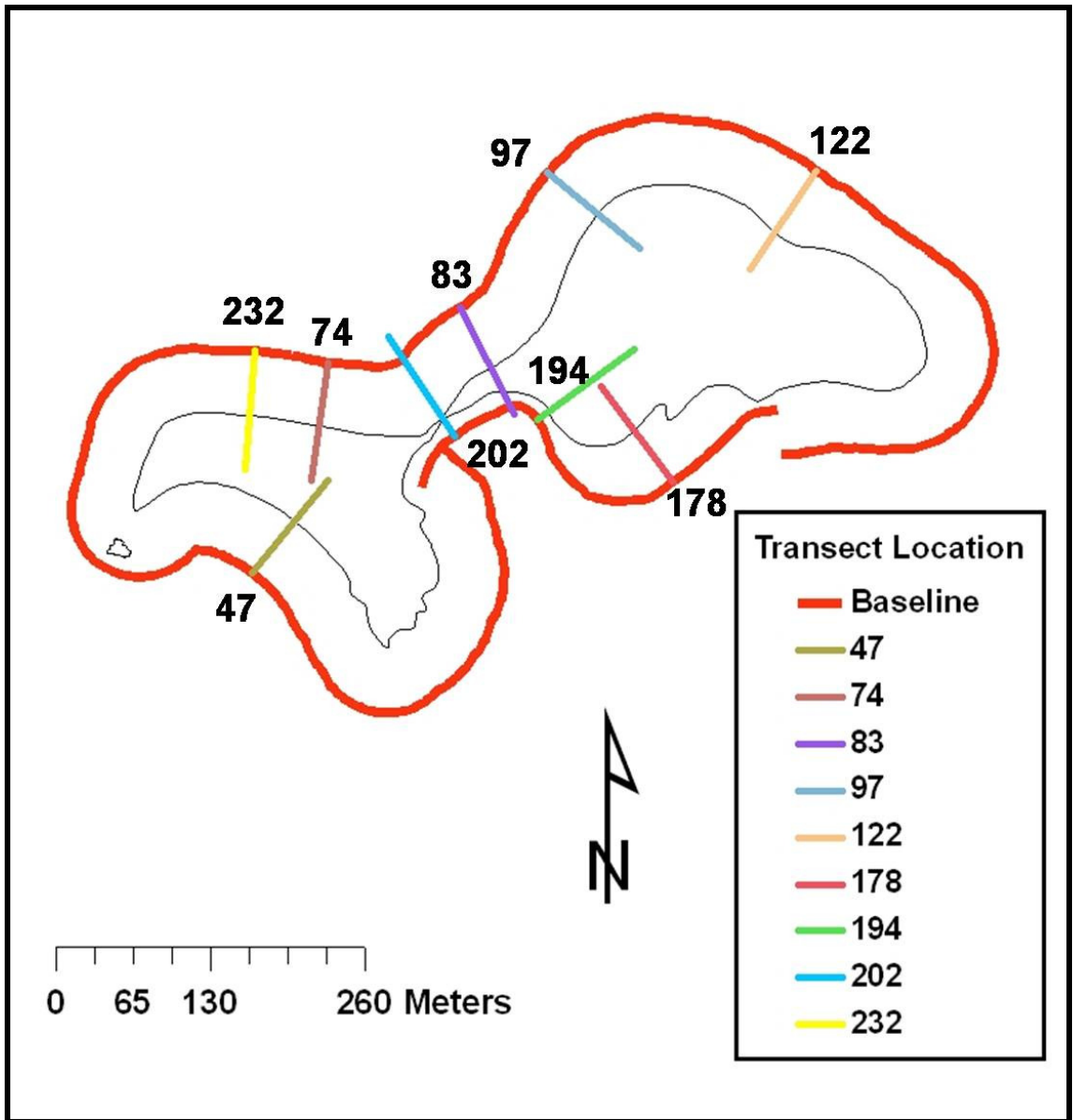


Figure 3.3. Shoreline transect (T_s) location map. Transects were chosen using two criteria, the first being their centered position within the geomorphic zone and, secondly, that they cross the shorelines at a near perpendicular angle.

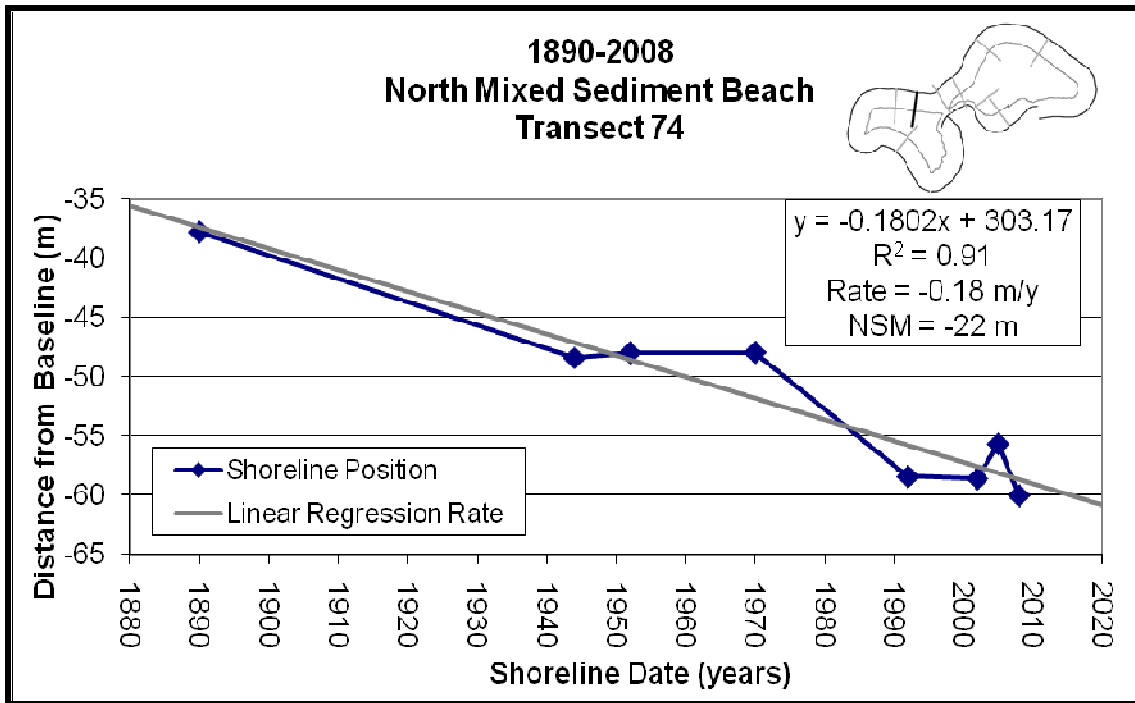


Figure 3.4. Linear regression analysis of T_s 74 along the NMSB for the 1890 dataset.

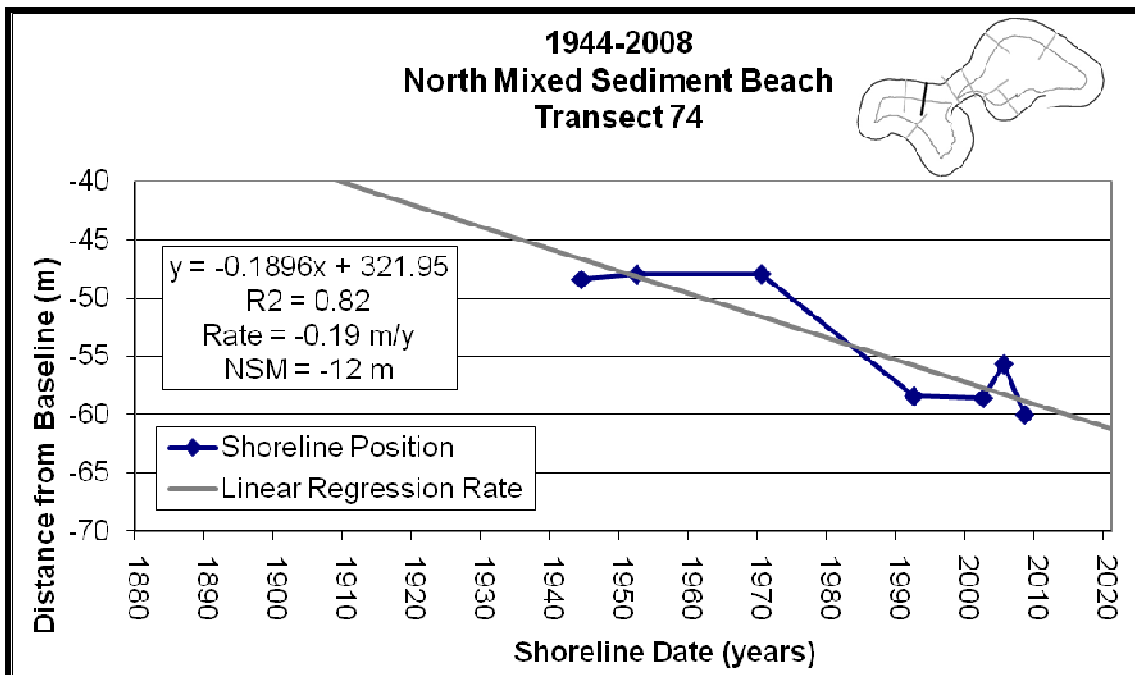


Figure 3.5. Linear regression analysis of T_s 74 along the NMSB for the 1944 dataset.

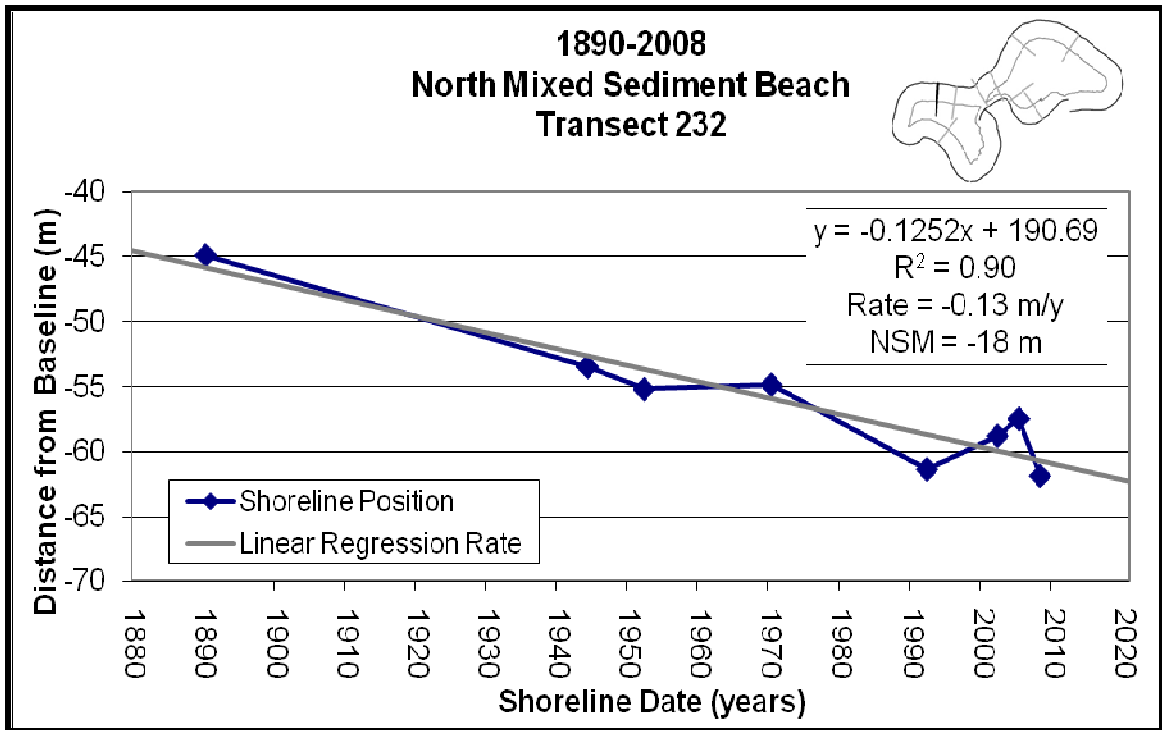


Figure 3.6. Linear regression analysis of T_s 232 along the NMSB for the 1890 dataset.

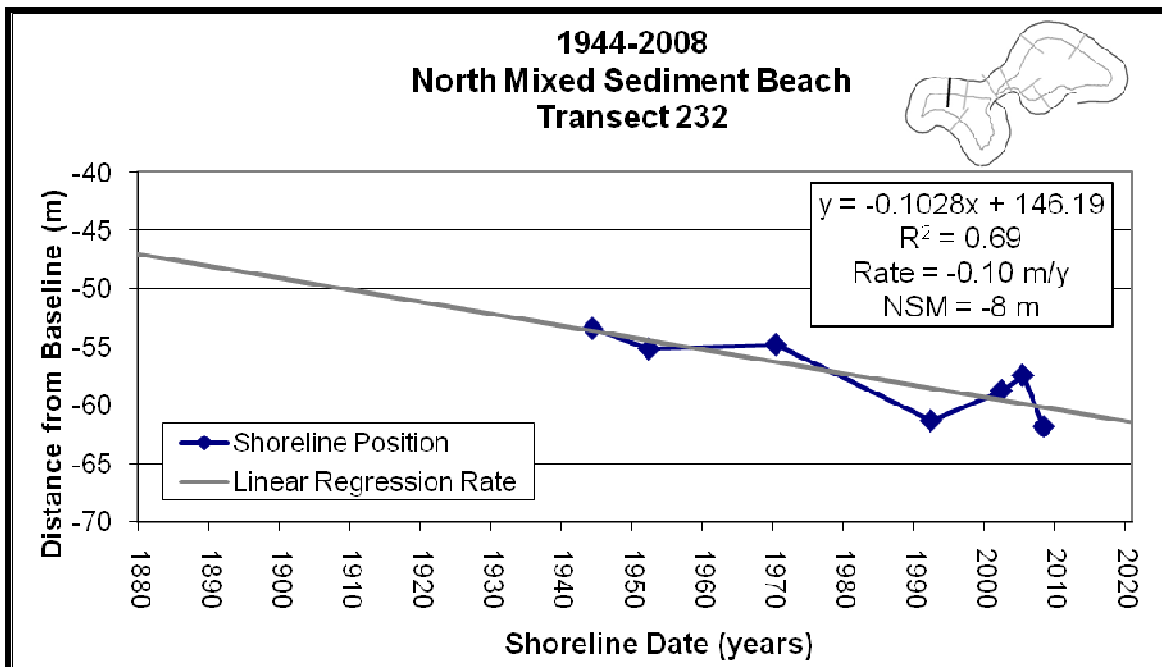


Figure 3.7. Linear regression analysis of T_s 232 along the NMSB for the 1944 dataset.

for T_s 74. The shoreline results from the analysis of T_s 232 and T_s 74 are consistent, showing a slow rate of erosion. The vegetation analysis of T_v 176 also showed a negative linear trend of loss (Figure 3.8). The LRR was -0.15 m/y, with an R² value of 0.65 (Figure 3.9). The vegline and shoreline showed identical landward retreat of 10 m between 1970-1992.

There is a strong correlation between the shoreline and vegetation results from the NMSB obtained from the analysis of the 1944 dataset. The results show that both the shoreline and the vegetation have retreated landward. There was a strong linear relationship found in the regression analysis of both the shoreline and vegetation datasets. If the processes that led to these changes remain the same, the results could provide accurate predictions of future trends that may occur in this area. Based on the trend line, the NMSB will continue to retreat landward during the next decade. In addition, the present rate of shoreline erosion along T_s 74 for the 1944 dataset of 0.19 m/y, will likely increase due to a predicted increase in the rate of SLR and the reoccurrence of significant storm surges in the coming decades. This area is an erosional hotspot and is one of the more vulnerable beaches on Rainsford Island. It is, therefore, considered one of the Island's Coastal Hazard Zones.

3.1.2 Southeast Sand Beach (SESB)

The analysis of T_s 202 along the SESB shows a steady seaward progradation of the shoreline (Figure 3.3). The 1890 dataset provided a LRR of 0.28 m/y, with an R² of 0.89 (Figure 3.10). During this period, the shoreline prograded seaward by 32 m.

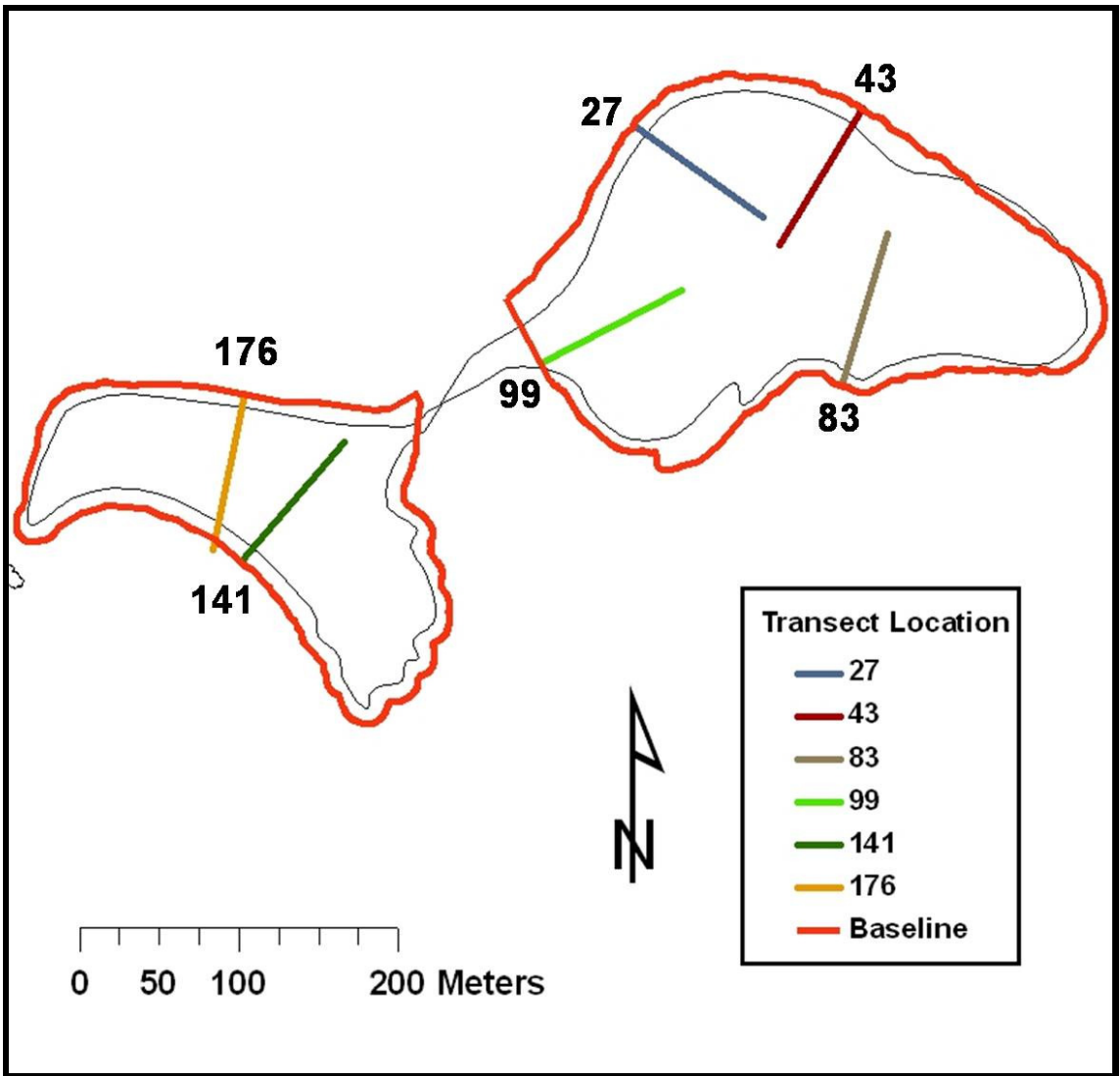


Figure 3.8. Vegetation transect (T_v) location map.

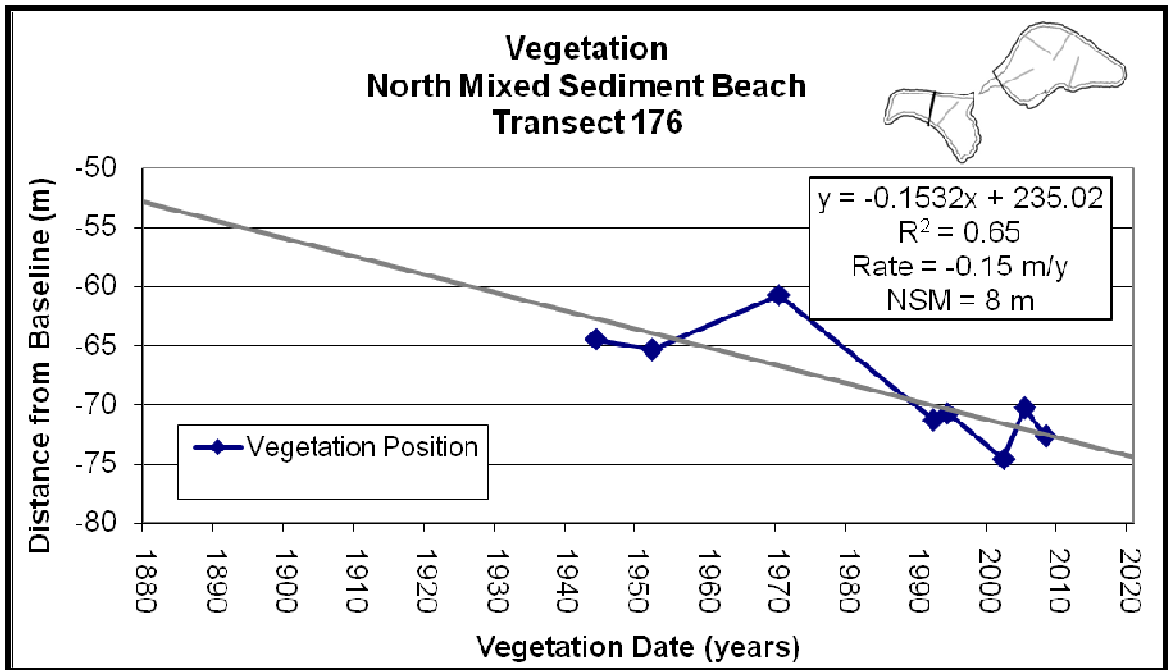


Figure 3.9. Linear regression analysis of T_v 176 along the NMSB for the 1944 dataset.

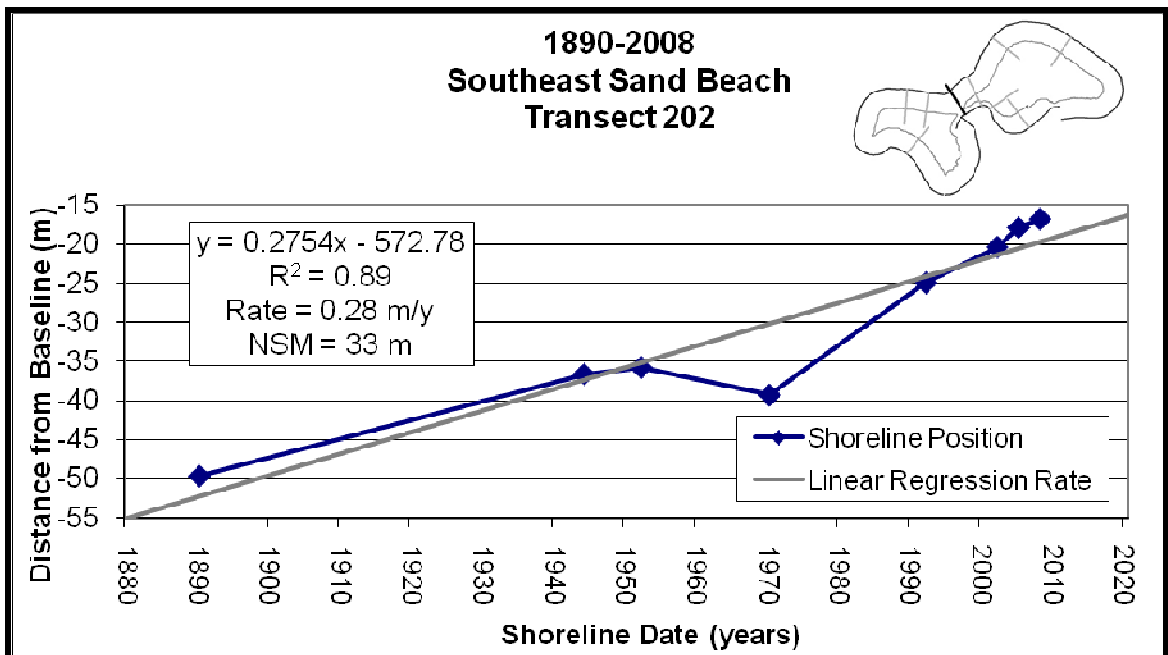


Figure 3.10. Linear regression analysis of T_s 202 along the SESB for the 1890 dataset.

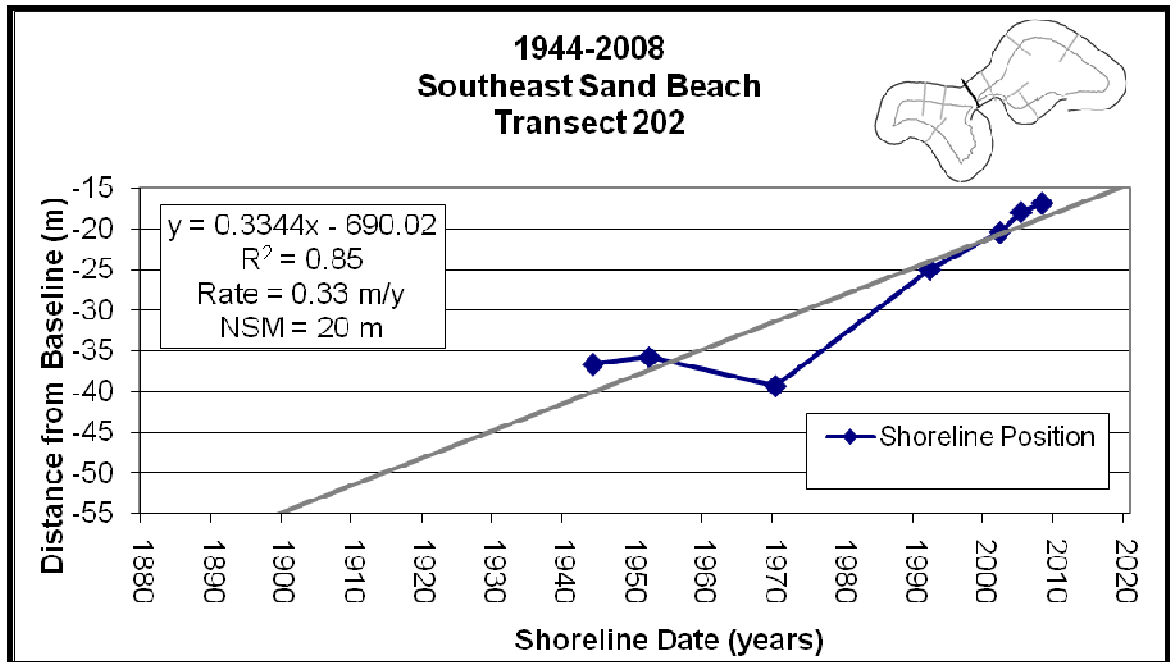


Figure 3.11. Linear regression analysis of T_s 202 along the SESB for the 1944 dataset.

The analysis of the 1944 dataset provides similar results with a LRR of 0.33 m/y and a seaward progradation of 20 m (Figure 3.11). The lower NSM in the 1944 dataset is a result of the 12 m of shoreline progradation between 1890 and 1944. The rate-of-change statistics remained consistent through both datasets indicating a positive linear relationship between the two. The high correlation between the two datasets provides strong evidence that the SESB will likely continue its positive trend of accretion during the next decade and is considered an accretion hotspot on Rainsford Island. As there is no vegetation on the low-lying spit, the vegetation analysis was not carried out.

3.1.3 Northwest Boulder Beach (NWBB)

Analysis of T_s 83 provided the results for the NWBB (Figure 3.3). This beach contains part of the low-lying spit connecting the two drumlins. The 1890 dataset provided a LRR of -0.19 m/y, with an R^2 value of 0.63 (Figure 3.12). Using the LMS method of regression analysis, which limits the weight of outlier data, gave a considerably higher rate-of-change of -0.33 m/y. The NSM for this transect indicated 17 m of erosion, while the SCE was over 26 m. Prior to 1944, the data indicates that the area remained relatively stable. The higher LMS rate and SCE are a result of the dynamic nature of the shoreline in this area after 1944, oscillating back and forth between erosion and accretion.

The results obtained from the analysis of the 1944 dataset show a considerably faster rate of erosion in this area. The biggest losses came between 1970 and 1990 when there was nearly 20 m of shoreline erosion. There was a LRR of -0.34 m/y with an R^2 value of 0.80 (Figure 3.13). Between 1992 and 2002 there was 10 m of accretion. For the remainder of the study period there were small amounts of erosion (2002 and 2005) and accretion (2005 and 2008).

The results from the analysis of T_v 27 provided the results for the vegetation analysis (Figure 3.8). The vegetation data supports the negative trend of loss found in the shoreline analysis with a LRR of -0.13 m/y and a LMS rate of -0.16 m/y (Figure 3.14). Between 1944 and 2008 the vegetation retreated landward by 12 m, a similar distance to the shoreline erosion. The combined results from the shoreline and vegetation analysis, which show a long running negative trend of erosion and retreat, indicate that this areas is an erosional hotspot on Rainsford Island.

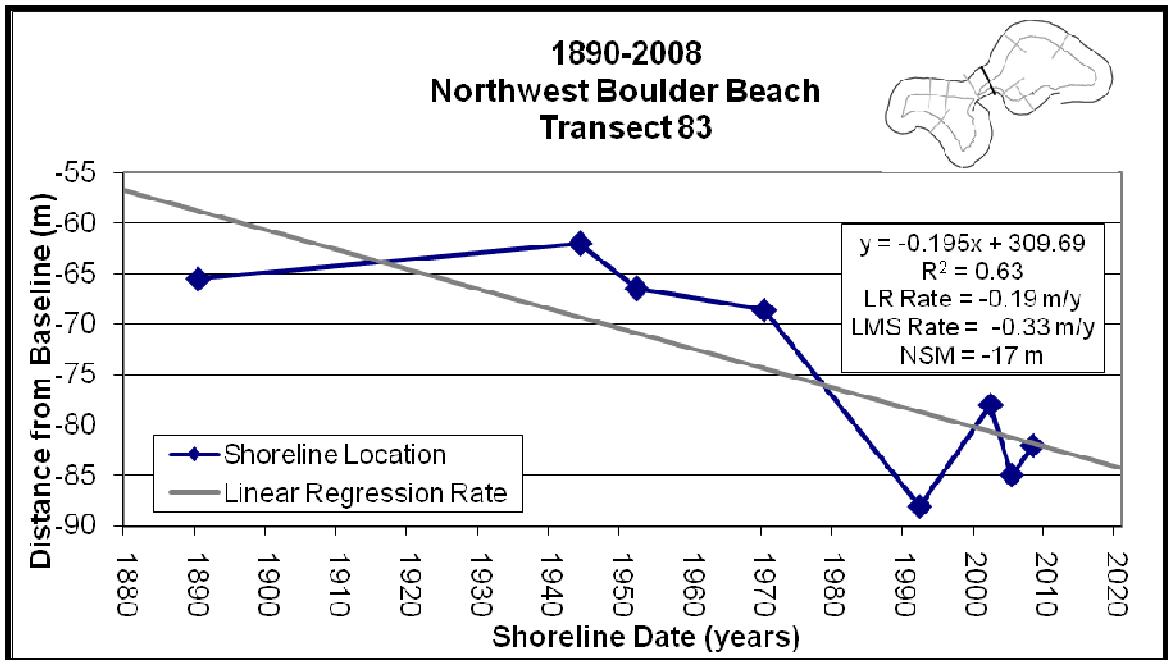


Figure 3.12. Linear regression analysis of T_s 83 along the NWBB for the 1890 dataset.

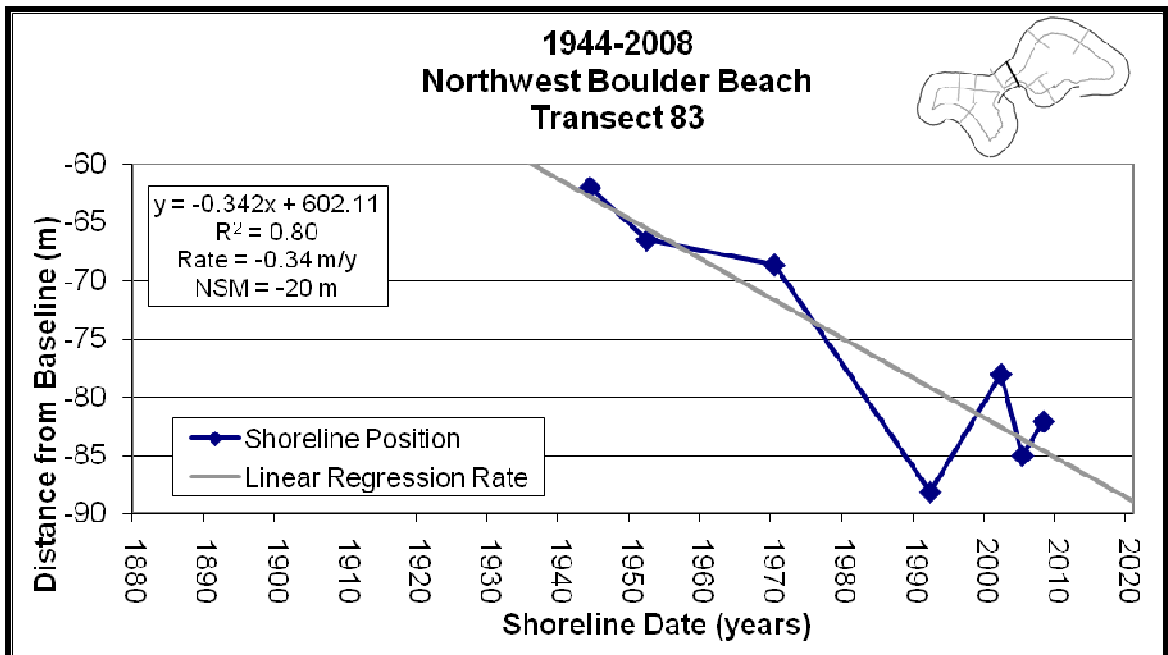


Figure 3.13. Linear regression analysis of T_s 83 along the NWBB for the 1944 dataset.

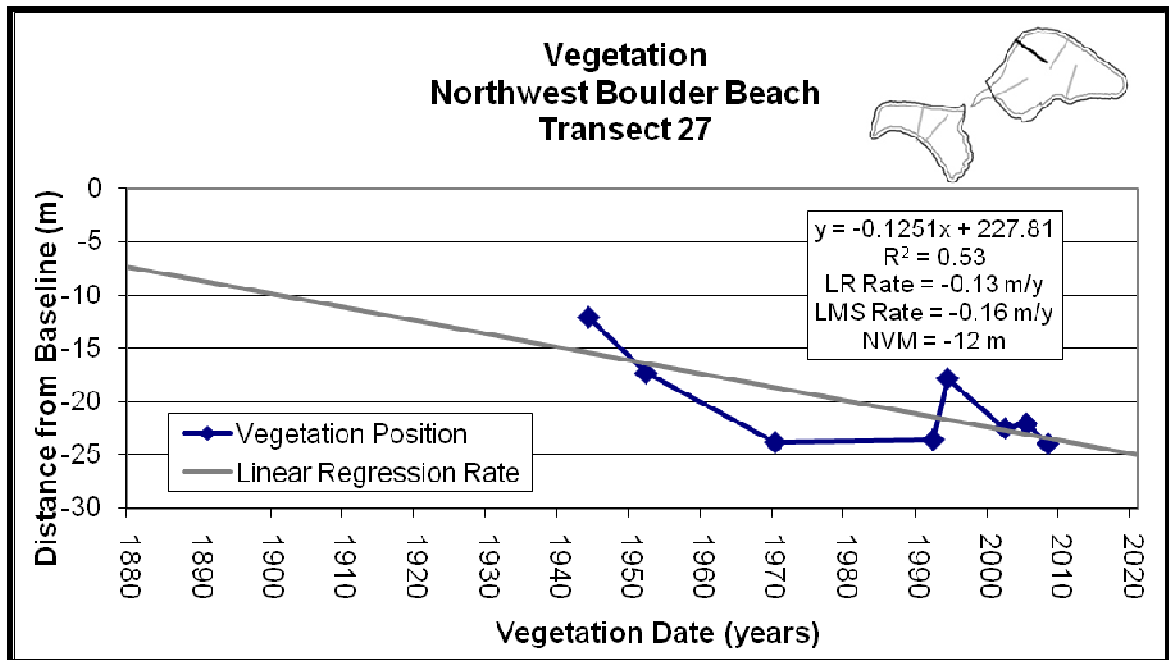


Figure 3.14. Linear regression analysis of T_v 27 along the NWBB for the 1944 dataset.

3.1.4 Seawall (SW)

The high bluffs of the north drumlin have been buffered from wave attack and erosion by the large granite seawall constructed in 1836. Despite the fact that it has been breached and collapsed in some areas, it still is largely intact and has likely limited the rate of erosion in the areas that remain armored. The combined shoreline and vegetation results from the 1944 datasets indicate that this area has been relatively stable and has experienced a lower rate of erosion than the other areas of Rainsford Island (excluding the bedrock outcrops).

T_s 97 and T_s 122 were employed to obtain the results for the shoreline analysis (Figure 3.3). The analysis of these transects for the 1890 dataset show the erosion of 10.8 m and 25 m

respectively, while the analysis of the 1944 dataset resulted in 4.55 m and 0.3 m of erosion respectively. This discrepancy in the datasets is primarily due to the extreme seaward position of the delineated shoreline on the historical map, creating outlier data points in the regression analysis. As the large granite blocks that make up the seawall are still physically aligned along this stretch of Island, and there are no signs of notable erosional events, the outlier data is likely due to a cartographic error rather than any significant erosional trend which may have occurred between 1890 and 1944. Due to this uncertainty, the 1944 dataset will be considered more valid for this area and the 1890 data set will not be discussed further.

The analysis of T_s 97 with the 1944 dataset provided a LRR of -0.08 m/y, with an R^2 value of 0.91 (Figure 3.15). The EPR supports the regression analysis providing a rate of -0.07 m/y. The analysis of T_s 122 with the 1944 dataset provided a LR rate of -0.3 m/y. (Figure 3.16).

The analysis of the vegetation data along the SW was carried out using T_v 43 (Figure 3.8). The results show a more significant rate of loss compared with the erosion of the shoreline. The LRR was -0.27 m/y with the vegetation retrograding landward by 16 m. This was more than three times that of the distance of the shoreline (Figure 3.17). The observed change in vegetation position is likely the result of bluff top erosion and mass wasting episodes. These processes are closely related to the geologic framework of the bluff and amount of precipitation, while the shoreline position is controlled by the buffering capacity of the seawall.

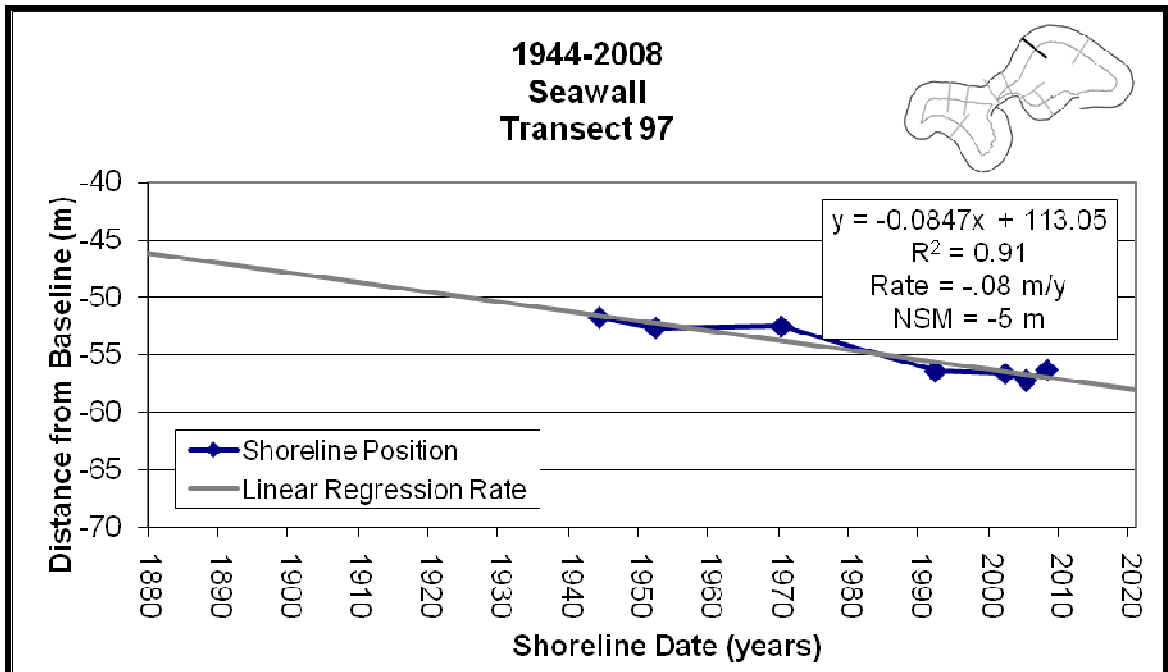


Figure 3.15. Linear regression analysis of T_s 97 along the SW for the 1944 dataset.

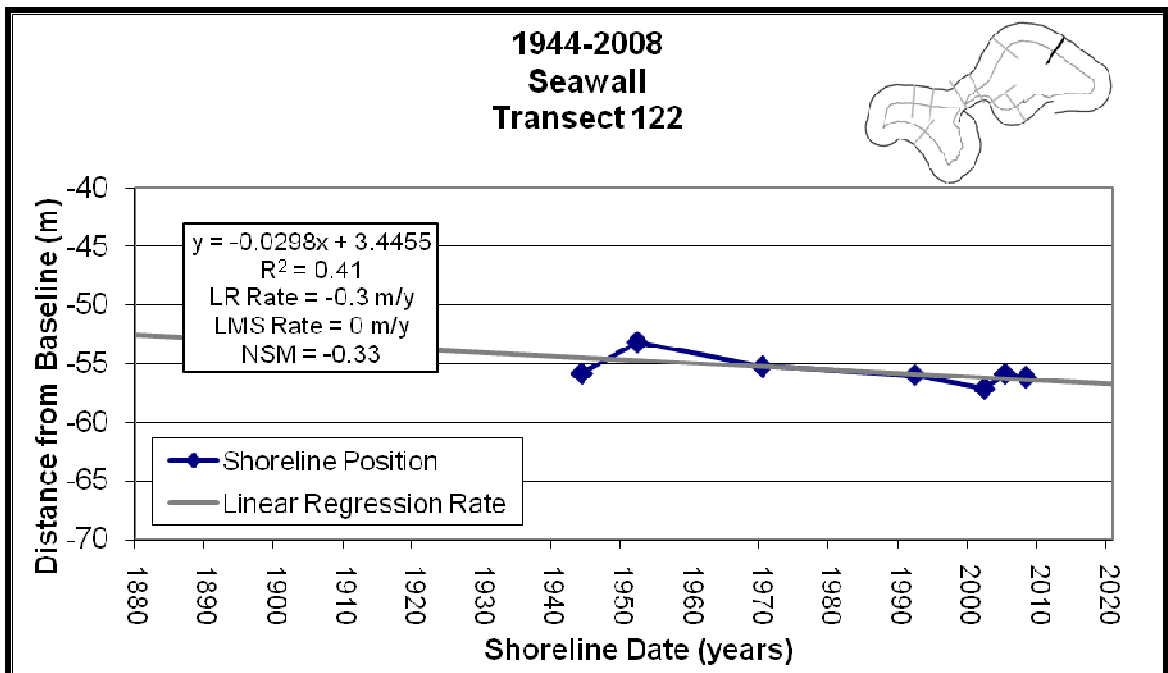


Figure 3.16. Linear regression analysis of T_s 122 along the SW for the 1944 dataset.

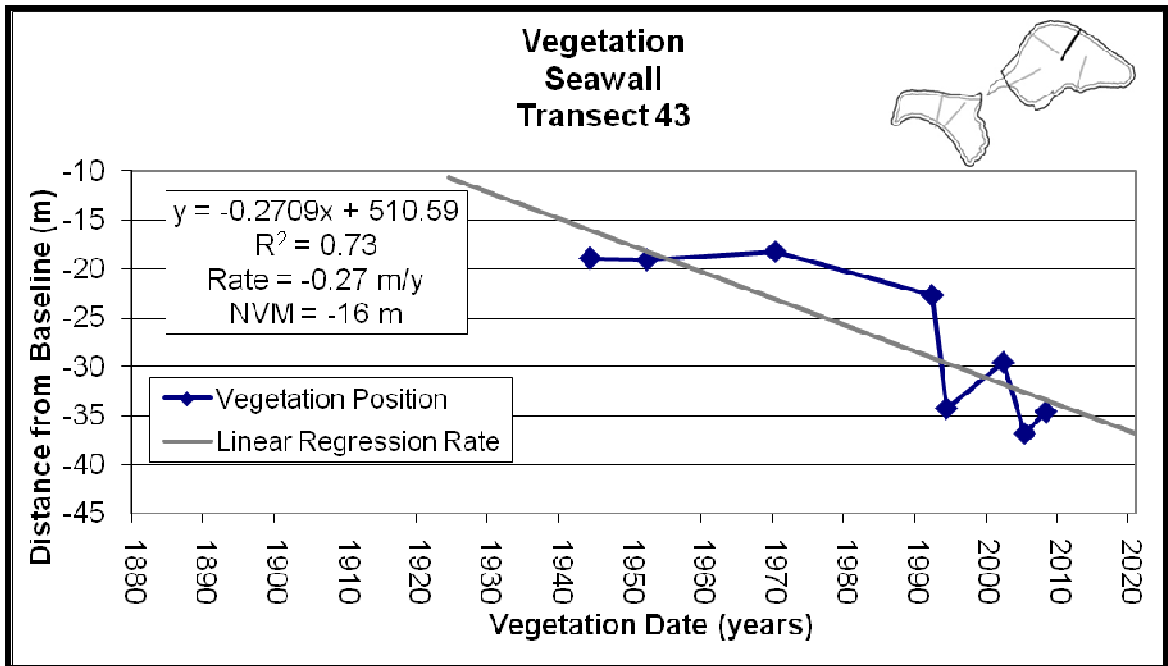


Figure 3.17. Linear regression analysis of T_v 43 along the SW for the 1944 dataset.

3.1.5 Southeast Boulder Beach (SEBB)

T_s 178 was used for the shoreline analysis of the SEBB (Figure 3.2). The analysis of the 1890 dataset provided a LRR of 0.20 m/y, with an R^2 value of 0.10 (Figure 3.18). The low R^2 value is primarily due to an outlier data point from the 1890 dataset. The EPR for this area was much higher at 0.36 m/y, with 43 m of shoreline progradation. Due to the low R^2 value the more robust LMS method was also considered. The LMS method limited the effect of the outlier data and provided a rate-of-change of -0.65 m/y, a rate supported by the analysis of the 1944 dataset results. Because the historical map appears relatively accurate along this area of the Island when compared with the HWL and MHW shorelines, this data point was not eliminated from the analysis.

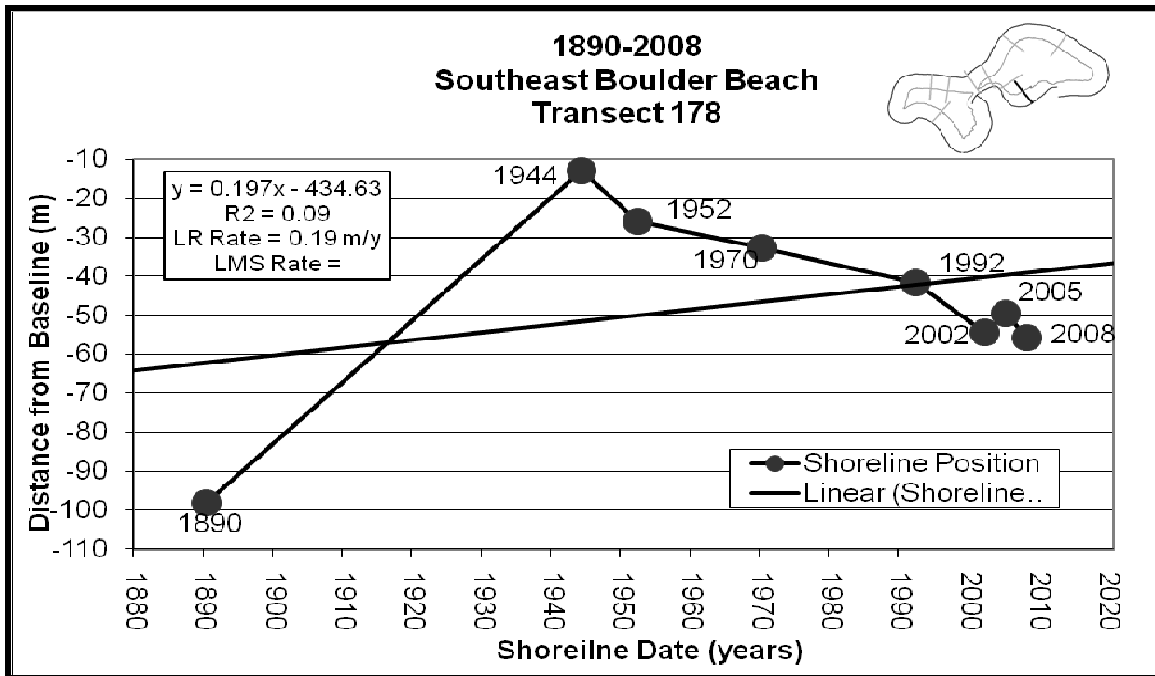


Figure 3.18. Linear regression analysis of T_s 178 along the SEBB for the 1890 dataset.

The results show that between 1890 and 1944, the area along T_s 178 accreted and dramatically prograded 86 m seaward. Historical records show that the “Portland Gale” of 1898, destroyed the large stone and timber wharf extending southward from the SEBB (Claesson and Carella, 2002). The partial removal of such a large coastal structure may have significantly altered sediment transport in this area, accounting for the rapid accretion. The analysis of the 1944 dataset provides a LRR of -0.59 m/y, with a R^2 value of 0.96 (Figure 3.19). After 1944, the shoreline reversed its trend of accretion and eroded 43 m.

Vegetation analysis of T_v 83 along the SEBB shows a loss of vegetation at a slower rate than that of the shoreline (Figure 3.8). The LRR between 1944 and 2008 was -0.23 m/y, with an R^2 value of 0.88 (Figure 3.20). During this time period the vegetation retreated landward 15 m.

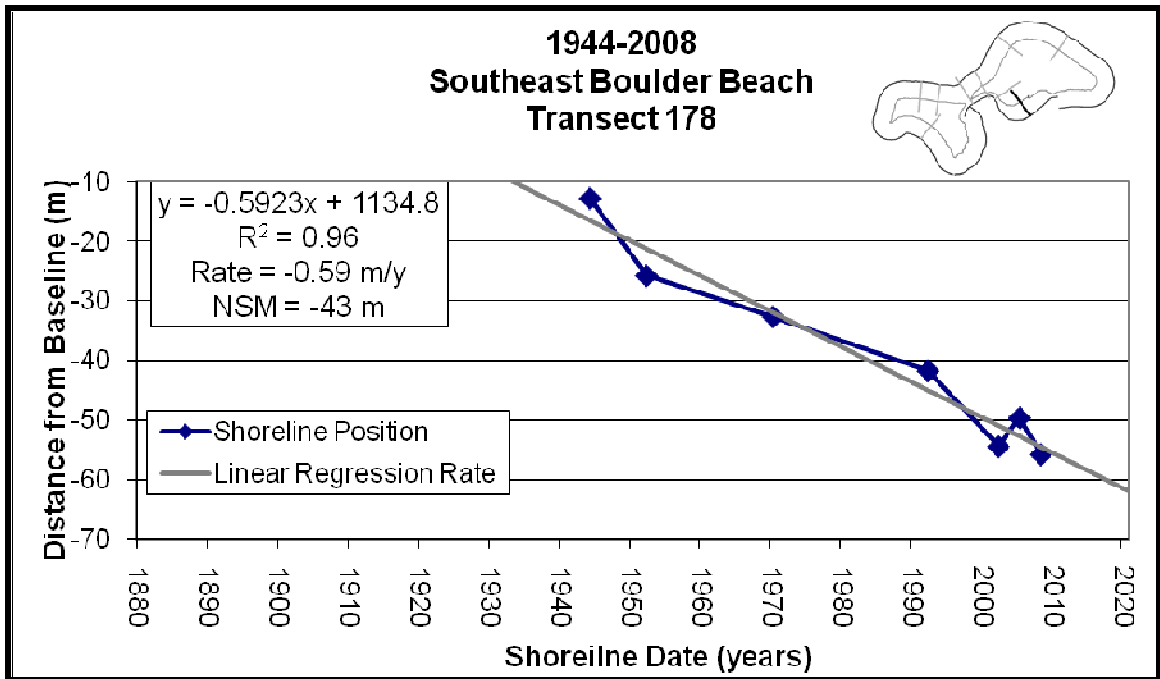


Figure 3.19. Linear regression analysis of T_s 178 along the SEBB for the 1944 dataset.

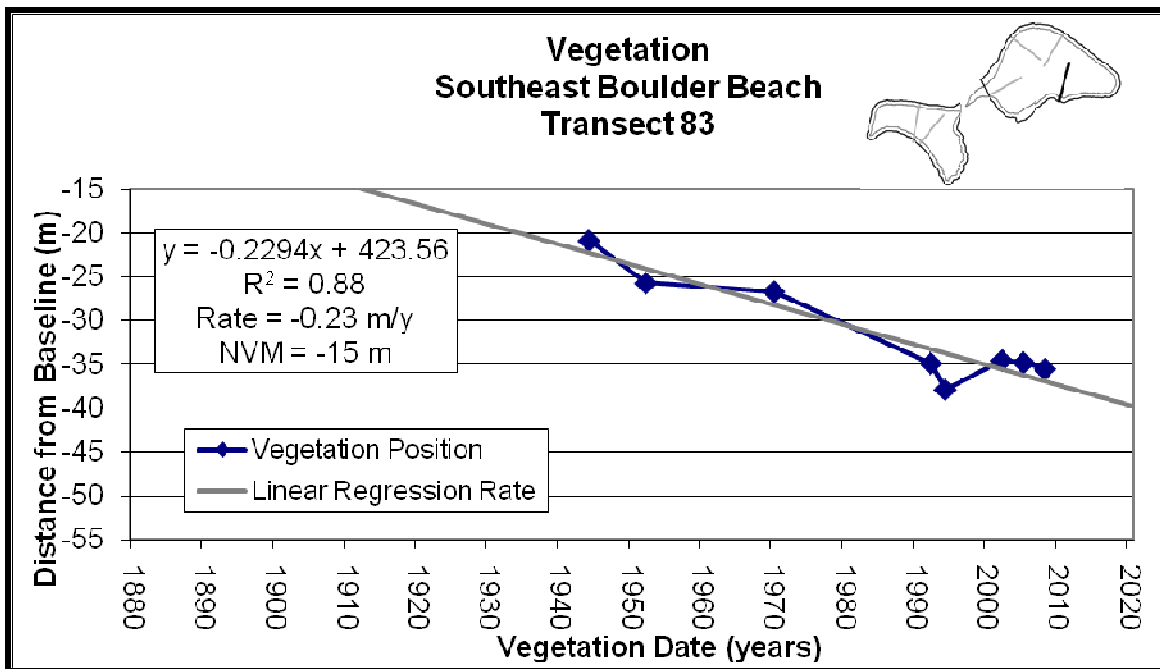


Figure 3.20. Linear regression analysis of T_v 83 along the SEBB for the 1944 dataset.

3.1.6 West Cove (WC)

The analysis of T_s 194 within the WC provided results that show the area has significantly accreted during the study period indicating that the WC is an accretion hotspot on Rainsford Island (Figure 3.3). The results obtained from the analysis of the 1890 dataset show that the cove has experienced accretion with 60 m of shoreline progradation. The LRR was 0.59 m/y with an R^2 value of 0.86 (Figure 3.21). The EPR gave a slightly lower rate of 0.51 m/y, reflecting the smaller amount of accretion that took place prior to 1944. A greater LRR of 0.83 m/y, with an R^2 value of 0.90, was seen in the analysis of the 1944 dataset (Figure 3.22). This steeper regression slope was primarily due to a rapid increase in the rate of accretion between 1970 and 1992. During this period, the shoreline rapidly prograded seaward 42 m, a distance which makes up the majority of the 50 m of NSM.

The vegetation analysis along T_v 99 shows that the vegetation oscillated throughout the study period with a slight negative trend (Figure 3.8). In contrast to the shoreline data which showed accretion, vegetation was being lost at the LRR of -0.41 m/y (Figure 3.23). The EPR was slightly lower at -0.29 m/y. Within the cove the NVM was -19 m, indicating a landward retreat between 1944 and 2008. However, as the SCE was 34 m, the area both advanced and retreated during the period. The greatest change occurred between 1994 and 2002 when the vegetation retreated landward 22 m. The contrasting results between the vegetation and shoreline data are attributed to the fact that coastal geomorphic change cannot always be correlated to changes in vegetation. Within the WC, the shoreline has rapidly prograded seaward while at the same time the vegetation has receded landward or was buried.

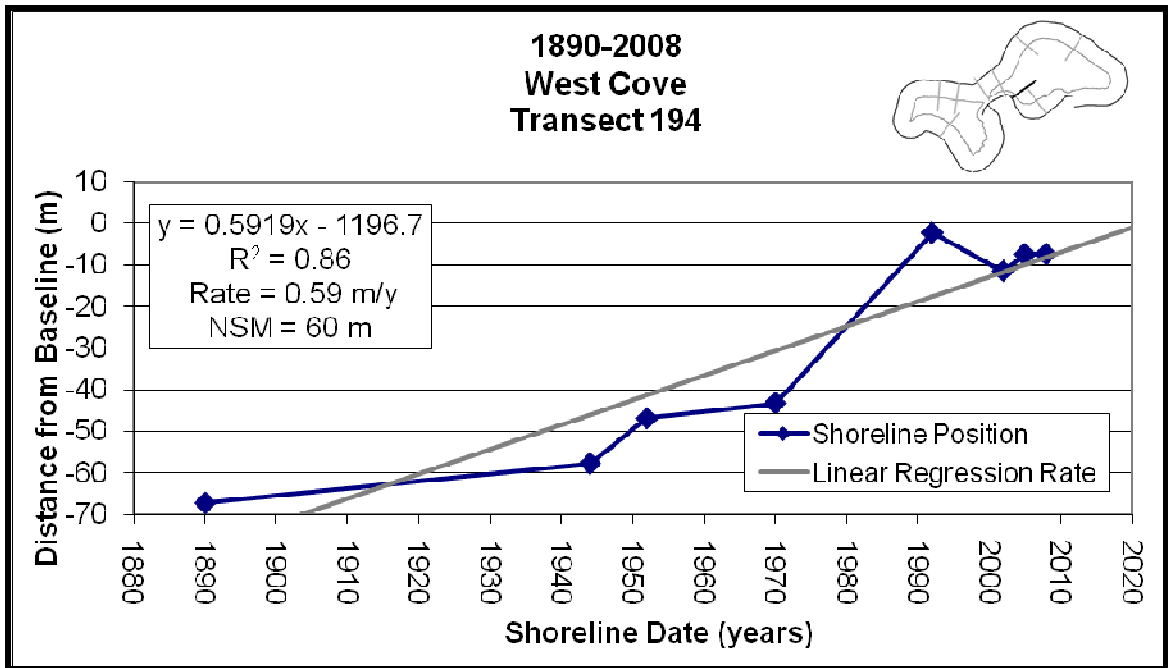


Figure 3.21. Linear regression analysis of T_s 194 along the WC for the 1890 dataset.

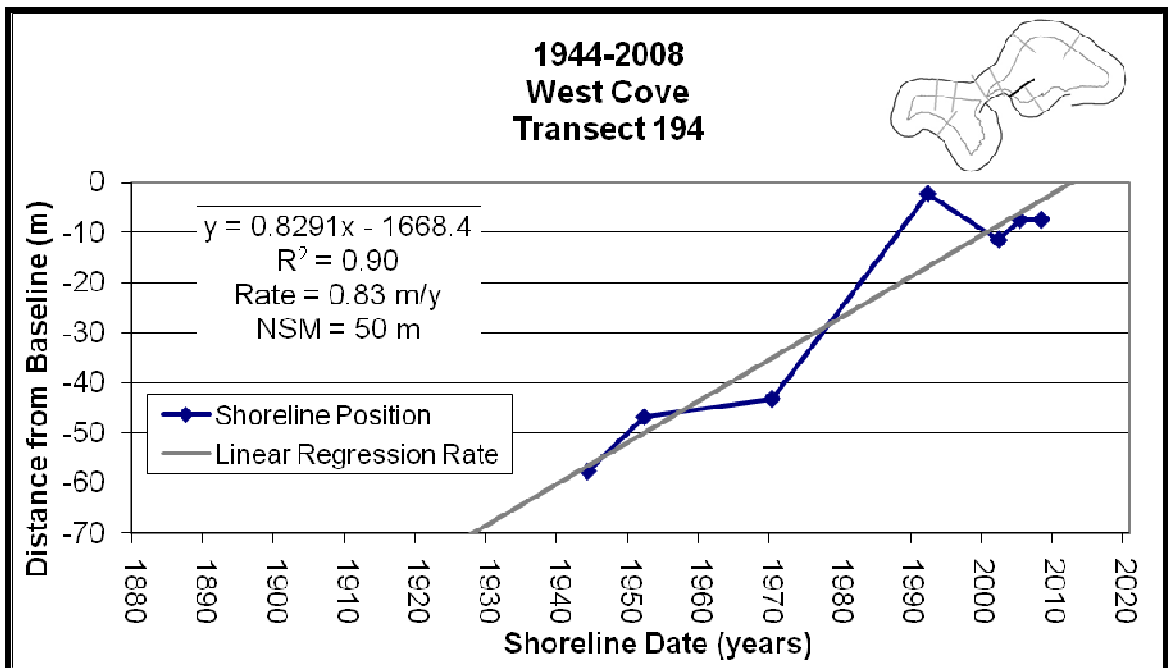


Figure 3.22. Linear regression analysis of T_s 194 along the WC for the 1944 dataset.

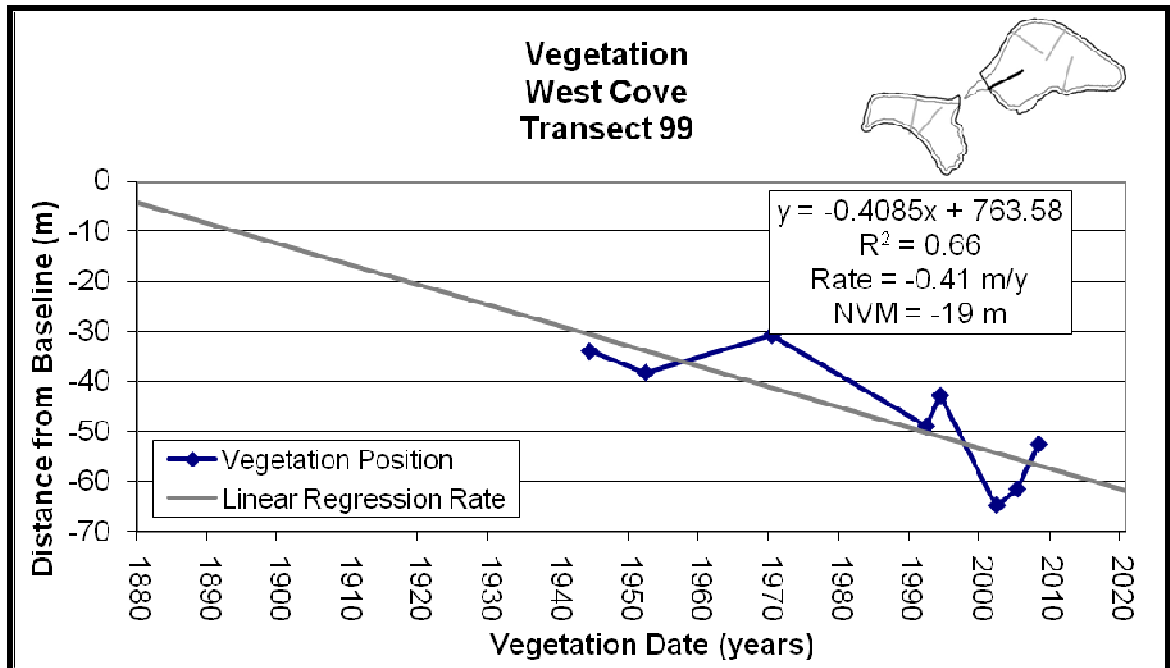


Figure 3.23. Linear regression analysis of T_v 99 along the WC for the 1944 dataset.

3.1.7 Southwest Sand Beach (SWSB)

The results obtained from T_s 47 show that the steep sloping SWSB has changed very little during the study period (Figure 3.3). This is likely a result of the two large bedrock outcrops on each terminus which serve to anchor the beach. Regression analysis of the 1890 dataset provided an accretion rate of 0.09 m/y, with an R^2 value of 0.80 (Figure 3.24). During the study period there was 10 m of shoreline progradation.

The analysis of the 1944 dataset provided similar results with a LRR of 0.05 m/y, with an R^2 value of 0.47 (Figure 3.25). The regression line had a relatively low correlation with the data points, with an R^2 value of only 0.48. Applying the LMS method provided a slightly higher accretion rate of 0.07 m/y. According to the NSM for the 1944 dataset there was 2 m

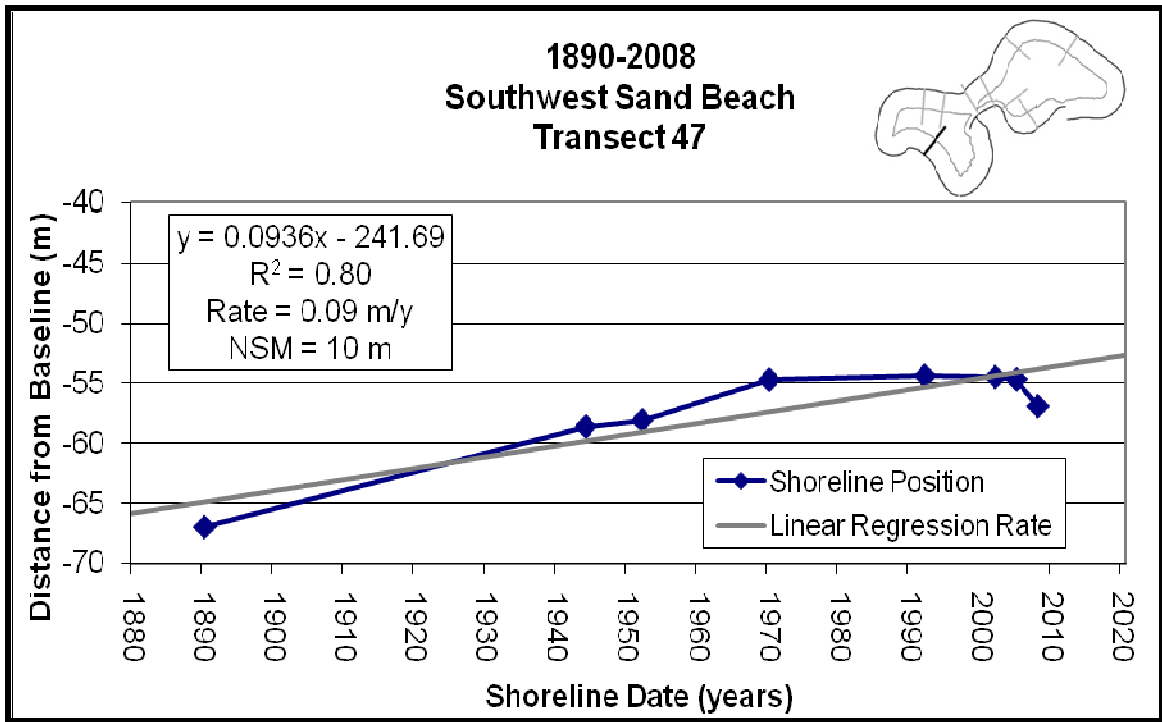


Figure 3.24. Linear regression analysis of T_s 47 along the SWSB for the 1890 dataset.

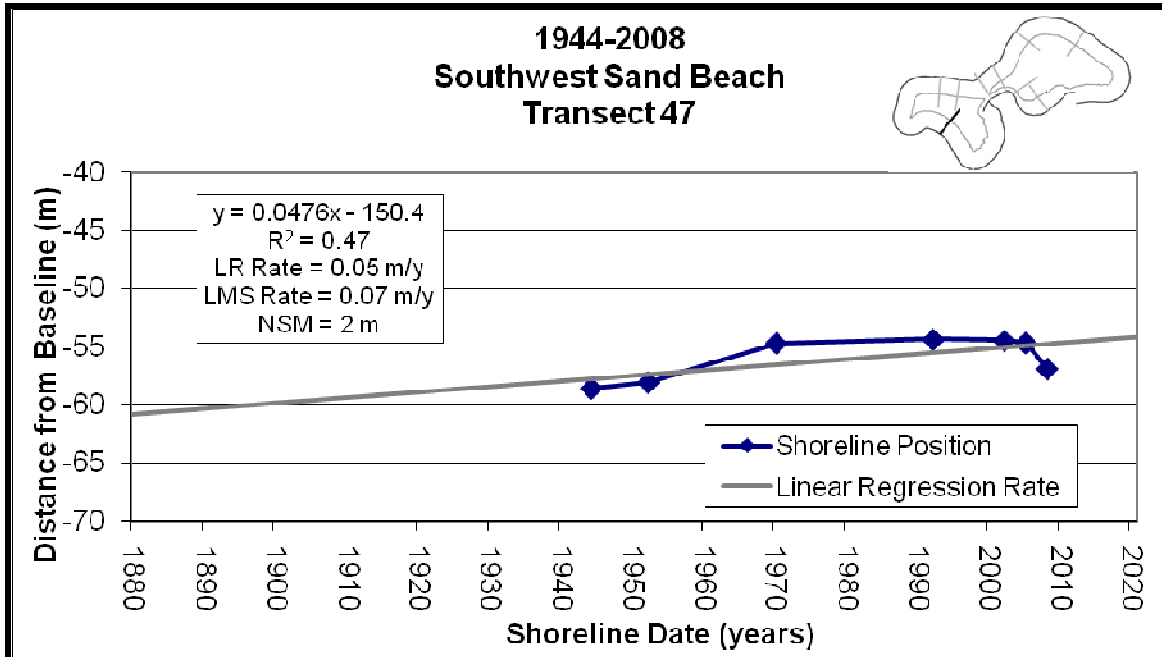


Figure 3.25. Linear regression analysis of T_s 47 along the SWSB for the 1944 dataset.

of shoreline progradation. Most of the accretion in this area occurred prior to 1970, as between 1970 and 2005 the beach remained relatively stable. Between 2005 and 2008 there was 2 m of erosion.

The vegetation analysis was carried out using T_v 141 (Figure 3.8). The results show a positive trend in vegetation gain, with some small periods of loss (Figure 3.26). The LRR of 0.20 m/y was over three times greater than that of the shoreline analysis. Between 1944 and 2008 the vegetated areas along this transect advanced seaward by 14 m.

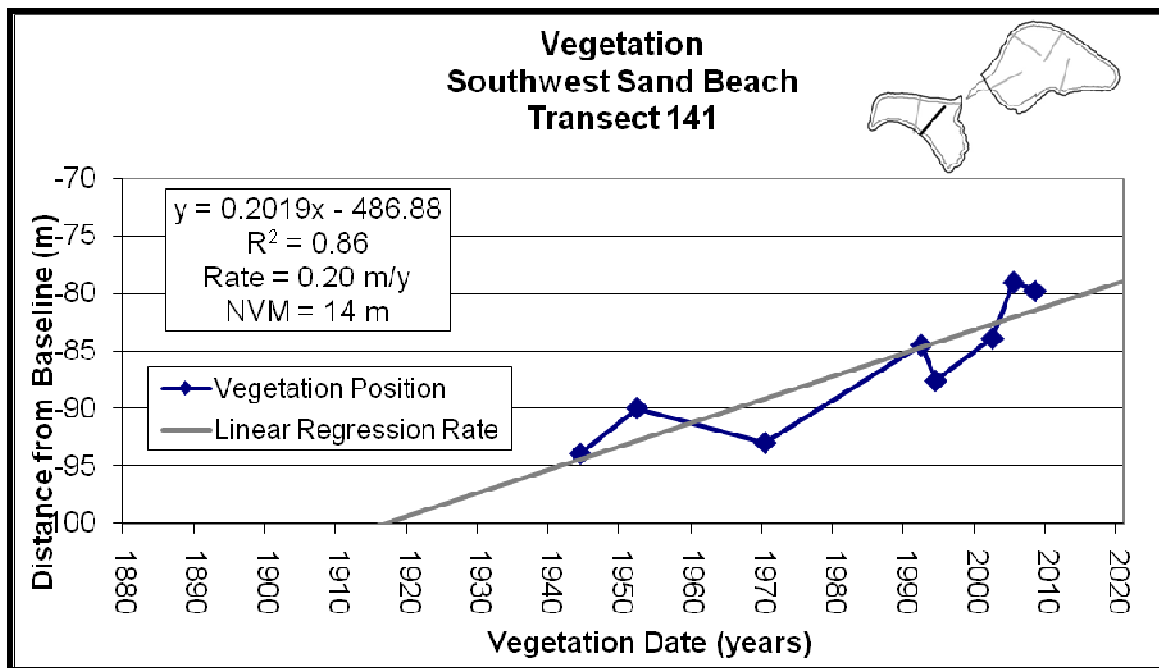


Figure 3.26. Linear regression analysis of T_v 141 along the SWSB for the 1944 dataset.

3.2 Comparison Analysis

The results obtained from the Comparison Analysis carried out within ArcMap are useful in identifying and quantifying the geomorphic trends occurring on Rainsford Island. ArcMap was used to create a single map for each comparison derived from the integration of datasets. Area measurements were obtained from the individual polygon features within the map. The results are given in m² of surface area that was eroded or accreted. The percentages given represent the area eroded or accreted, divided by the total area of the polygon basefile in the comparison of the two datasets.

3.2.1 Shoreline Data Compared to 2008 Basefile

The comparison analysis carried out, using the 2008 polygon as the basefile, provides strong evidence for an erosional trend occurring on Rainsford Island over the past century. The results indicate that most of the erosion took place after 1970 (Figure 3.27). The comparison of the USGS historical map and the 2008 orthophoto represents the longest temporal range of this study, and showed the erosion of 11,368 m² of Rainsford Island (Table 3.1). This was over 14% of the Island's area and supports the erosional trends seen in the DSAS analysis for the same time period. The accuracy in determining the amount of shoreline change occurring between two data sets increases with the length of time between them.

The comparison of the 1944 polygon file also showed a dramatic loss in area of 7,085 m² or 9% of the Island's coastal area eroded between 1944 and 2008 (Figure 3.28). These losses were also observed between 1952 and 2008 where 8,295 m² or 11% of the area eroded.

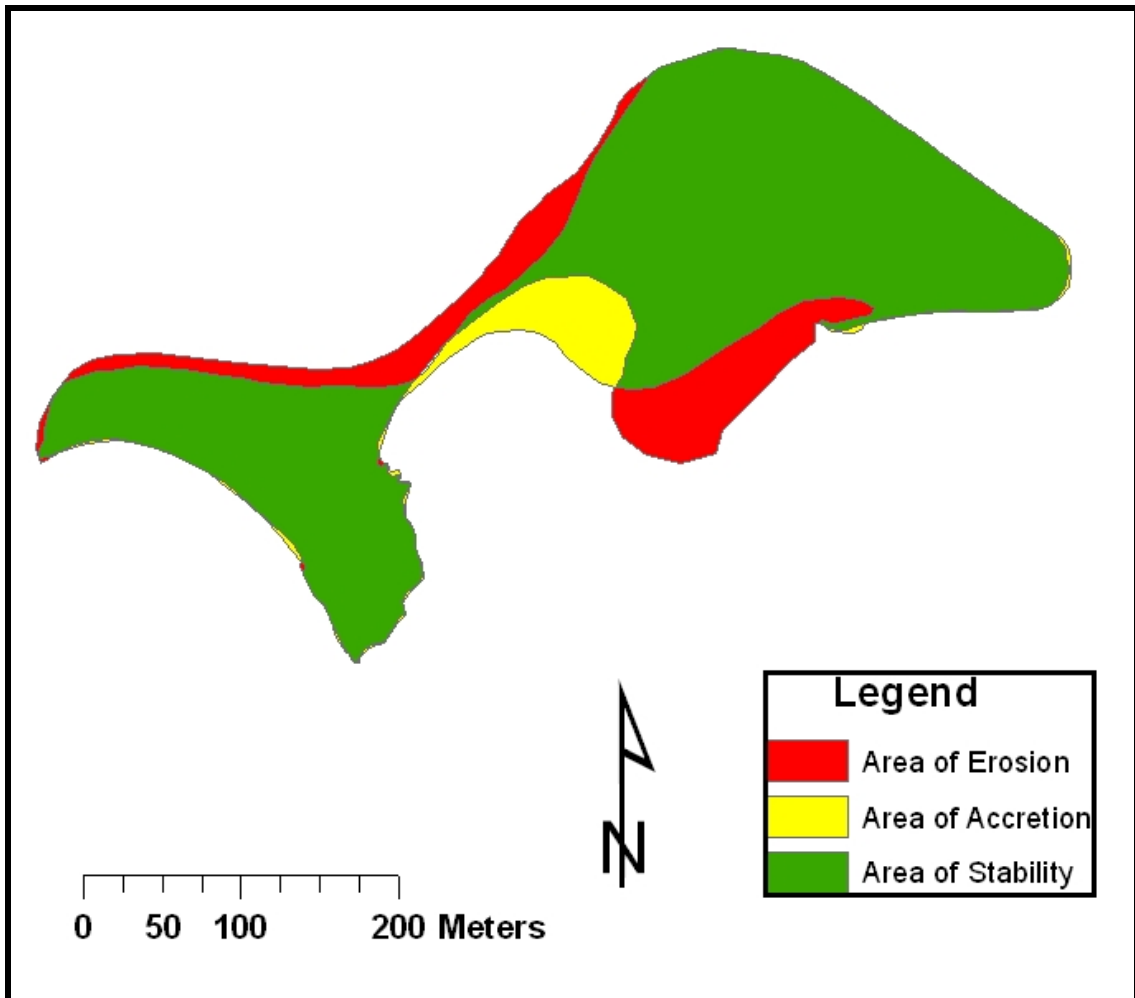


Figure 3.27. Map of Rainsford Island showing shoreline change occurring between 1944 and 2008. This comparison spans a time period of 64 years and shows the Island's shoreline has changed in some areas while others, buffered by the seawall and bedrock outcrops, have remained relatively stable. The areas of erosion are shown in red, areas of accretion in yellow, and areas of stability in green. The comparison of the 1944 and 2008 polygon files showed a dramatic loss in area with 7,085 m² or 9% of the Island being eroded.

Shoreline Date	Basefile	Area Accreted (m ²)	Area Eroded (m ²)	Area Accreted/Eroded (m ²)	Percent Island
1890	2008	4,940	16,308	-11,368	14%
1944	2008	4,916	12,001	-7,085	9%
1952	2008	2,839	11,134	-8,295	11%
1970	2008	2,406	3,117	-711	1%
1992	2008	426	2,844	-2,418	4%
2001	2008	1,124	2,485	-1,361	2%
2005	2008	1,076	4,670	-3,594	5%

Table 3.1. Results from the shoreline comparison analysis using the 2008 basefile. Each shoreline polygon file was compared to the 2008 polygon file and area differences and similarities were quantified in m². The percent calculation was made by dividing the net accretion or erosion figure by the total area of the basefile polygon. This calculation provides a ballpark estimate of the percent change in area on the Island.

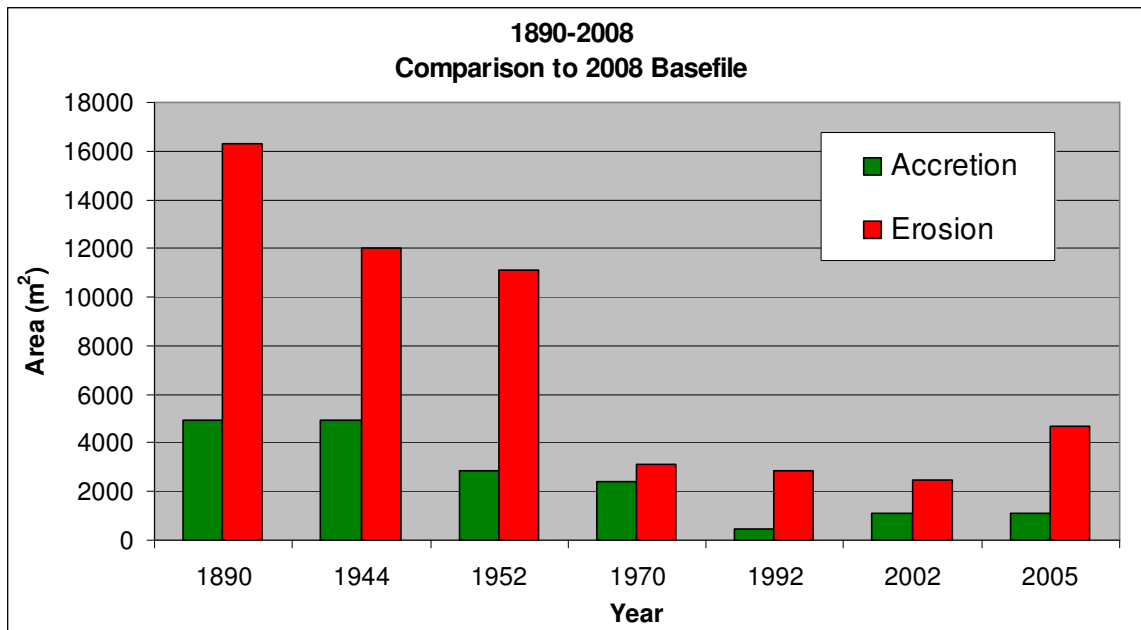


Figure 3.28. Bar graph showing results of 2008 basefile comparison.

There were similar amounts of erosion seen in the comparisons of the 2008 basefile with the historical map, the 1944 dataset, and the 1952 dataset. The similar amounts of erosion between each comparison indicate that much of this erosion occurred after 1952. The comparison of the 1970 through 2005 polygon files showed a much smaller trend of erosion with only a 711 m² loss of area in the 1970 comparison.

3.2.2 Data Comparison to the Mean High Water Offset-Corrected Shoreline.

Employing the MHW offset-corrected shoreline as the basefile provided an opportunity to incorporate the LIDAR/ tidal datum derived shoreline into the Comparison Analysis. The results of the comparison were similar to those obtained using the 2008 basefile with a few notable differences.

The data shows that 9,072 m² of the Rainsford Island coastline was lost between 1890 and 2002 (Figure 3.29). In 1944, there was erosion of 6% of the Island's area, and in 1952 erosion of 8% (Table 3.2). The comparison of the 1970 data continued the same trend with erosion of 7,023 m². Between 1970 and 1992 there was a threefold drop in erosion, with only 2,608 m² or 4% of the Island area eroded. The comparisons of the 1992 through 2008 data indicated stability with some small amounts of accretion (2002 and 2008) and erosion (2005).

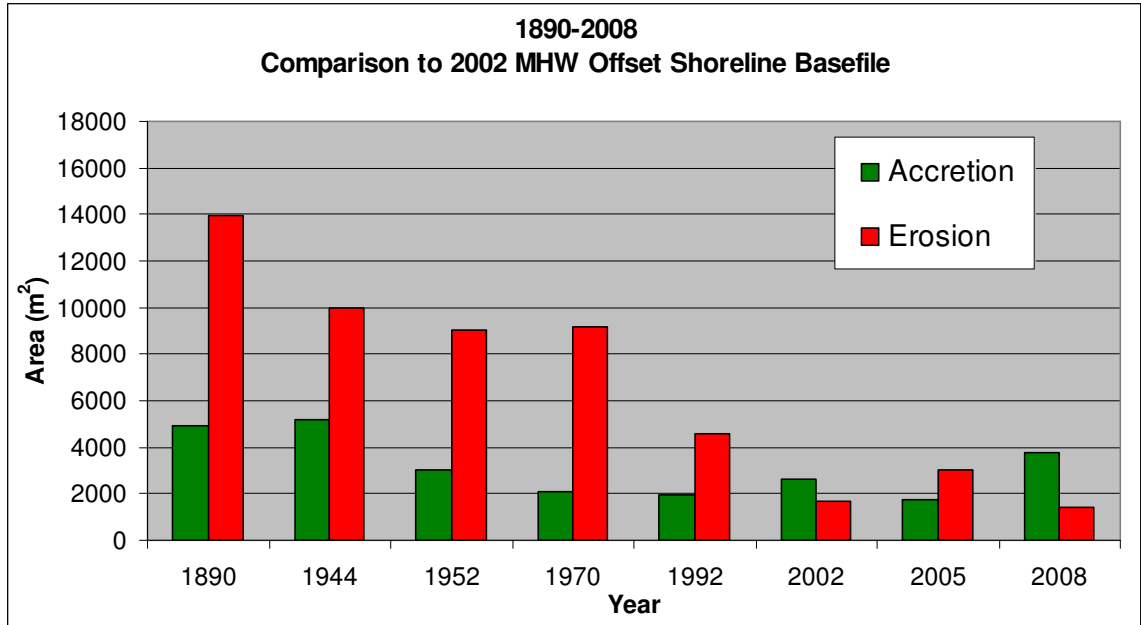


Figure 3.29. Bar graph showing results of MHW offset shoreline basefile comparison.

Shoreline Date	Basefile	Area Accreted (m ²)	Area Eroded (m ²)	Area Accreted/Eroded (m ²)	Percent Island
1890	2002 MHW	4,915	13,987	-9,072	11%
1944	2002 MHW	5,180	9,970	-4,790	6%
1952	2002 MHW	3,038	9,037	-5,999	8%
1970	2002 MHW	2,119	9,142	-7,023	9%
1992	2002 MHW	1,956	4,564	-2,608	4%
2002	2002 MHW	2,651	1,717	934	3%
2005	2002 MHW	1,737	3,036	-1,299	2%
2008	2002 MHW	3,744	1,448	2,296	3%

Table 3.2. Results from the shoreline comparison analysis using the Mean High Water Offset-Corrected Shoreline basefile. Each shoreline polygon file was compared to the MHW offset shoreline polygon file and area differences and similarities were quantified in m².

3.2.3 Vegetation Comparison to 2008 Basefile

The analysis of the Island's vegetation polygon files compared to the 2008 basefile also shows a reduction of the vegetated area prior to 1970, with periods of increase and decrease after this point (Figure 3.30). The 1944 and 1952 comparisons both showed the vegetation retreating landward by 11% and 10%, with 6,279 m² and 5,642 m² of retreat respectively (Table 3.3). These losses are comparable to the Island area loss of 9% and 11% obtained when using the 2008 basefile. There was a 2% gain in 1970, and in both 1992 and 2002 comparisons there was an 8% loss in the vegetated areas of the Island. In 2005 the area remained relatively stable.

3.2.4 Shoreline Comparison Analysis Between Datasets

Between 1890 and 1944, 4,281 m² of the coastline on Rainsford Island eroded, representing 5% of the Island's surface area at that time (Figure 3.31). Between 1944 and 1952 there was 1,210 m² of accretion, which began a positive trend of shoreline progradation that would continue until 1970 (Table 3.4). Between 1952 and 1970, the coastal areas of Rainsford Island increased by 7%. During this period, nearly 6,000 m² of area was created by the seaward progradation of the shoreline.

The comparison between the 1970 and 1992 polygons provided results which indicate the 25-year positive trend of accretion ends with a rapid erosion of the Island's area. The data suggests that between 1970 and 1992, the Rainsford Island shoreline was dramatically eroded (Figure 3.32). Due to this erosion, the Island decreased in area by 11% or 9,000 m². This

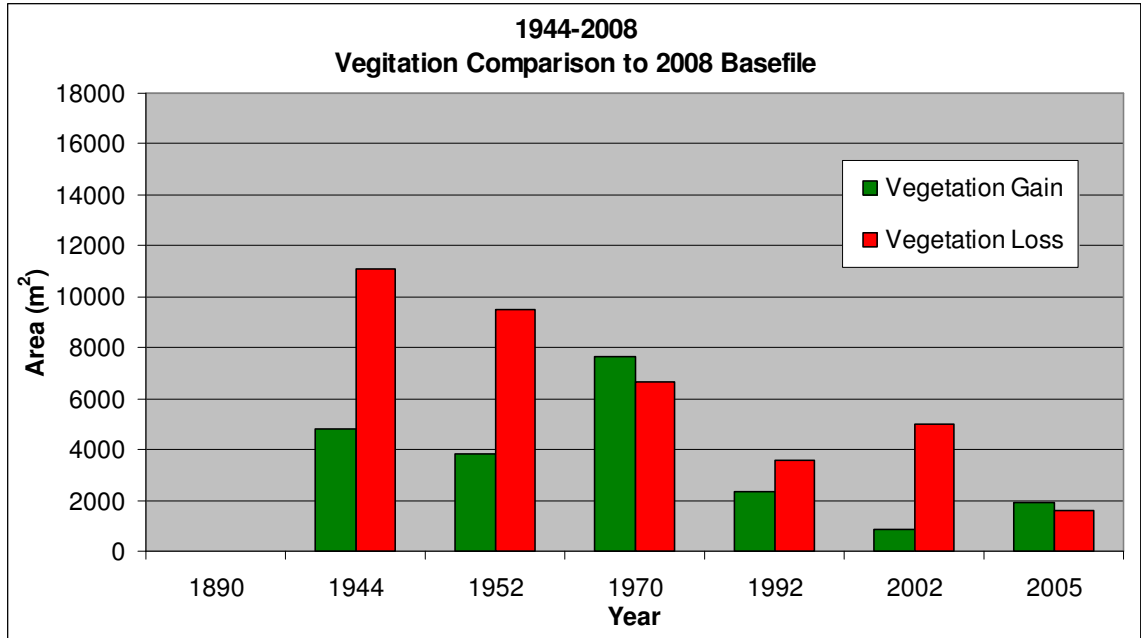


Figure 3.30. Bar graph showing results of vegetation comparison using 2008 basefile.

Vegetation Date	Basefile	Area Gained (m ²)	Area Lost (m ²)	Area Gained/Lost (m ²)	Percent Island
1944	2008	4,798	11,077	-6,279	11%
1952	2008	3,842	9,484	-5,642	10%
1970	2008	7,653	6,630	1,023	2%
1992	2008	2,368	3,557	-1,189	2%
2002	2008	855	4,964	-4,109	8%
2005	2008	1,891	1,618	273	1%

Table 3.3. The results from the vegetation comparison analysis using the 2008 basefile. Each of the vegetation polygon files was compared to the 2008 polygon file and area differences and similarities were quantified.

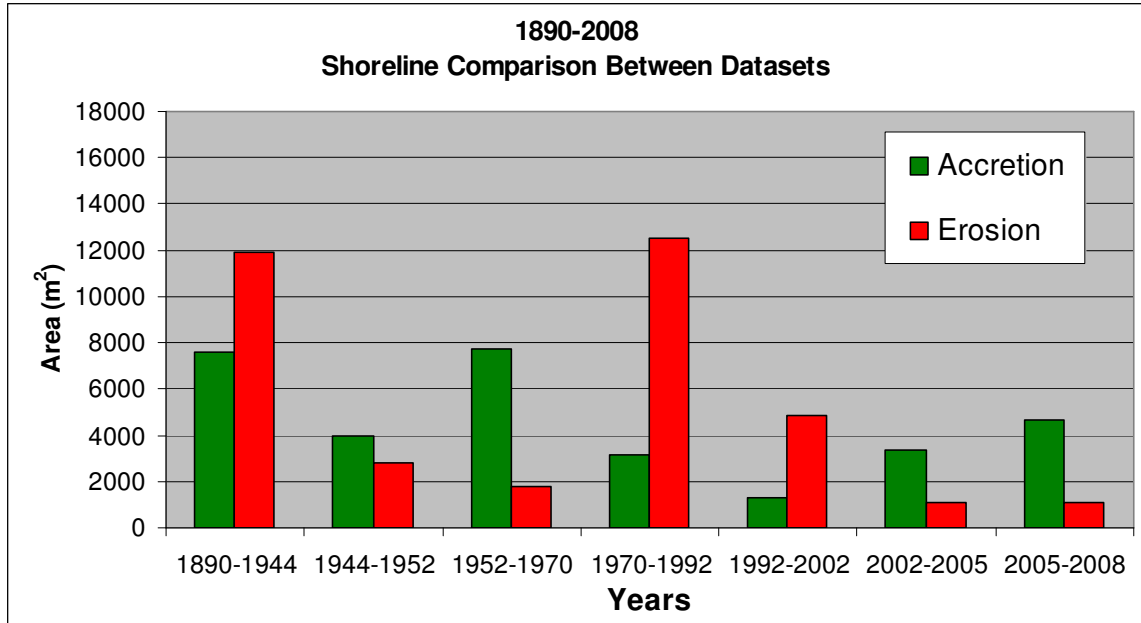


Figure 3.31. Bar graph showing results of shoreline comparisons between datasets.

Shoreline Date	Basefile	Area Accreted (m ²)	Area Eroded (m ²)	Area Accreted/Eroded (m ²)	Percent Island
1890	1944	7,614	11,895	-4,281	5%
1944	1952	3,988	2,778	1,210	2%
1952	1970	7,740	1,747	5,993	7%
1970	1992	3,117	12,502	-9,385	11%
1992	2002	1,284	4,826	-3,542	5%
2002	2005	3,339	1,106	2,233	3%
2005	2008	4,670	1,076	3,594	5%

Table 3.4. Results from the shoreline comparisons between datasets. Each shoreline polygon file was compared to the next year polygon file. These comparisons provided the ability to more specifically identify when the shoreline changes occurred.

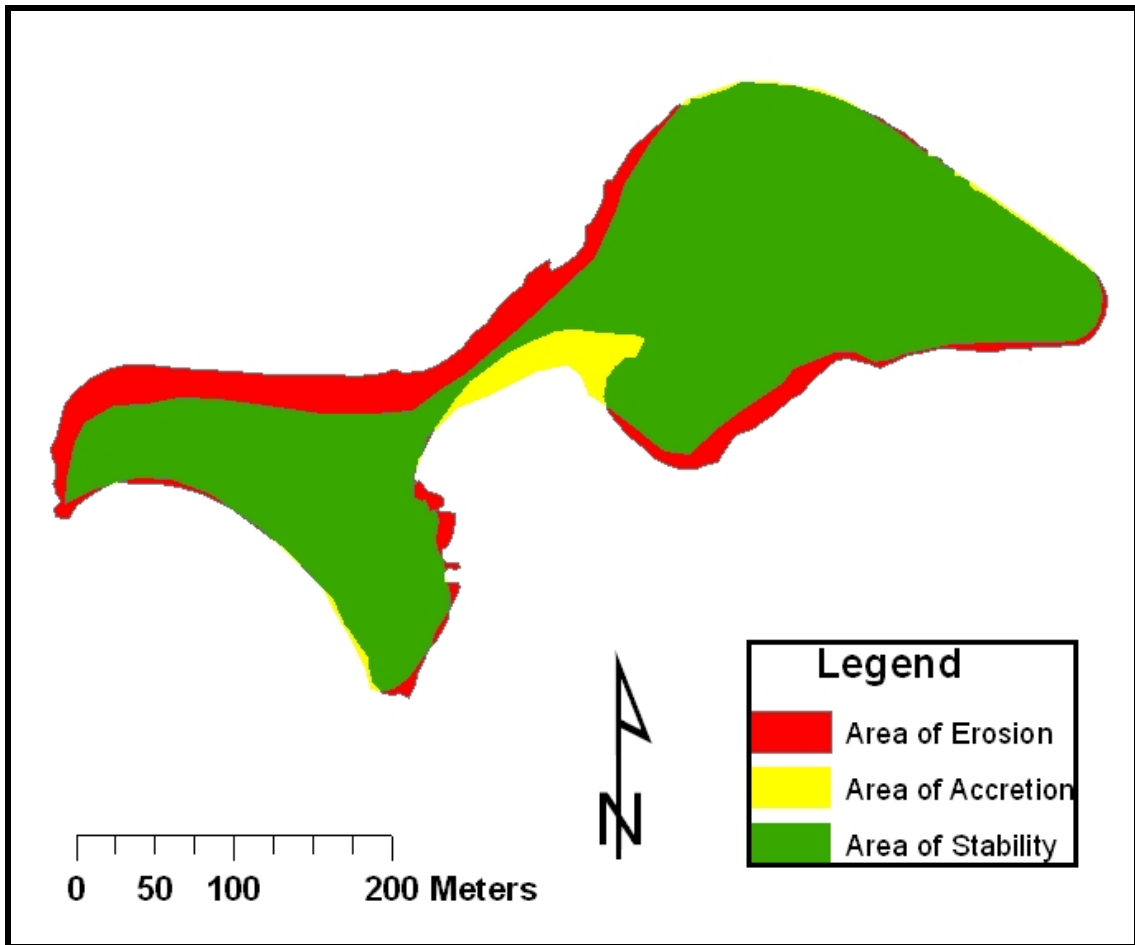


Figure 3.32. Map of Rainsford Island showing shoreline change occurring between 1970 and 1992. The area of loss (erosion) is shown in red, area of gain (accretion) in yellow, and area of stability in green. During this period over 9,385 m² or 11% of the Island's area was eroded away, most of which occurred on the northern beaches. While erosion was occurring on the north side of the Island the WC was accreting.

trend of erosion continued in the analysis of the 1992 and 2002 data. After this point, the erosional trend again reversed itself and between 2002 and 2008 there were accretions of 2,233 m² and 3,594 m² respectively.

3.2.5 Vegetation Comparison Analysis Between Datasets

The vegetation comparison analysis between consecutive datasets provided various results with periods of both expansion and contraction (Figure 3.33). Between 1944 and 1952, there was little change in vegetation, between 1952 and 1970 there was a loss of 6,667 m² or 12% of the vegetated areas on the Island (Table 3.5). The results obtained from the vegetation analysis are negatively correlated to the shoreline results for the same period, which showed 6,000 m² of accretion. Between 1970 and 1992 there was a gain of 2,212 m² or 4% of the vegetated areas on the Island, and between 1992 and 2002 there was a 5% increase of 2,920 m². The comparison of the vegetation between 2002 and 2005 shows another significant loss. During this period, 4,234 m² or 9% of the vegetated areas were lost. The vegetated areas remained relatively stable in the 2005 comparison.

3.3 Mean High Water Visual Analysis

The analysis of the MHW shoreline, with the historical maps and aerial photographs was carried out to observe and determine the long term coastal trends that have occurred on Rainsford Island. Despite the fact that this analysis is not quantitative, it is nonetheless very useful in assessing how the Island's shoreline is changing over time. In conjunction with the

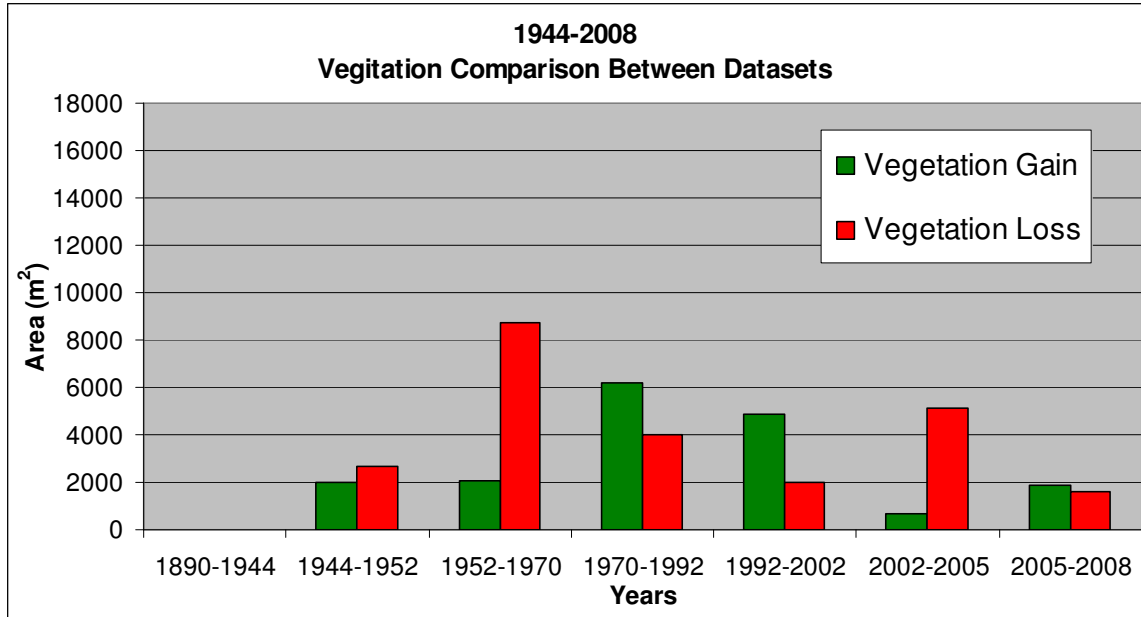


Figure 3.33. Bar graph showing results of vegetation comparisons between datasets.

Vegetation Date	Basefile	Area Gained (m ²)	Area Lost (m ²)	Area Gained/Lost (m ²)	Percent Island
1944	1952	2,000	2,636	-636	1%
1952	1970	2,099	8,766	-6,667	12%
1970	1992	6,225	4,013	2,212	4%
1992	2002	4,899	1,979	2,920	5%
2002	2005	697	5,120	-4,423	9%
2005	2008	1,892	1,618	274	1%

Table 3.5. Results from the vegetation comparisons between datasets.

other results, this information is beneficial to understanding how the shoreline evolved on Rainsford Island.

3.3.1 Mean High Water Shoreline and the 1890 Historical Map

The visual analysis of the MHW shoreline with the USGS historical map provides a clear picture of the broad coastal trends that have occurred on Rainsford Island during the past century (Figure 3.34). The southeast migration of the low-lying spit, quantified in the other results, is evident. The landward position of the MHW shoreline along the spit indicates that erosion has occurred on the northern beaches. This observation is supported by the results obtained from the DSAS analysis of the NWBB, which puts the distance of the southeast migration at 20 m.

The seaward position of the MHW shoreline in the area of the WC and SESB indicates that accretion has occurred in these areas. This is another observation which is supported by the DSAS results. The close match between the MHW shoreline and the mapped shoreline along the southern bedrock outcrop indicates that this area has remained relatively stable during the last century, which would be expected. Also evident through these observations is the 10 m of accretion obtained from the DSAS results along the SWSB. In this area, the MHW shoreline sits seaward of the mapped shoreline. This analysis is also beneficial in identifying possible cartographic errors, as was the case along the northeast section of the seawall discussed in Section 3.1.4. As the MHW shoreline passes well landward of the delineated shoreline on the historical map and through a portion of the upper bluff, it provides further evidence of a mapping discrepancy in this area. This is

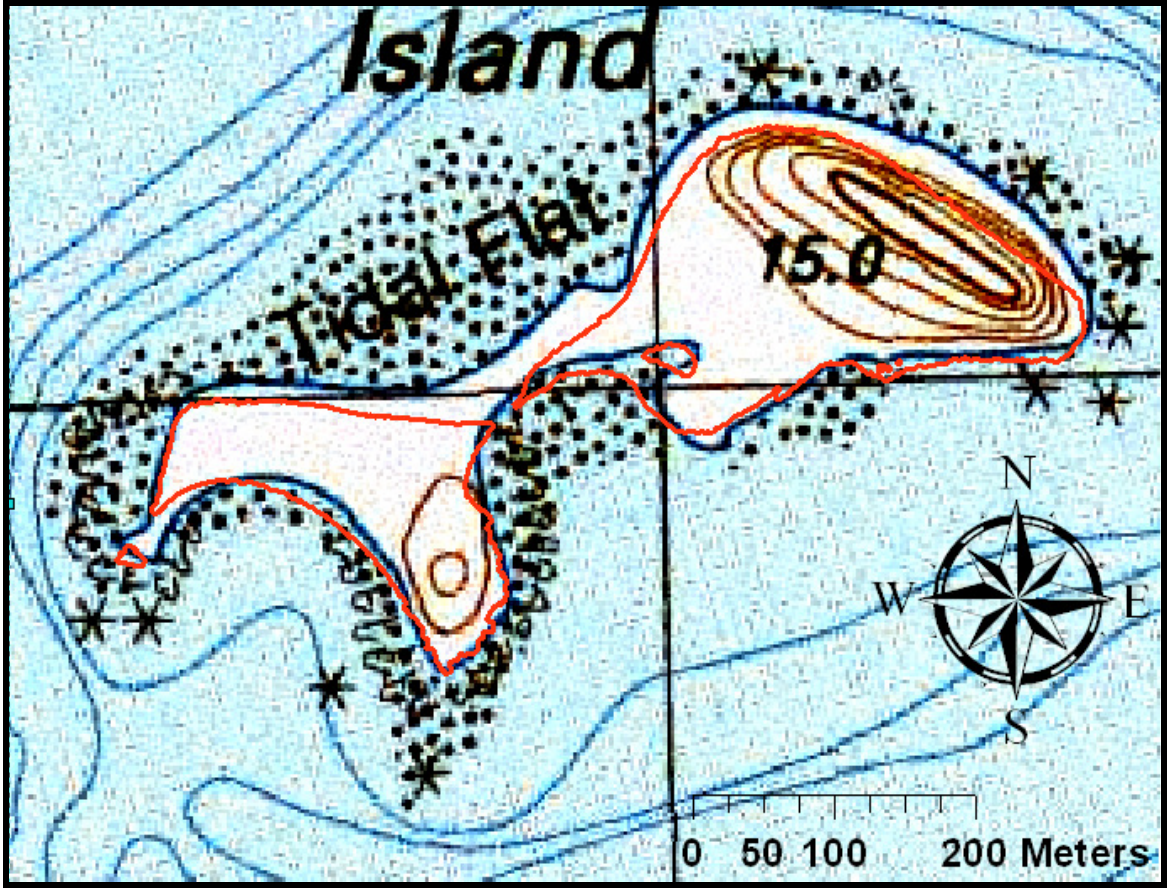


Figure 3.34. Historical USGS quadrangle map of Rainsford Island with MHW shoreline. The map was provided by MassGIS and is the earliest dataset used in this study. The figure shows the effectiveness of integrating an objectively created MHW shoreline shown in red with historical datasets to visually assess long term coastal trends.

affirmed by the fact that the MHW shoreline follows the seawall closely when overlaid on the 1944-2008 aerial photographs.

3.3.2 Mean High Water Shoreline and the 1904 Historical Map

The integration of the 1904 historical map and the MHW shoreline provides an excellent means by which to assess how the coastal changes occurring during the past century have impacted the Island's infrastructure, much of which is now considered historically sensitive (Figure 3.35). The accuracy of the delineated shoreline in the 1904 georectified map is unknown, but there are likely some discrepancies as was the case with the USGS map. For example, there is little alignment between the MHW shoreline and the map's shoreline along the western point of the south drumlin, while along the northern seawall there is a close fit. Despite these inaccuracies, it still provides useful information on the general location and size of the historical buildings and coastal infrastructure that once encompassed much of the Island. Through the integration of the MHW shoreline with this map, it is possible to assess which sites have already been destroyed and those that may become vulnerable in the future.

During the period between 1904 and 2002, major geomorphic changes occurred on Rainsford Island, impacting much of its infrastructure. One of the most striking observations is the apparent erosion of the SEBB indicated by the landward position of the MHW shoreline in this area. As a result of the erosion, the ice house, three other unnamed buildings, and the stone and timber wharf have all been destroyed. The DSAS analysis supports these observations showing 42 m of erosion in this area. As historical records indicate, this wharf

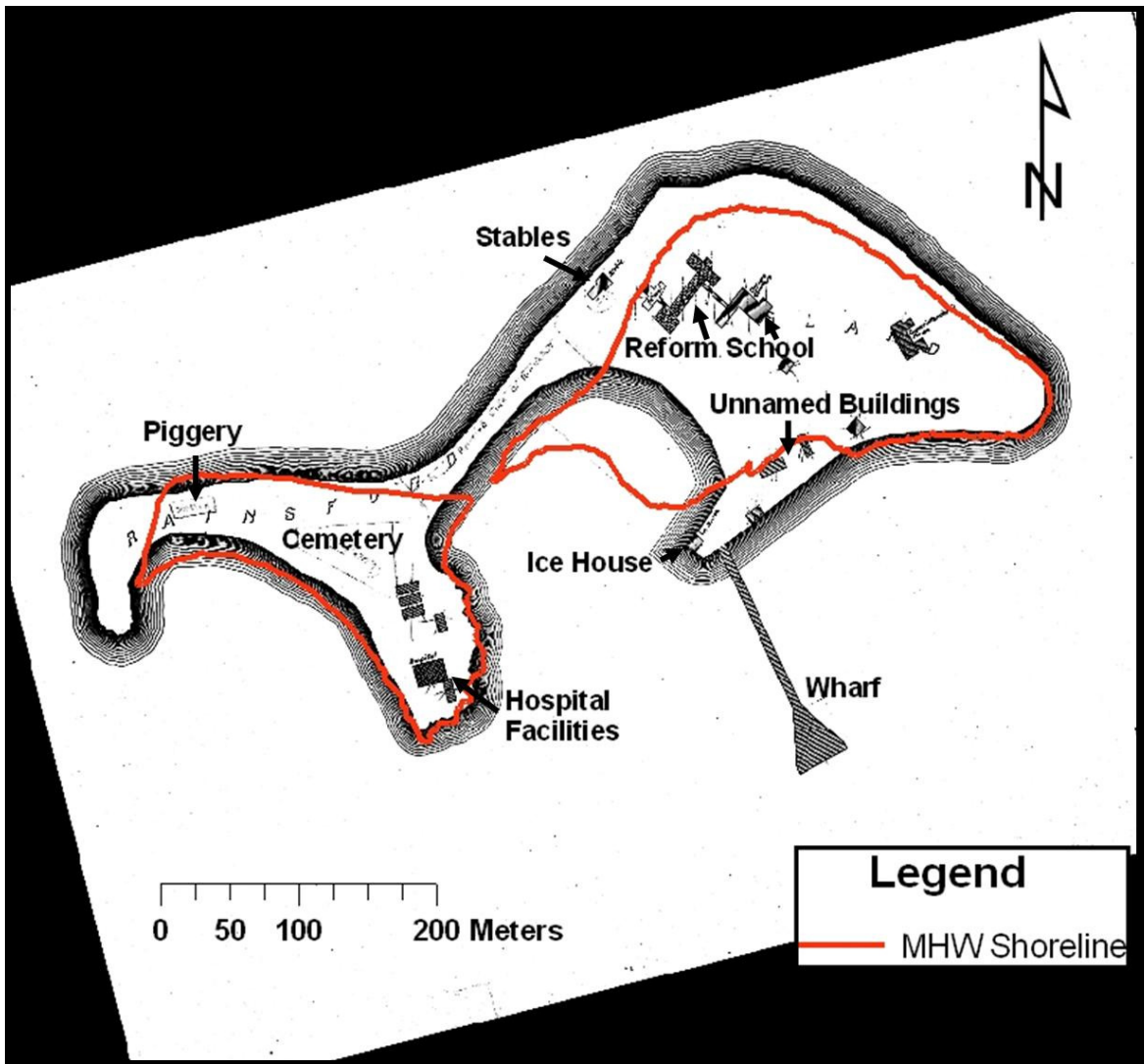


Figure 3.35. Historical 1904 georeferenced map of Rainsford Island with MHW shoreline. This map provides the locations of the historically sensitive sites on Rainsford Island. Numerous buildings can be seen seaward of the MHW shoreline shown in red indicating that they have been lost to erosion. Other buildings observed near the MHW shoreline are vulnerable and may soon meet the same fate.

was destroyed by the 1898 “Portland Gale.” This map was likely created prior to this date as the wharf is observed intact on the 1904 map.

A building identified on the map as the “Stable,” located along the NWBB, has also been destroyed as it sits well seaward of the MHW shoreline. Other structures are located a short distance landward of the MHW shoreline and may soon meet a similar fate. One of which, located on the northwestern shore of the north drumlin, is a school building from the House of Reformation built in 1895. The still intact foundation of the “Piggery” located on the north beach of the south drumlin presently sits directly on the MHW shoreline and is currently in the splash zone, becoming partially submerged during spring tides.

3.3.3 Mean High Water Shoreline and the 1944 Aerial Photograph

Overlaying the MHW shoreline on the 1944 georectified aerial photograph provided an effective tool to observe and assess coastal trends that have occurred between 1944 and 2002 (Figure 3.36). The continued southeast migration of the spit has resulted in erosion on the northern beaches and accretion along the southeastern beaches. The seaward position of the MHW shoreline within the WC clearly shows the large amount of filling and accretion that has occurred in this location. As the progradation of the shoreline within the WC and the southeast migration of the spit are observed on both historical maps and the 1944 overlay, it can be concluded that most of these geomorphic changes occurred after 1944.

According to the DSAS results, the SEBB from which the stone and timber wharf extended appears to have dramatically accreted between 1890 and 1944, and then reversed its trend and eroded just as rapidly. The DSAS results show that initially there was a

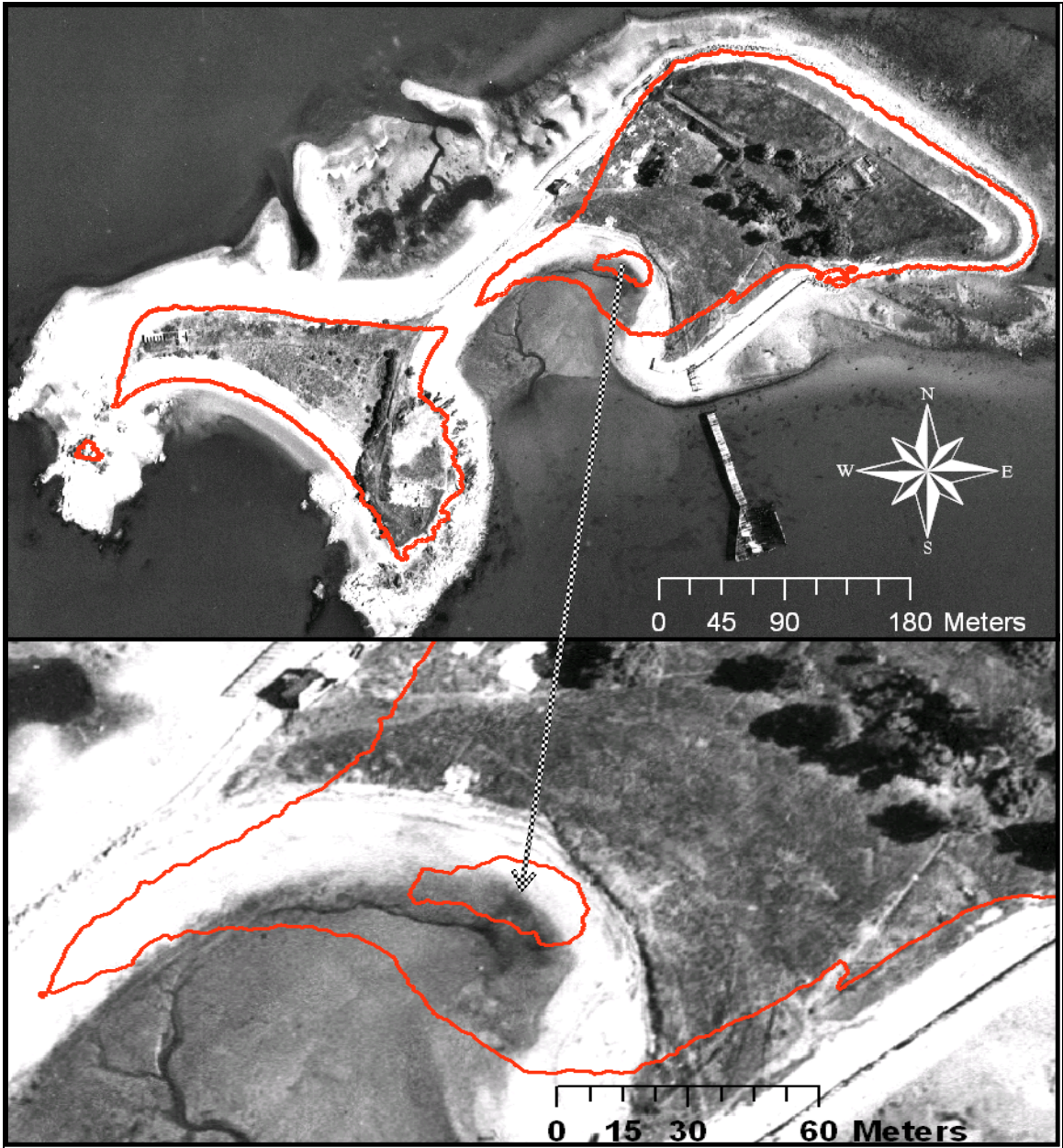


Figure 3.36. 1944 aerial photograph with MHW shoreline. The area of the WC is magnified in the lower image indicated by the arrow. The dramatic accretion that occurred within the cove between 1944 and 2002 is clearly observable. The southeast migration of the low elevation sand spit connecting the two drumlins is also made evident in this image, while other areas of the Island, including those buffered by the seawall, have remained relatively stable. A building identified as a Stable along the northwestern beach is observed well seaward of the MHW shoreline indicating that it has been lost to the rising seas.

progradation of the shoreline of 86 m prior to 1944. After this point, the shoreline began its steady landward retreat of 42 m between 1944 and 2002. As discussed previously, this may be evidence for a large change to sediment transport along this portion of the Island due to the 1898 destruction of the wharf. However, cartographic error on the 1890 and 1904 maps cannot be ruled out.

3.4 Flood Hazard Predictive Maps

The predictive maps are based on a static SLR model which does not take into account erosion and accretion. The elevation of the MHW is instantaneously raised by 1 m, 2 m, and 3 m, on the Rainsford Island DEM, and areas that fall below this elevation are shown as inundated. The geomorphic structure of the Island is not taken into account, which inevitably raises some uncertainties to the predictions. Because these predictions assume a stable landscape, they may be more accurate for storm surge events rather than sea-level rise over time. This is due to the fact that sea-level rise occurs gradually, altering coastal geomorphic processes. In contrast, storm surges happen within one or two tidal cycles and may either rapidly alter coastal geomorphology or preserve the landscape. The degree of alteration relates to storm dynamics and the geologic framework of the Island.

3.4.1 1-Meter Flood Hazard Map

The predictive map displaying the possible inundation in response to a 1-m rise in sea-level or storm surge event is based on the tidal datum derived MHW elevation value. A 1-m rise in sea-level has been predicted to occur by the end of the 21st century (IPCC, 2007).

This elevation was therefore applied in this scenario. Under this scenario, 26% of Rainsford Island would become inundated (Figure 3.37). The bedrock and seawalled portions of the Island are resistant to the 1-m SLR or storm surge. This is a direct result of the vertical to near vertical slope of the coastline in these areas. However, even on these well buffered coastlines, there is some inundation.

The inundation of the spit is also evident with flooding occurring on the northern shores of the Island. The map shows inundation of the WC. This is an example of where the accuracy of the prediction may be questionable due to the omissions of erosional and depositional trends, as the other quantitative results in the study show a consistent positive trend of accretion within the WC.

The map indicates that 1-m of SLR or a powerful storm surge event would completely submerge some areas containing sensitive historical sites including the Rainsford Island Cemetery, located within the center of the south drumlin. The inundated triangular area in this location coincides closely with the borders of this extremely sensitive site (Figure 1.8).

3.4.2 2-Meter Flood Hazard Map

Under a scenario where there is a storm surge or SLR of 2-m, over 60 % of the Island would be inundated (Figure 3.38). The more likely event to occur in the near future is a large storm surge resulting from a Nor'easter or hurricane and not a rapid rise in sea-level, which occurs more gradually. If a 2-m storm surge were to occur the inundation may not be permanent as flooding waters would eventually retreat and return to pre-storm elevations.

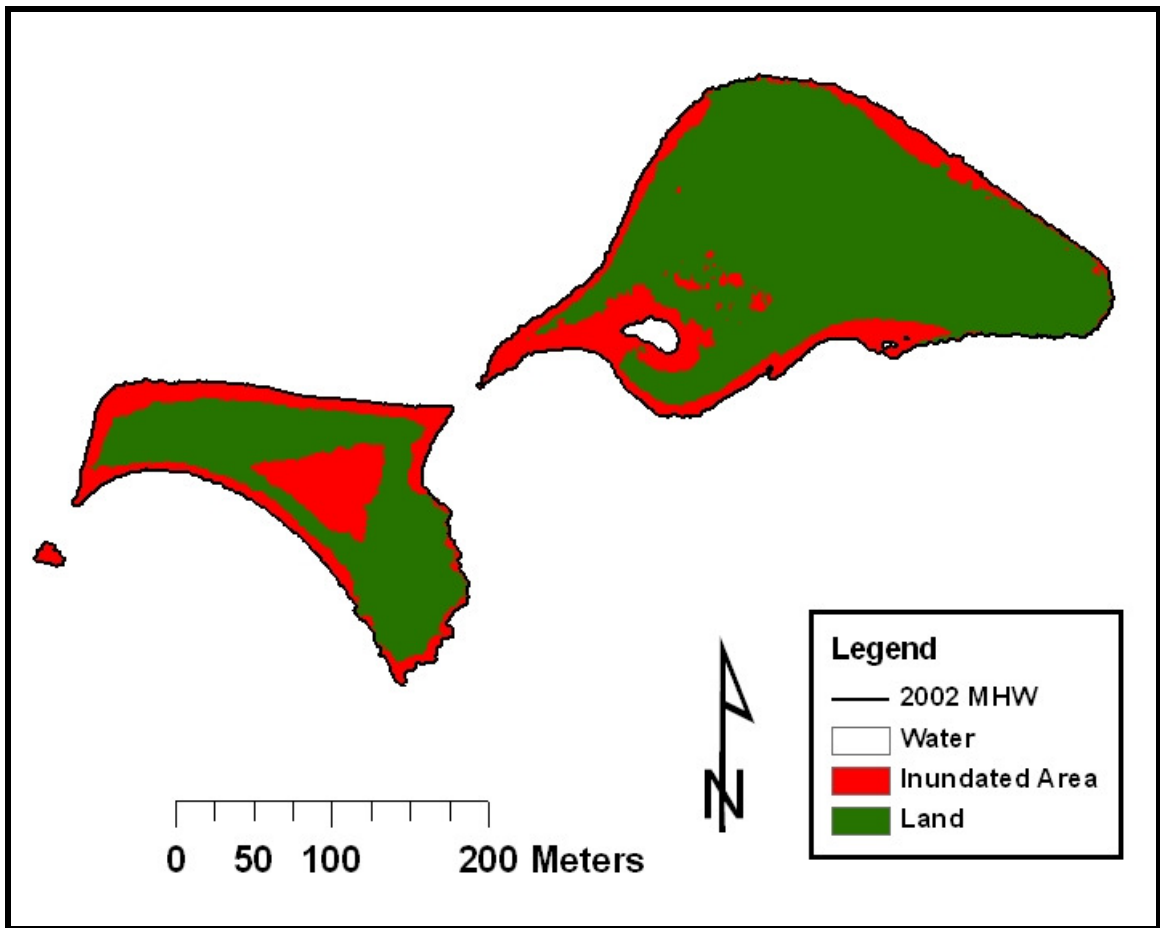


Figure 3.37. 1-Meter Flood Hazard Map. Inundated areas are shown in red and the MHW shoreline is represented by the black line. Under this scenario, much of the Island’s shoreline would likely experience some degree of erosion except for areas buffered by the seawall and bedrock outcrops and those areas that have shown long term trends of accretion such as in the West Cove. The triangular shaped inundated area on the south drumlin is the precise location of the Rainsford Island Cemetery, a highly sensitive archeological site.

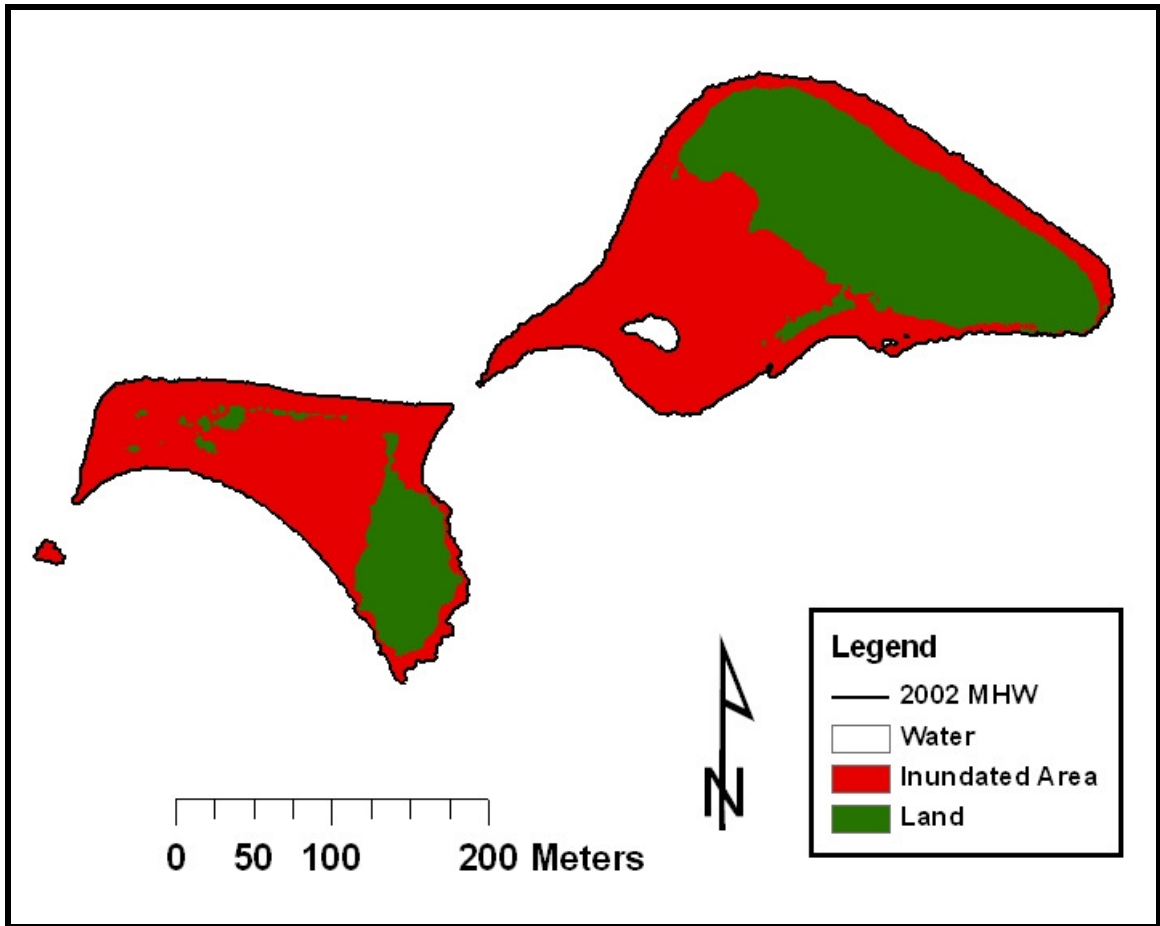


Figure 3.38. 2-Meter Flood Hazard Map. Inundated areas are shown in red and the MHW shoreline is represented by the black line. Under this scenario, the Island would effectively be cut in two with the majority of the low-lying areas of the north and south drumlins becoming submerged.

The bedrock and seawall areas of the Island that had remained relatively stable in response to a 1-m flood became inundated under the 2-m scenario. Once the elevation of the vertical to near vertical shoreline in these areas is overtopped, the landward areas once protected become inundated. With a 2-m storm surge, the seawall becomes ineffective at buffering the bluffs from erosional processes. This would result in the bluffs becoming undercut by wave attack at their base leading to bluff slides and mass wasting events. The bedrock outcrop's vertical elevation along the south drumlin is considerably higher than that of the seawall. As a result, the inundation in this area is significantly less than along the seawall.

3.4.3 3-Meter Flood Hazard Map

The elevation value of the current 100-year flood in Boston Harbor is currently set at 3 m. Kirshen et al. (2009), has reported that under the higher emission scenarios presented by the IPCC (2007), the occurrence of the 100-year flood event may reoccur at intervals of 8 years or less in the Boston Harbor area as a result of anthropogenic climate change, and may increase in elevation by over 1-m. An event such as this would completely change the coastal geomorphology of Rainsford Island as can be seen in the 3-m Flood Hazard Map (Figure 3.39). With 66% of the Island becoming inundated, the only untouched areas would be the higher elevation areas of the north and south drumlins. The erosion that would follow the inundation would be dependent on the geologic framework of the Island. The unconsolidated clays and soils that make up the bluff would rapidly be eroded by coastal processes while the granite bedrock outcrop would likely stay intact.

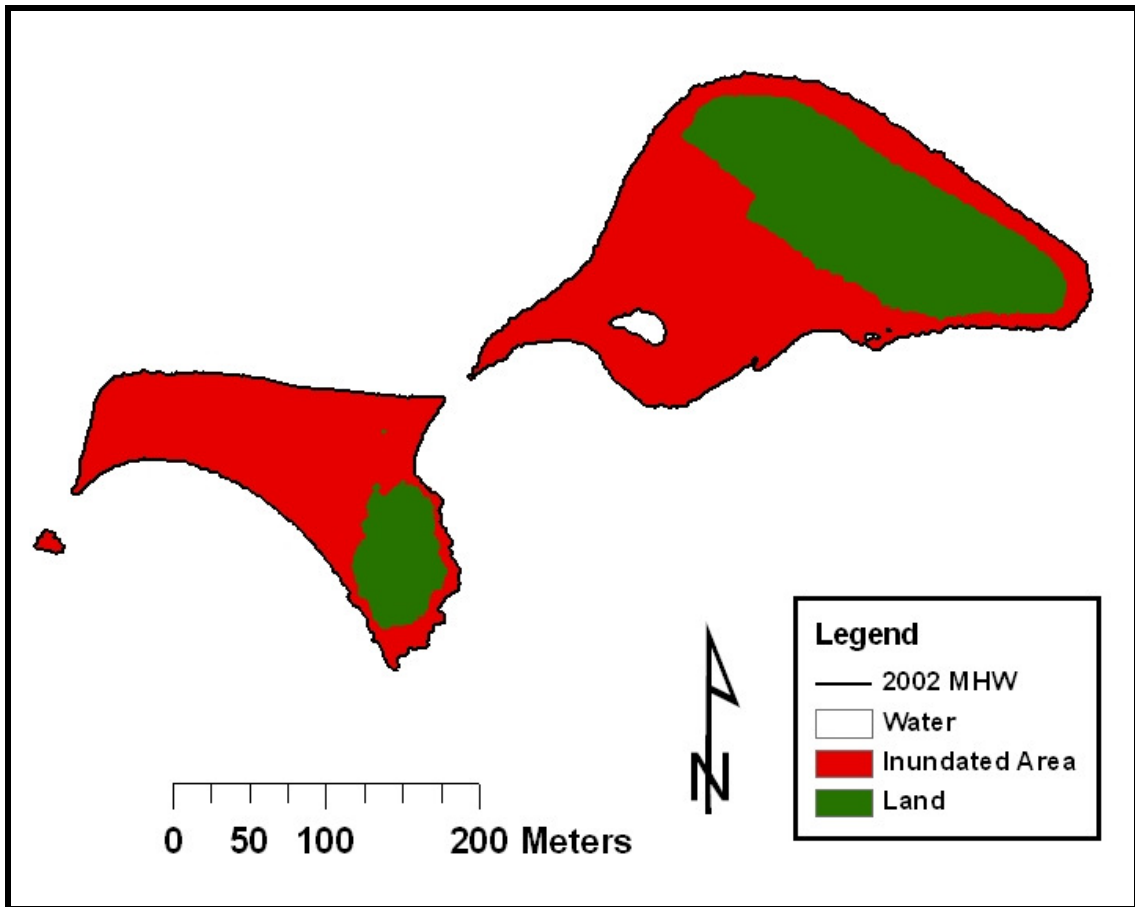


Figure 3.39. 3-Meter Flood Hazard Map. Inundated areas are shown in red and the MHW shoreline is represented by the black line. This scenario displays the possible implications of the predicted increase in elevation and reoccurrence of the 100-year flood event which is currently set at 3 meters. A storm surge of this elevation would result in the almost complete inundation of the Island and the loss of numerous sensitive historical and archeological sites.

CHAPTER 4

DISCUSSION

4.1 Data Integration

Integrating the multiple data sources within a GIS and developing methods and techniques to carry out geospatial and statistical analysis presented some of the most difficult challenges of this study. Integrating and managing data, which varied from 19th century historical maps to state-of-the art LIDAR data, was challenging and introduced some uncertainties into the study. As is the case with most shoreline change analysis studies that utilize a manually-created proxy based shoreline, there were inherent uncertainties in this subjective process. The manual visual identification of the shoreline feature was heavily dependent on the quality and temporal coverage of the available data.

Collecting the image data to carry out this investigation was difficult, as historical aerial photographs and maps are located in the archives and basements of a number of different agencies and institutions. By reviewing the literature of past studies that utilized aerial photographs in Boston Harbor, we learned of the existence of some of the photographs used in this study. As many of these studies were decades old, the challenge was in tracking down where the actual photographs were located.

RISES corresponded with seven different entities to obtain the images used in this study. These included the Massachusetts State Archives, the National Archives, the University of New Hampshire, the City of Boston, and numerous others. In some cases we knew of the existence of a particular aerial photograph, but could not pinpoint their exact location. This included aerial photographs from 1938, 1966, and 1977. Including these datasets would have greatly enhanced the temporal coverage of the investigation but they proved elusive and, therefore, could not be included.

RISES sought to acknowledge the uncertainties that arose from the quality and temporal coverage of the data sources and took every step possible to reduce their influence on the results of the study. ERDAS Imagine software was successfully employed to georeference and standardized the data by bringing all image data into the same coordinate system and spatial resolution. Through the standardization of the geospatial data, many of the potential uncertainties which may have been introduced by utilizing multiple data sources of varied temporal and spatial resolution, was reduced.

The methods used in RISES to define and identify the HWL feature within the available data were based on well established protocols and proven techniques which have successfully been employed in previous shoreline change analysis studies (e.g. Zhang, et al., 2002; Douglas and Crowel, 2000; Himmelstoss, et al., 2006). This required a thorough review of the available literature and the development of new techniques and methods specific to this investigation. RISES chose to utilize the HWL as the indicator feature by which to delineate the shoreline and defined it as the “most seaward wrack line” on the beach face. This definition ran contrary to many studies which primarily defined the HWL as the “wet-dry

boundary” on the beach face. Due to the steep and dynamic Rainsford Island shoreline, as well as the inconsistent temporal resolution of the image data, the wet-dry boundary was difficult to consistently identify and its exclusive use was not possible. The wrackline was a feature that was clearly discernable throughout the data sources. This allowed for the accurate and consistent delineation of the Island’s shoreline.

In order to enhance the confidence in the results obtained from the shoreline analysis, RISES also carried out vegetation analysis. The vegetation line is a clearly discernable feature which could confidently be identified and delineated throughout the image data. Although in some cases the vegetation results ran contrary to those of the shoreline, the two predominately followed similar trends. By supporting the shoreline data, the vegetation analysis improved confidence in the results obtained.

RISES also eliminated potential uncertainties in the process of delineating the shorelines by eliminating data sources in which the HWL could not be consistently identified. The 1972, 1988, and 1994 aerial photographs initially obtained for the investigation were eliminated as their inclusion may have introduced a degree of error that would have reduced the accuracy of the results of the investigation. This was done at the cost of temporal coverage, as data from these years would have increased the temporal resolution of the study.

In addition to the quality and temporal coverage of the available data sources, the success of accurately delineating the shorelines was also heavily dependent on the skills and experience of the interpreter. Ensuring that the interpreter had the necessary skills and experience to accurately delineate the features was also an important step taken to reduce potential uncertainties within the study. This was achieved through developing the skills and

experience of the interpreter through his participation and completion of the Graduate Certificate in Geographic Information Science program at the University of Massachusetts, Boston, and hundreds of hours of hands on experience.

One of the most important ways RISES sought to ensure its accuracy and eliminate potential errors was to carry out four different types of analyses in order to determine the shoreline evolution of Rainsford Island. These included the comparison analysis, the DSAS analysis, the MHW overlay analysis, and the predictive mapping. Through the employment of four separate forms of analysis and methods, potential errors were reduced and the coastal geomorphic trends found in one form of analysis could be compared with the others. Combined, these methods greatly enhanced the confidence of the studies' results and improved the overall accuracy of the investigation.

4.2 Digital Shoreline Analysis System (DSAS)

The employment of the DSAS extension for ArcMap greatly improved the study. The DSAS extension has numerous benefits over older methods employed in shoreline change studies. These benefits include the ability to integrate multiple datasets, identify specific areas of change, calculate rate-of-change statistics, and visually display results. Prior to obtaining the extension, it was unclear how RISES would proceed. It was initially planned to manually create transects and calculate statistics within ArcMap, though at the time it was unclear how specifically to go about this. If the methods could not be automated and had to be carried out manually, it would have been a painstaking and time consuming process. Fortunately, while reviewing literature on the subject, a study that had utilized the extension was found (Harris, et

al., 2005). After becoming aware of the existence of the software, it was a simple matter of visiting the USGS website indicated in the article and downloading the free software and instruction manual (Thieler, et al., 2008).

One of the greatest benefits gained from utilizing the DSAS extension was the efficient calculation of rate-of-change statistics. The use of established statistical techniques has recently become an essential aspect of any credible shoreline change study. RISES relied heavily on linear regression (LR) analysis for computing the change through time of the vegetation and shoreline positions. The LR method minimizes potential random errors and short term variability introduced by the manual delineation of shorelines and the variance in data sources. It also is purely computational, easily applied, and based on established statistical techniques (Himmelstoss, 2009). LR also includes all of the available data and is especially effective at calculating long-term rates of change in shoreline investigations (Crowell and Leatherman, 1999).

Despite the benefits of employing the LR method, it may, at times, be more appropriate to utilize the least median of squares (LMS) method, which is another rate-of-change statistic calculated within DSAS. Because the LR method employs all of the available data regardless of changes in trend or accuracy, it is susceptible to outlier effects and may also underestimate the rate-of-change over shorter periods of time (Genz, et al., 2007). Outlier data is introduced in shoreline change studies through the use of multiple data sources and the manual delineation of the shore and vegetation lines. Due to these potential uncertainties when using LR, it was appropriate to employ the LMS method when low R^2 values indicated a possible outlier data point.

The LMS method is more effective in limiting the influence that anomalous data has on the slope of the regression line and is a more robust statistic estimator in some cases. This study found that when R^2 values were high, the LRR and LMS rates were similar, while when R^2 values were low, the LRR was found to be substantially lower (Table 4.1). The utilization of both regression methods reduced some uncertainties within the study and in doing so enhanced its accuracy.

TRANSECT NUMBER	LMS	LRR	R²
47	0.07	0.09	0.8
74	-0.2	-0.18	0.92
83	-0.33	-0.19	0.63
97	-0.1	-0.1	0.97
122	-0.02	-0.18	0.71
178	-0.65	0.2	0.1
194	0.81	0.59	0.86
202	0.31	0.28	0.89

Table 4.1. Comparison of rate-of-change statistics. LRR and LMS rates were similar in cases where there was high R^2 values. Such is the case with Transect 47. When low R^2 values were present, the LRR was significantly lower, as in the case with Transect 83 and 178.

Despite the overriding benefits of employing the DSAS extension, there were some difficulties encountered in its application. Setting up the shoreline data for analysis was at times tedious, and problems were encountered due to the specific formats needed to integrate data. For example, on one occasion, a date was entered in the wrong format and statistics could not be generated. A two second change to the format immediately solved the problem, but not before hours were spent trying to trouble shoot it.

There was also a question raised on how effective DSAS would be when applied to a significantly smaller spatial area than that for which it was originally designed. One of the first applications of DSAS was in a study investigating shoreline change on the long straight beaches of Maryland's Assateague Island National Seashore (Harris, et al., 2005). These sandy beaches were over a kilometer in length and relatively straight compared with the dynamic shape of Rainsford Island. On Rainsford Island, particularly around the WC and spit, there were large variations in the historical shoreline positions making it difficult to attain a perpendicular angle at the shoreline/transect vertices (Figure 4.1).

RISES attempted to alleviate some of the uncertainties that arose by applying the DSAS extension to such a small spatial area. This was achieved by manually editing the baseline and individual transects in order to attain a near perpendicular angle at the vertices. The ability to edit the baseline and individual transects was a new feature included in the 2008 DSAS version 4.0, which came out just in time for its application in RISES (Thieler, et al., 2008). This feature greatly improved the DSAS extension and made it more effective at determining shoreline rate-of-change statistics on small spatial scales.

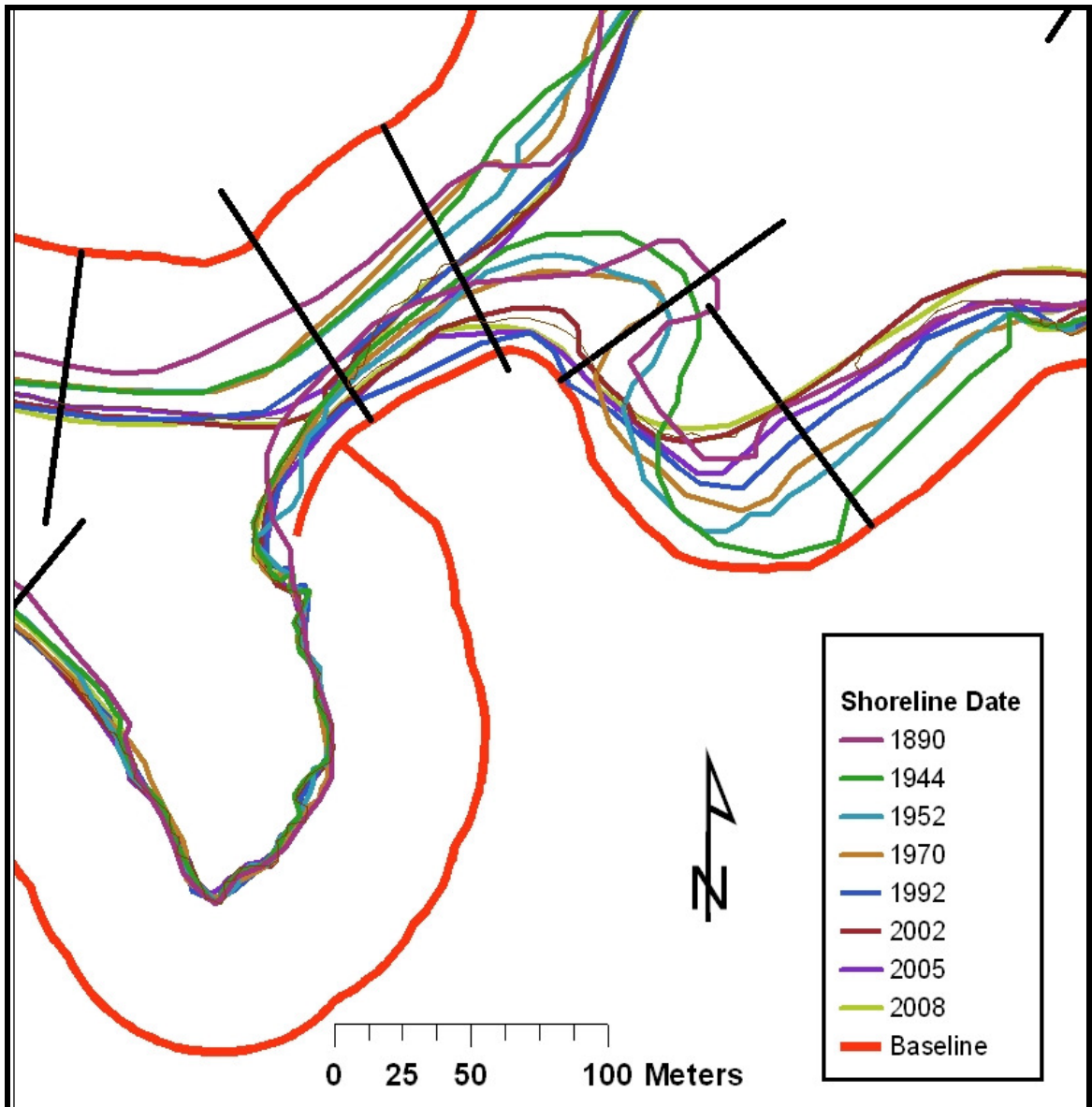


Figure 4.1. Dynamic nature of historical shoreline positions. The close up of Rainsford Island shows the dramatic fluctuations in shoreline position that occurred over the study period. The transects shown in black and the baseline shown in red were manually edited in an attempt to achieve a near perpendicular angle at the transect-shoreline vertices.

4.4 Areas of Significant Coastal Change

4.4.1 Southeast Boulder Beach (SEBB)

The SEBB was one of the areas of Rainsford Island that experienced significant geomorphic changes during the study period (Figure 4.2). Although there was an overall negative trend of erosion along this stretch of the coastline between 1944 and 2008, the DSAS statistics revealed a rapid rate of accretion prior to 1944 (Figure 4.3). After 1944, the positive trend reversed itself and an erosional trend was established for the remainder of the study period resulting in this area becoming an erosional hotspot on Rainsford Island.

It was previously discussed that the “Portland Gale” of 1898 destroyed the large stone and timber wharf that extended from this beach and may have been the mechanism that led to this trend reversal. One possible scenario is that the wharf may have reduced sediment transport while in place resulting in the offshore buildup of sediments. Once sediment transport was restored after the destruction of the wharf in 1898, these offshore sediments may have rapidly been transported onshore, accounting for the rapid progradation of 86 m of shoreline prior to 1944. Once the bulk of these sediments had been transported onshore, natural coastal processes were restored and a negative erosional trend was established.

However, due to the absence of 50 years of data between 1890 and 1944, and a lack in understanding the coastal processes occurring in this area, it is difficult to make any conclusions. In addition, the 1938 Hurricane, one of the largest storms of the century, occurred during this time period, making it even more difficult to identify the underlying processes that resulted in the trend reversal.

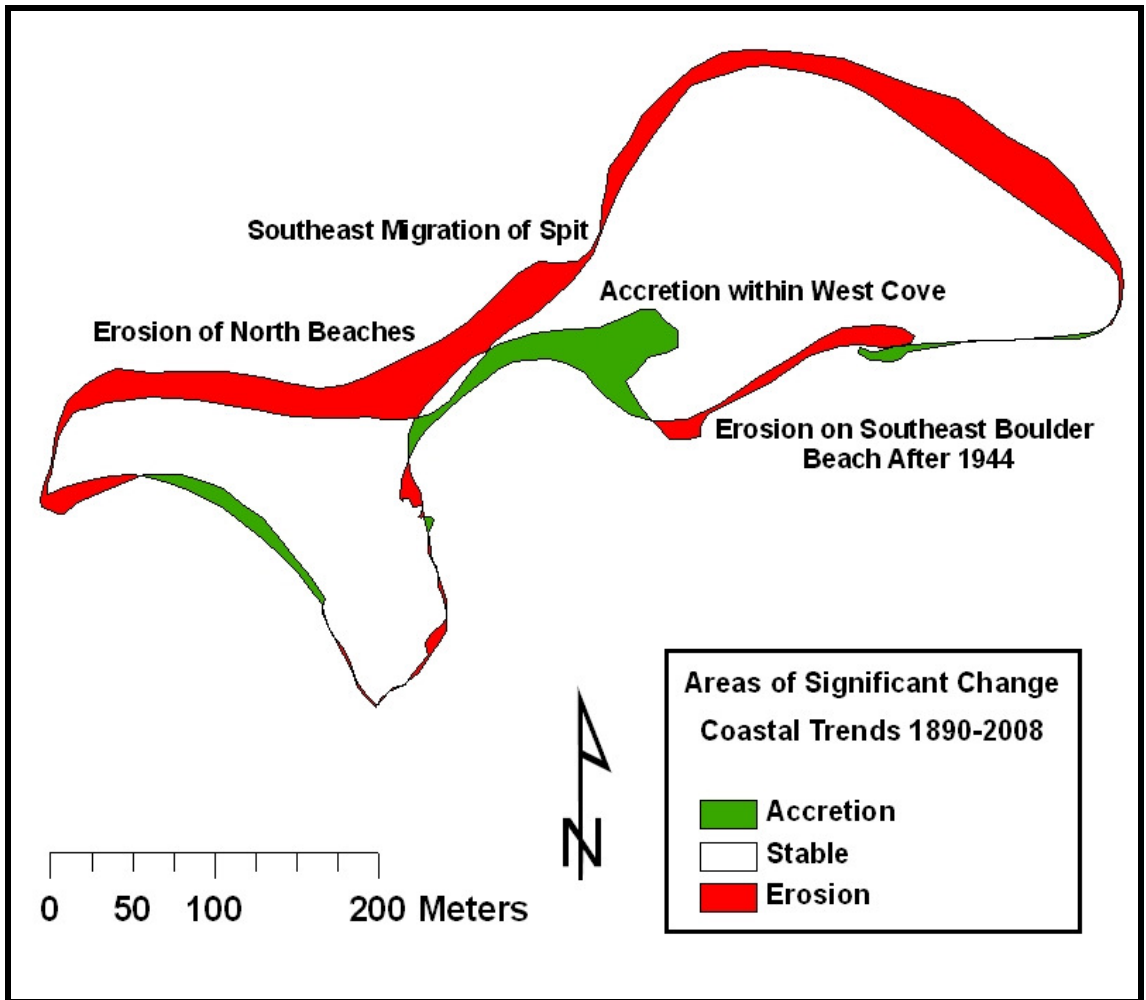


Figure 4.2. Areas of significant change. This map highlights the areas of Rainsford Island that experienced the greatest degree of change between 1890 and 2008.

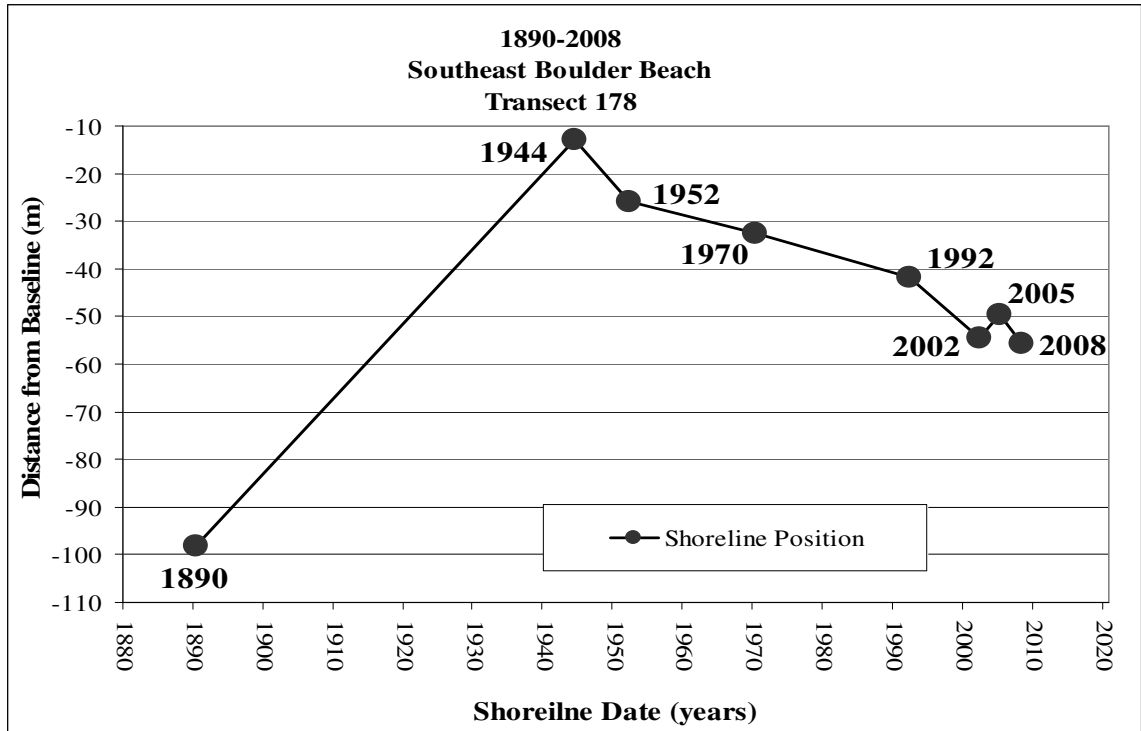


Figure 4.3. Dynamic shoreline trends along the SEBB.

4.4.2 Migration of low-lying spit

One of the most striking coastal geomorphic trends identified in RISES was the southeast migration of the sand and gravel spit that connects the two drumlins. This trend was clearly observed in the comparison and overlay analysis and quantified through the DSAS statistics (Figure 4.3). Between 1944 and 2008 the spit steadily migrated in a southeast direction, resulting in 20 m of accretion along its southeast side and 20 m of erosion along its northwest side.

The regression analysis provided a strong negative correlation between the shoreline results of the NWBB and those from the SESB. This was expected as they both encompass

one side of the spit. The LRR for the two beaches was negatively correlated at 0.33 m/y and -0.34 m/y respectively. The coastal processes that led to the migration of the spit also influenced other nearby areas, including the WC, which will be discussed in the next section. If this trend continues, there will be further erosion along the NMSB leaving low elevation areas of the south drumlin vulnerable to future storm surges.

4.4.3 West Cove (WC)

The area of the WC experienced significant geomorphic change during the study period with over 50 m of shoreline progradation. The rapid filling and accretion within the cove was clearly observed on the MHW overlays and comparison maps and quantified through the DSAS analysis (Figure 4.3). The results indicate that the majority of this accretion took place after 1944 and was likely coupled to the southeast migration of the sand and gravel spit.

The vegetation analysis did not support the shoreline results within the WC. While the shoreline rapidly prograded 50 m seaward, the vegetation retrograded landward by 20 m. This may be attributed to the fact that while there was significant shoreline progradation, a large 36 m diameter oval-shaped area in the center of the cove still remained below the MHW elevation (Figure 4.4). Due to the low elevation in this area, saltwater likely seeps upwards through the sediment pores during high tides, making it difficult for vegetation to take root. This may be one factor that accounts for the negative correlation between the shore and vegetation data.

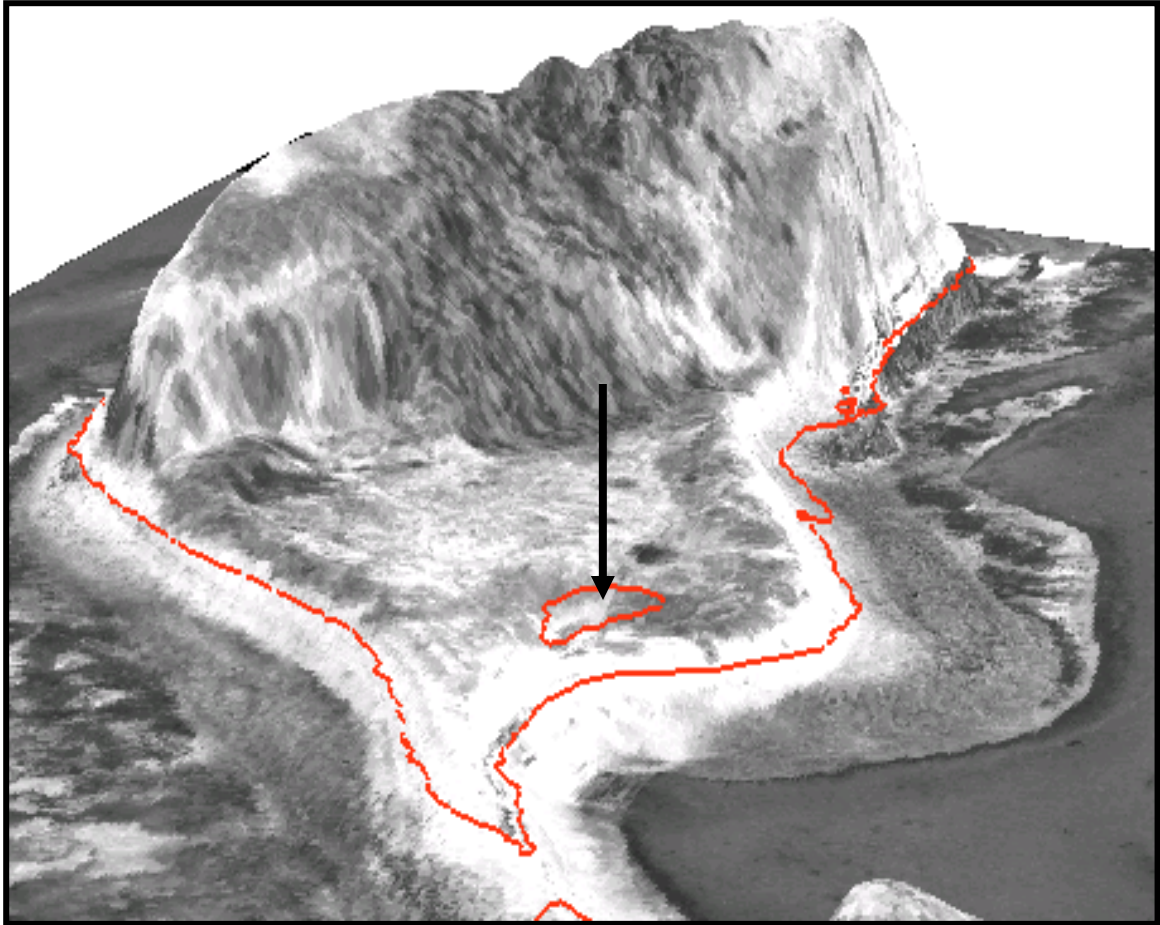


Figure 4.4. Area below MHW elevation within WC. This image looking northeast provides a good example of how different datasets can be effectively integrated within a GIS. Three data sources, including the MassGIS LIDAR DEM, the LIDAR/tidal datum derived MHW shoreline shown in red, and the high resolution 2002 orthophotograph, were integrated to create this image using ESRI's ArcScene software. A 5-meter vertical exaggeration was applied in its creation. The area below the MHW elevation within the WC is indicated by the black arrow.

4.5 Coastal Hazard Zones on Rainsford Island

4.5.1 Designation of Coastal Hazard Zones

RISES designated an area as a “Coastal Hazard Zone” if it met any two of the following three criteria:

1. DSAS regression analysis with strong linear correlations indicates a continuation of the negative erosional trend during the next decade.
2. The comparison and overlay analysis indicates that the area has experienced a consistent trend of erosion during the past fifty years.
3. The area is vulnerable to coastal flooding as indicated by the 1-Meter Flood Hazard Map.

4.5.2 North Beaches

The NWBB and the NMSB are erosional hotspots and both fulfill all of the above criteria. These beaches have therefore been identified as Coastal Hazard Zones (Figure 4.5). Observations of both the comparison analysis and the MHW overlay clearly indicate a long running erosional trend. This trend was quantified through regression analysis.

The NMSB has long buffered the low elevation areas of the south drumlin from erosional processes. The strong linear correlation in the regression analysis indicates that if coastal processes remain the same, this area will continue its negative trend of erosion during the next decade further reducing its buffering capacity. This would leave the low elevation areas of the south drumlin highly vulnerable to coastal flooding.

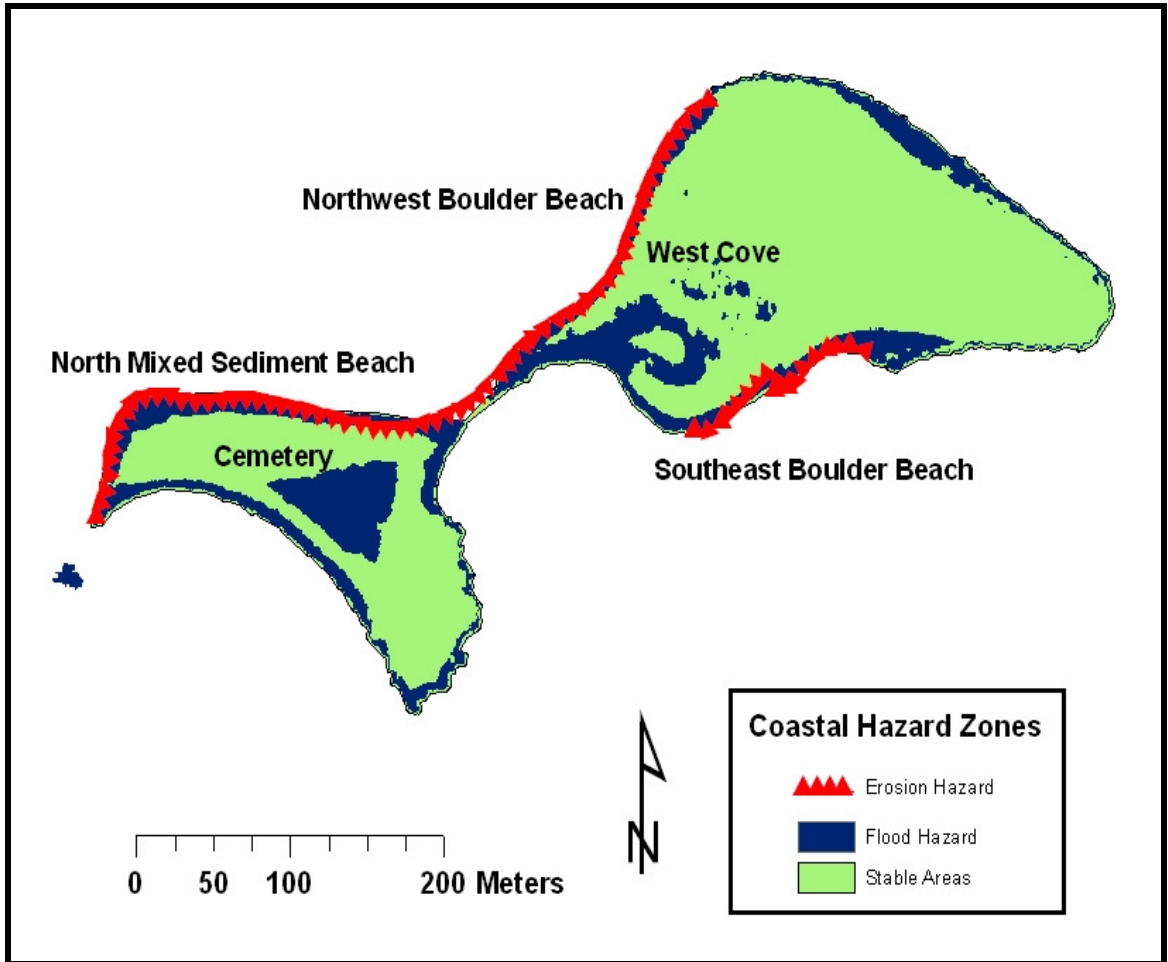


Figure 4.5. Coastal Hazard Zone Map. Areas that are vulnerable to erosion are shown in red, areas that are vulnerable to flooding resulting from storm surges are shown in blue, and stable areas are shown in green. Areas that would likely become inundated with one meter of sea-level rise include the West Cove and the cemetery located within the low-lying areas of the south drumlin.

4.5.3 Cemetery

Due to the continued erosion of the NMSB, and the predictive map which shows the area is vulnerable to coastal flooding, the low elevation area of the south drumlin has been identified as a Coastal Hazard Zone (Figure 4.5). This area contains the Rainsford Island Cemetery, which likely faces the greatest threat from the large storm surges associated with Nor'easters. The submergence of this highly sensitive historical site presents enormous challenges to coastal managers and policy makers as a major storm event, comparable to the Nor'easters of the past, may bring human remains to the surface. The cemetery is a highly sensitive historical and cultural site containing the graves of individuals that provide a rich chronology of events that led to the establishment of the United States of America. Those laid to rest in the cemetery include numerous victims of the devastating 18th century small pox epidemic as well as veterans of the Revolutionary War, the War of 1812, and the Civil War. In order to preserve the integrity of this site, immediate action would be required in order to mitigate and prepare for future erosional events.

4.5.4 Southeast Boulder Beach (SEBB)

The SEBB has been identified as a Coastal Hazard Zone (Figure 4.5). The regression analysis of the 1944 dataset shows a strong linear correlation in the data and a likely continuation of the negative erosional trend during the next decade. This area is also vulnerable to coastal flooding as indicated by the 1-Meter Flood Hazard Map. A storm surge of 1-m would fully submerge this area and likely cause further erosion to occur. The

comparison and overlay analysis provide further support for the designation of this area as a Coastal Hazard Zone.

4.6 Future Research

There are many aspects of RISES that could be enhanced by further research. The first of these entails incorporating previously unattainable historical aerial photographs. Recently, aerial photographs from 1938, 1966, and 1978 have been located. Locating and obtaining these images for use in RISES was unsuccessful, despite the fact it was known they existed. With some additional effort, these images could be obtained and integrated within the DSAS analysis. Their inclusion would increase the temporal and spatial resolution of the original study and provide the ability to more accurately determine specific time periods when coastal trends occurred. Incorporating the 1938 aerial photograph would expand the temporal coverage of the aerial data by six years and may provide insights into how the infamous 1938 Hurricane impacted the coastal areas of Rainsford Island.

Another way to improve RISES would be to employ geophysical equipment in order to locate and determine the extent of subsurface over-wash fans deposited during large storm events. A geophysical survey of the terrestrial areas of the Island, utilizing ground penetrating radar (GPR), may provide the ability to link coastal trends identified in RISES with specific storm events such as the “Blizzard of 78.” Insights gained through GPR surveys may be helpful in understanding the mechanisms behind the rapid rate-of-change statistics found during certain periods of time, as was the case on Rainsford Island between 1970 and 1992.

A portion of Rainsford Island has already been surveyed, including the area containing the cemetery. In a previous investigation, Gontz (2008) determined the location and extent of the cemetery through the use of GPR (Figure 4.7). Other areas of the Island were also surveyed including much of the WC. However, the data has yet to be processed and analyzed. Future work would include processing and analyzing the previously collected data and performing additional field surveys.



Figure 4.6. Ground penetrating radar (GPR) survey of Rainsford Island Cemetery. Dr. Allen Gontz pulls a GPR antenna with Chris Maio in tow holding the laptop computer and GPR backpack receiver. The data obtained from this survey enabled the determination of the extent and boundary of the cemetery (Gontz, 2008). Other data collected remains unprocessed (Photo by Jonathon Wiggs).

The coming release of the 2009 LIDAR data for Boston Harbor presents many new exciting research opportunities. With a second LIDAR data set, in which a 2009 MHW shoreline could be derived, a high resolution objective shoreline change study could be conducted (Figure 4.6). The exclusive use of LIDAR-tidal datum derived shorelines would eliminate all of the inherent uncertainties found within traditional shoreline change studies, such as the variability in data sources and the errors associated with the manual delineation of shorelines.

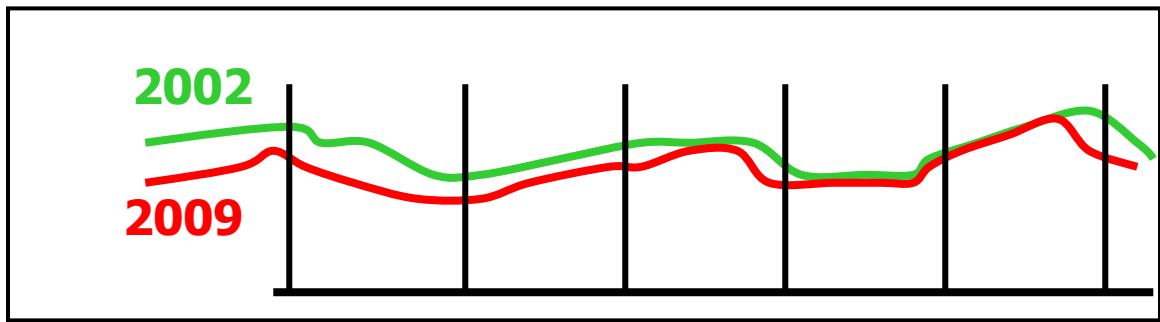


Figure 4.7. Shoreline change analysis employing two LIDAR datasets. The integration of the previously created 2002 MHW shoreline, represented by the green line, and a 2009 MHW shoreline, represented by the red line, would enable for a high resolution statistically robust shoreline change study. This could be carried out within the DSAS extension using an objectively created baseline and transects represented above by the black lines. By utilizing shorelines derived from high resolution LIDAR and statistically derived tidal datums, all uncertainties associated with manually created proxy-based shorelines are eliminated.

Although the temporal resolution of the study utilizing the previously created 2002 MHW shoreline and a new 2009 MHW shoreline would only cover seven years, its high resolution and accuracy would provide robust statistics with predictive capabilities unattainable in the past. It would also be the first study of its kind in the Boston Harbor area and provide a baseline for future research.

After developing the methods and techniques needed to carry out a shoreline change analysis using two sets of LIDAR data on Rainsford Island, it could be applied to a much larger area, potentially encompassing all of Boston Harbor. This would provide accurate high resolution information that could significantly enhance the ability of local coastal managers and policy makers to address the challenges presented by the predicted rise in sea-level and increased occurrence and intensity of storm surges associated with climate change.

CHAPTER 5

ITEMIZED CONCLUSIONS

5.1 Itemized Conclusions

The Rainsford Island Shoreline Evolution Study (RISES) successfully integrated multiple data sources of varying spatial and temporal resolutions within a GIS and developed new methods and techniques in order to enable the geospatial analysis of the integrated data. Through this successful integration and analysis the investigation accurately mapped, calculated rate-of-change statistics, located accretion and erosion hotspots, and identified coastal hazard zones vulnerable to flooding and erosion. RISES also provided robust statistical based results that will benefit future coastal zone management decisions and provide guidance for future shoreline studies in Boston Harbor. The following itemized conclusions are the main findings of this study.

1. **Rainsford Island has experienced a negative trend of erosion during the study period.** The longest temporal coverage utilizing the aerial photographs spans a period of 64 years and provides the highest confidence calculation of the total area above the HWL lost to erosion. During the period between 1944 and 2008, 9% of the Island's coastline and 11% of its vegetation was lost to erosion. Although there were areas of erosion and accretion on the Island, the results indicate an overall general trend of erosion and a net loss of surface area above the HWL.
2. **There were three erosional hotspots identified on Rainsford Island, which include the Southeast Boulder Beach, the Northwest Boulder Beach, and the North Mixed Sediment Beach.** These beaches have been identified as coastal hazard zones. Regression analysis of these areas provided negative rates of erosion of over 0.5 meters per year. The strong linear correlation between the historical shoreline positions in these areas enabled for a high degree of confidence in the prediction that these beaches will likely continue their negative trend of erosion during the next decade.
3. **There were two accretion hotspots identified on Rainsford Island; the West Cove and Southeast Sand Beach.** The highest rate-of-change statistic within RISES was obtained from the regression analysis of the WC data. Once open to the sea and used as a mooring lagoon for visiting boats prior to 1952, the small lagoon rapidly accreted

at a rate of 0.83 meters per year. As a result of the rapid filling, there was over 50 m of shoreline progradation in this area.

The second accretion hotspot on Rainsford Island was along the SESB, which is in close proximity to the WC. In conjunction with the filling of the WC, this beach advanced seaward 33 m. The mechanism which led to the accretion in both of these areas was likely related to the same coastal processes.

4. **Coastal flooding resulting from a storm surge would likely inundate much of the Island's shoreline and other low elevation areas above the high water line (HWL).** While the shoreline would only be flooded during the duration of the storm event due to the steep seaward slope of the beaches, the low elevation areas on the north and south drumlins could potentially remain submerged. One of these areas containing the Island's cemetery has been identified as a Coastal Hazard Zone.

5. **The greatest period of coastal geomorphic change on Rainsford Island occurred between 1970 and 1992.** During this period there was a rapid landward retreat of the shoreline with a loss of over 9,000 m² of the Island's surface area. Most of the erosion during this period occurred in the areas previously identified as erosional hotspots. The data indicates that the majority of the southeast migration of the spit and the filling of the WC occurred during this 22-year period. It is unclear whether the mechanism behind these dramatic coastal changes was related to the enormous storm surges associated with the "Blizzard of 78" or the "Perfect Storm," but these record

breaking Nor'easters likely played a significant role in the shoreline evolution of Rainsford Island. Further geophysical evidence would be required to conclusively draw these linkages.

APPENDIX A. IMAGE DATA: SOURCES AND INFORMATION

AERIAL PHOTOGRAPH

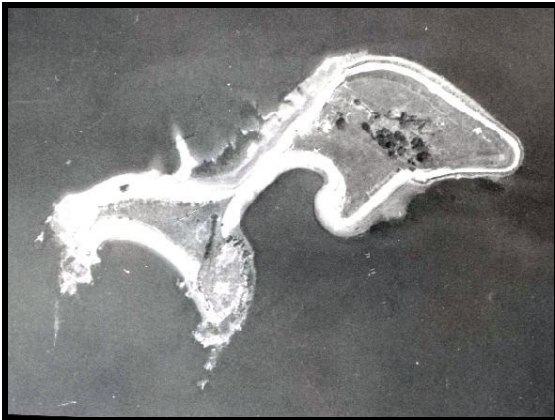
SOURCE

1944 Black and White



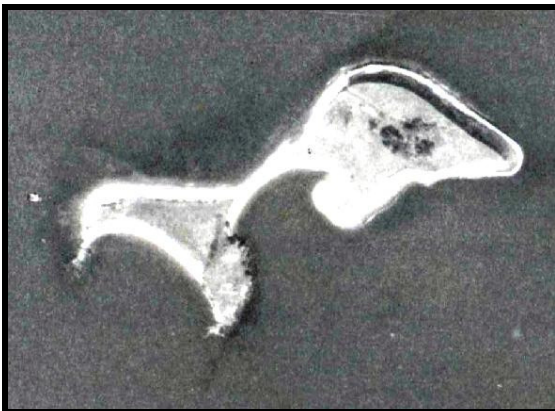
The 1944 aerial photograph was obtained on a CD as a GeoTIFF file from the principle investigator on the 2001-2002 Rainsford Island Archeological Survey. The 1944 image proved to be a crucial dataset for this investigation as it marked the earliest high quality image used in the study.

1952 Black and White



The 1952 aerial photograph was provided by the Massachusetts Office of Cultural Resources, Division of Planning as digitized JPEG files. This unrectified photograph was of relatively good quality.

1970 Black and White

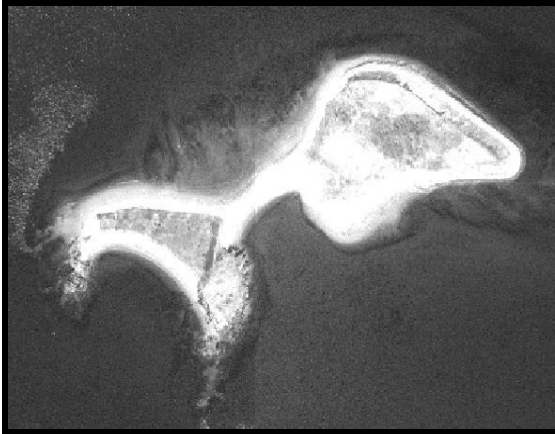


The 1970 aerial photograph was provided by the Massachusetts Office of Cultural Resources, Division of Planning as digitized JPEG files. This photograph is of poor quality and therefore introduced some potential uncertainties into the study.

AERIAL PHOTOGRAPH

SOURCE

1992 Black and White



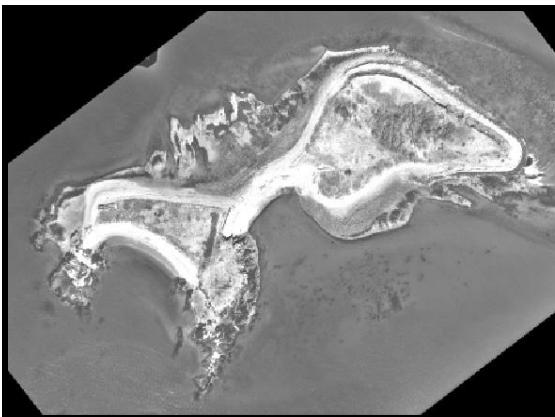
This orthophotograph was obtained from the Massachusetts Office of Geographic and Environmental Information (MassGIS). The aerial photograph was taken during a 1992 Spring survey. The two orthophotos containing the area of Rainsford Island were identified with the MassGIS Orthoimage Index as tiles 245894 and 249894. The image has a 1–2 meters per pixel resolution and is of relatively poor quality.

1994 Color



This orthophotograph was obtained from the Massachusetts Office of Geographic and Environmental Information (MassGIS). The aerial photograph was taken during the Fall of 1994 and has a 1-meter per pixel resolution. This image was eliminated from the shoreline analysis as the HWL indicator feature was not visible due to the “bleach white” appearance of the beaches. As the vegetation was clearly visible, the image was included in that aspect of the study.

2002 Black and White



The 2002 high resolution aerial photograph was obtained on a CD as a GeoTIFF file from the principle investigator on the 2001-2002 Rainsford Island Archeological Survey. The unrectified image was taken in March, 2002 and is of excellent quality.

AERIAL PHOTOGRAPH

SOURCE

2005 Color



This orthophotograph was obtained from the Massachusetts Office of Geographic and Environmental Information (MassGIS). The aerial photograph was taken during April of 2005 and has a 0.5-meter per pixel resolution. The image was of excellent quality and therefore employed as the source data to which the unrectified photographs were georeference.

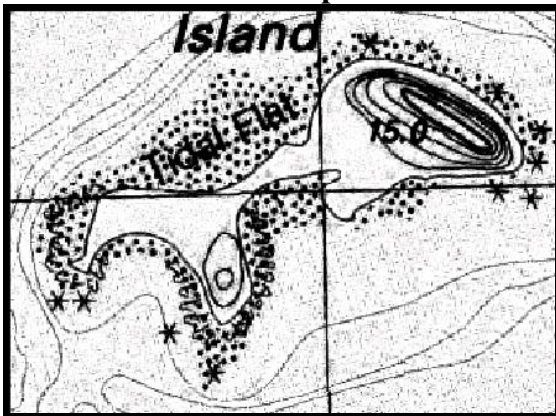
2008 Color



This orthophotograph was obtained from the Massachusetts Office of Geographic and Environmental Information (MassGIS). The aerial photograph was taken during the spring of 2008 and has a 1-meter per pixel resolution. The 2008 image is of excellent quality and provides the most recent data utilized in the study.

HISTORICAL MAP

1890 Map



The digital georeferenced 15-minute USGS topographic quadrangle map was obtained from the Massachusetts Office of Geographic and Environmental Information (MassGIS). The original map was obtained by MassGIS from the Harvard Map Collection and dates to circa 1890, though the exact date is uncertain. The georeferenced map has a 5.4 meter per pixel resolution and was employed to lengthen the temporal range of this study.

APPENDIX B. BOSTON HARBOR TIDAL DATUM

Sep 24 2009 17:28

ELEVATIONS ON STATION DATUM
National Ocean Service (NOAA)

Station: 8443970

T.M.: 0 W

Name: BOSTON, BOSTON HARBOR, MA

Units: Meters

Status: Accepted

Epoch: 1983-2001

Datum	Value	Description
MHHW	4.205	Mean Higher-High Water
MHW	4.071	Mean High Water
DTL	2.640	Mean Diurnal Tide Level
MTL	2.624	Mean Tide Level
MSL	2.660	Mean Sea Level
MLW	1.178	Mean Low Water
MLLW	1.074	Mean Lower-Low Water
GT	3.131	Great Diurnal Range
MN	2.893	Mean Range of Tide
DHQ	0.134	Mean Diurnal High Water Inequality
DLQ	0.104	Mean Diurnal Low Water Inequality
HWI	3.74	Greenwich High Water Interval (in Hours)
LWI	9.93	Greenwich Low Water Interval (in Hours)
NAVD	2.752	North American Vertical Datum
Maximum	5.675	Highest Water Level on Station Datum
Max Date	19780207	Date Of Highest Water Level
Max Time	10:36	Time Of Highest Water Level
Minimum	-0.061	Lowest Water Level on Station Datum
Min Date	19400324	Date Of Lowest Water Level
Min Time	00:00	Time Of Lowest Water Level

To refer Water Level Heights to a Tidal Datum, apply the desired Datum Value.

Click [HERE](#) for further station information including New Epoch products.

To refer Water Level Heights to either

NGVD (National Geodetic Vertical Datum of 1929) or

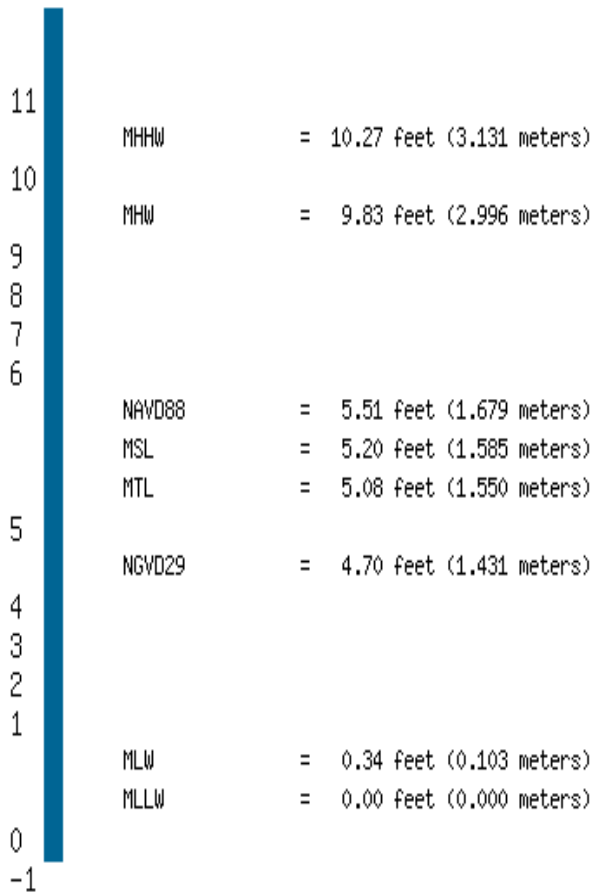
NAVD (North American Vertical Datum of 1988), apply the values located at:

[National Geodetic Survey](#)

APPENDIX C. NATIONAL GEODETIC SURVEY ELEVATION DATA

Elevation Information

PID: MY0555
 VM: 185
 Station ID: 8443970
 Epoch: 1983-2001
 Date: Thu Sep 24 17:33:40 EDT 2009



The NAVD 88 and the NGVD 29 elevations related to MLLW were computed from Bench Mark, K 12, at the station.

APPENDIX D. DIGITAL SHORELINE ANALYSIS SYSTEM (DSAS)
TRANSECT RESULTS

DATASET	TRANSECT NUMBER	EPR	SCE	NSM	LMS	LRR	R²
1890-2008 Shoreline	47	0.09	12.59	10.05	0.07	0.09	0.8
1890-2008 Shoreline	74	-0.19	22.2	-22.2	-0.2	-0.18	0.92
1890-2008 Shoreline	83	-0.14	26.15	-16.55	-0.33	-0.19	0.63
1890-2008 Shoreline	97	-0.09	11.7	-10.8	-0.1	-0.1	0.97
1890-2008 Shoreline	122	-0.21	26	-25.03	-0.02	-0.18	0.71
1890-2008 Shoreline	178	0.36	85.43	42.5	-0.65	0.2	0.1
1890-2008 Shoreline	194	0.51	64.93	59.8	0.81	0.59	0.86
1890-2008 Shoreline	202	0.28	32.81	32.81	0.31	0.28	0.89
1944-2008 Shoreline	47	0.03	4.23	1.69	0.07	0.05	0.47
1944-2008 Shoreline	74	-0.18	12.05	-11.58	-0.21	-0.19	0.82
1944-2008 Shoreline	83	-0.31	26.15	-20.09	-0.28	-0.34	0.8
1944-2008 Shoreline	97	-0.07	5.45	-4.55	-0.09	-0.08	0.91
1944-2008 Shoreline	122	-0.01	3.98	-0.33	-0	-0.03	0.41
1944-2008 Shoreline	178	-0.67	42.93	-42.93	-0.6	-0.59	0.96
1944-2008 Shoreline	194	0.79	55.45	50.32	0.78	0.83	0.9
1944-2008 Shoreline	202	0.31	22.49	19.82	0.6	0.33	0.85
1944-2008 Vegetation	27	-0.19	11.85	-11.85	-0.16	-0.13	0.53
1944-2008 Vegetation	43	-0.25	18.58	-15.68	-0.29	-0.27	0.73
1944-2008 Vegetation	83	-0.23	17.05	-14.69	-0.19	-0.23	0.88
1944-2008 Vegetation	99	-0.29	34.16	-18.68	-0.31	-0.41	0.66
1944-2008 Vegetation	141	0.22	14.96	14.21	0.19	0.2	0.79
1944-2008 Vegetation	143	0.21	13.67	13.67	0.17	0.17	0.86
1944-2008 Vegetation	176	-0.13	13.83	-8.15	-0.11	-0.15	0.65
1944-2008 Vegetation	183	-0.24	15.99	-15.2	-0.23	-0.24	0.85

REFERENCES LIST

- Anders, F.J, and Byrnes, M.R., 1991. Accuracy of shoreline change rates as determined from maps and aerial photographs. *Shore and Beach*, 59(1), 17-26.
- Arendt, A.A., Echelmeyer, K.A., Harrison, W.D., Lingle, C.S., and Valentine, V.B., 2002. Rapid Wastage of Alaska Glaciers and Their Contribution to Rising Sea Level. *Science*, 297(5580), 382–386.
- Aubrey, D.W., 1994. Geomorphology of Spectacle Island and Boston Harbor, Massachusetts, 10,000 Years B.P.–present. In: *The Spectacle Island Site: Middle to Late Woodland adaptations in Boston Harbor, Suffolk County Massachusetts, Central Artery/Tunnel project*, Ed. McHargue, G., Appendix A: Timelines Inc.
- Bell, E.L., 2009. Cultural Resources on the New England Coast and Continental Shelf: Research, Regulatory, and Ethical Considerations from a Massachusetts Perspective. *Coastal Management*, 37, 17-53.
- Berkland, E., 2009. Personal Communication. City of Boston, Archeologist. August 29, 2009.
- Boak, E.H. and Turner, I.L., 2005. Shoreline definition and detection: a review. *Journal of Coastal Research*, 21(4), 688–703.
- Church, J.A., Godfrey, J.S., Jackett, D.R., and McDougall, T.J., 1991. A Model of Sea Level Rise Caused by Ocean Thermal Expansion. *Journal of Climate*, 4, 438–456.
- Claesson, S.H., and Carella, E., 2002. Rainsford Island Archaeological Reconnaissance and Management Plan. Boston Landmarks Commission.
- Clark, G., Moser, S., Ratick, S., Dow, K., Meyer, M., Emani, S., Jin, W., Kasperson, J., Kasperson, R., Schwarz, H., 1998. Assessing the vulnerability of coastal communities to extreme storms: the case of Revere, MA, USA. *Mitigation Adaptation Strategies Global Change*, 3, 59-82.
- Cooper, M., Beevers, M., Oppenheimer, M., 2005. Future sea level rise and the New Jersey Coast, assessing potential impacts and opportunities. Woodrow Wilson School of Public and International Affairs. Princeton University, Princeton, NJ.
- Costanza R., d'Arge R., de Groot, R., Farber, S., Grasso, M., Hannon, B., Limburg, K., Naeem, S., O'Neill, R.V., Paruelo, J., Raskin, R.G., Sutton, P., van den Belt, M., 1997. The value of the world's ecosystem services and natural capital. *Nature*, 60, 253–387.

- Cracknell, A.P., 1999. Remote sensing techniques in estuaries and coastal zones—an update. *International Journal of Remote Sensing*, 19(31), 485-496.
- Crowell, M., and Leatherman, S.P., 1999. Coastal erosion mapping and management. *Journal of Coastal Research*, SI(28), 196.
- D'Entremont, J., and Snow, E.R., 2002. *The Islands of Boston Harbor, 1630-1971*. Commonwealth Ed., Boston, MA.
- Dobson, J.E., Bright, E.A., Ferguson, R.L., Field, D.W., Wood, L.L., Haddad, K.D., Iredale, H. III., Jensen, J.R., Klemas, V.V., Orth, R.J., and Thomas, J.P., 2003. NOAA Coastal Change Analysis Program (C-CAP): guidance for regional implantation, NOAA Technical Report, NMFS 123(1995).
- Dolan, R., Fenster, M.S., and Holme, S.J., 1991. Temporal Analysis of Shoreline Recession and Accretion. *Journal of Coastal Research*, 7(3), 723-744.
- Dolan, R., Hayden, B.P., and May, S.L., 1983. Erosion of the U.S. shorelines. In: Komar, P.D. (Ed.), *CRC Handbook of Coastal Processes and Erosion*, CRC Press, 285-299.
- Donnelly, J.P., 2006. A revised late Holocene sea-level record for northern Massachusetts, USA. *Journal of Coastal Research*, 22(5), 1051–1061.
- Douglas, B.C., and Crowell, L.M., 2000. Long-term shoreline position prediction and error propagation. *Journal of Coastal Research*, 16(1), 145-152.
- Douglas, B.C., Crowell, L.M., and Honeycutt, M.G., 2002. Discussion of Fenster, M.S.; Dolan, R., and Morton, R.A., 2001. Coastal Storms and Shoreline Change: Signal or Noise. *Journal of Coastal Research*, 17(3), 714-720.
- Douglas, B.C., and Crowell, L.M., and Leatherman. S.P., 1998. Considerations for shoreline position prediction. *Journal of Coastal Research*, 14(3), 1025-1033.
- Emery, K.O., and Aubrey, D.G., 1991. Sea levels, land levels, and tide gauges. *Science*, 254(5030), 448-455.
- Fahker, B., 2001. Where is the shoreline? The answer is not as simple as one might expect. *Hydro International*, 515, 6-9.

- Fairbanks, R.G., 1989. A 17,000-year glacio-eustatic sea level record: influence of glacial melting rates on the Younger Dryas event and deep-ocean circulation. *Nature*, 342, 637-642.
- Farrell, S., Leip, T., Spekr, B., and Mauriello, M., 1999. Mapping erosion hazard areas in Ocean County. *Journal of Coastal Research*, SI(28), 50-57.
- Fenster, M.S., Dolan, R., and Morton, R.A., 2001. Coastal storms and shoreline change: Signal or noise? *Journal of Coastal Research*, 17(3), 714-720.
- Genz, A.S., Fletcher, C.H., Dunn, R.A., Frazer, N., and Rooney, J., 2007. The predictive accuracy of shoreline change rate methods and alongshore beach variation on Maui, Hawaii. *Journal of Coastal Research*, 87(19). 23-34.
- Galgano, F.A., Douglas, B.C., and Leatherman, S.P., 1998. Trend and variability of shoreline position. *Journal of Coastal Research*, SI(26), 282-291.
- Galgano, F.A., Leatherman, S.P., and Douglas, B.C., 2004. Inlets Dominate U.S. East Coast Shoreline Change. *Journal of Coastal Research*, In Press.
- Goldsmith, R., 1991. Stratigraphy of the Milford-Dedham zone, eastern Massachusetts; an Avalonian terrane. In: Chapter E., The bedrock geology of Massachusetts. U.S. Geological Survey Professional Paper, 1366(E-J), E1-E62.
- Gontz, A., 2008. The suitability of ground penetrating radar for assessment of the Rainsford Island Cemetery and applications toward its use in developing a conservation plan. Report Submitted to: City Archaeology Program Environment Department, City of Boston.
- Gorman, L., Moranc., A., and Lakson, R., 1998. Monitoring the coastal environment. Part IV. Mapping, shoreline changes, and bathymetric analysis. *Journal of Coastal Research*, 14(1), 61-92.
- Harris, M., Brock, J., Nayegandhi, A., and Duffy, M., 2005. Extracting shorelines from NASA airborne topographic lidar-derived digital elevation models: Reston, VA. USGS Open-file report, 1427(2005).
- Himmelstoss, E., Fitzgerald, D.M., Rosen, R., and Allen, J.R., 2006. Bluff Evolution of coastal drumlins; Boston Harbor Islands, Massachusetts. *Journal of Coastal Research*, 22(5), 1230-1240.

- Himmelstoss, E.A. 2009. "DSAS 4.0 Installation Instructions and User Guide" In: Thieler, E.R., Himmelstoss, E.A., Zichichi, J.L., and Ergul, A., 2009. Digital Shoreline Analysis System (DSAS) version 4.0 — An ArcGIS extension for calculating shoreline change. USGS Open-file report, 1278(2008).
- Intergovernmental Panel on Climate Change (IPCC), 2007. Summary for Policy Makers: Working Group I (WGI) Fourth Assessment Report (AR4). (Eds Solomon, S. et al.), Cambridge Univ. Press, 2007.
- Kaye, C.A., and Barchoorn, E.S., 1964. Late Quaternar sea-level change and crustal rise at Boston, MA, with notes on autocompaction of peat. *Geological Society of America Bulletin*, 75, 63-80.
- Kirshen, P., Watson, C., Douglas, E., Gontz, A., Lee, J., and Tian, Y., 2007. Coastal flooding in the Northeastern United States due to climate change. *Springer*, 13(2008), 437–451.
- Kirshen, P., Ruth, M., Anderson, W., and Lakshmanan, T.R., 2004. Infrastructure systems, services and climate change: integrated impacts and response strategies for the Boston metropolitan area. Final Report to US EPA ORD, EPA Grant Number: R.827450–01.
- Knebel, H.J., Rendigs, R.R., Oldale, R.N., and Bothner, M.H., 1993. Sedimentary framework of Boston Harbor, Massachusetts. In: Fletcher, C.H. III., and Wehmler, J. (Eds.), *Quaternary Coasts of the United States: Marine and Lacustrine Systems*, SEPM Special Publication(48), 35-43.
- Leatherman, S., and Douglas, B., 2003. Sea-level and coastal erosion require large-scale monitoring. *EOS Transactions of the American Geophysical Union*, 84(2), 13-16.
- Leatherman, S.P., Eskandary, L.S., 1999. Evaluation of coastal erosion hazards along Delaware's Atlantic Coast. *Journal of Coastal Research*, SI(28), 43-49.
- Ledoux, L., and Turner, R.K., 2002. The economic value of wetland services: a meta-analysis. *Ocean & Coastal Management*, 45(2002), 583–616.
- List, J.H., and Farris, A.S., 1999. Large-scale shoreline response to storms and fair weather. *Proceedings of the Coastal Sediments*, (1999), 1324-1337.
- Liu, H., Sherman, D., and Songgang, G.U., 2007. Automated extraction of shorelines from airborne light detection and ranging data and accuracy assessment based on Monte Carlo simulation. *Journal of Coastal Research*, 23(6), 1359–1369.

- Luedtke, B.E., 2000. Archaeology on the Boston Harbor Islands after 25 years. *Bulletin of the Massachusetts Archaeological Society*, 61(1), 2-11.
- Luedtke, B.E., 1984. Preliminary Report on an Archaeological Survey of the Southern Half of Long Island, MA. Report Submitted to the Massachusetts historical Commission.
- Lydia, C.L., A., Louise, S.L., Starkhouse, B., and Sumaila, U.R., 2009. An overview of socio-economic and ecological perspectives of Fiji's inshore reef fisheries. *Marine Policy*, 33(5), 807-817.
- MacQuarrie, B., 2009. Nature, abuse imperil a harbor island heritage. *Boston Globe*, 275(58), February 27, 2009.
- Maiti, S., Bhattacharya, A.K., 2009. Shoreline change analysis and its application to prediction: A remote sensing and statistics based approach. *Marine Geology*, 257(2009), 11-23.
- Martinez, M.L., Intralawan, A., Vazquez, G., Perez-Maqueo, O., Sutton, P., Landgrave, R., 2007. The coasts of our world: Ecological, and Social Importance. *Ecological Economics*, 63, 11-23.
- MassGIS., 2003. Boston Harbor LIDAR Metadata. Executive Office of Environmental Affairs, Boston, Massachusetts. <http://www.mass.gov/mgis/>.
- McBride, R.A., Taylor, M.J., and Byrnes, M.R., 2007. Coastal morphodynamics and Chenier-Plain evolution in southwestern Louisiana, USA: a geomorphic model. *Geomorphology*, 88(3-4), 367-422.
- McBride, R.A., Penland, S., Hiland, M.W., Williams, S.J., Westphal, K.A., Jaffe, B.E., and Sallenger, H., Jr., 2002. Analysis of Barrier Shoreline Change in Louisiana from 1853 1989. In: *Louisiana Barrier Island Erosion Study: Atlas of Shoreline Changes*, Chapter 4. USGS, I(2150).
- McBride, R.A., Huand, M.W., Penland, S., Williams, S.J., Byrnes, M.R., Westfhal, K.S., Jaffe, B.E., and Sallenoer, A.H., 1991. Mapping barrier island changes in Louisiana: techniques, accuracy, and results. *Proceedings of the Coastal Sediments 1991*, Seattle, Washington, 1011-1026.
- Moore, L.J., Ruggiero, P., and List, J.H., 2006. Comparing mean high water and high water line shorelines: Should proxy-datum offsets be incorporated into shoreline change analysis? *Journal of Coastal Research*, 22(4), 894-905.

- Newman, W.A., Berg, R.C., Rosen, P.S., and Glass, H.D., 1990. Pleistocene stratigraphy of the Boston Harbor drumlins, Massachusetts. *Quaternary Research*, 34(2), 148-159.
- NOAA., 2007. National Oceanic and Atmospheric Administration, Center for Operational Oceanographic Products and Services, Tides and Currents. <http://tidesandcurrents.noaa.gov/>.
- Oldale, R.N., 1985. A drowned Holocene Barrier Spit off Cape Ann, Massachusetts. *Geology*, 13, 59-70.
- Oldale, R.N., Colman, S.M., and Jones, G.A., 1993. Radiocarbon Ages from Two Submerged Strandline Features in the Western Gulf of Maine and a Sea-Level Curve for Northeastern Massachusetts Coastal Region. *Quaternary Research*, 40, 38-45.
- Oldale, R.N., and Colman, S.M., 1992. On the age of the penultimate full glaciation of New England. *Geological Society of America*, SP(270), 317-326.
- Oldale, R.N., Wommack, L. E., and Whitney, A.B., 1983. Evidence for a Postglacial Low Relative Sea-Level Stand in the Drowned Delta of the Merrimack River, Western Gulf of Maine. *Quaternary Research*, 19, 325-336.
- Parker, B., 2003. The difficulties in measuring a consistently defined shoreline: the problem of vertical referencing. *Journal of Coastal Research*, 38, 44-56.
- Peltier, W.R., and Tushingham, A.M., 1989. Global sea level rise and the greenhouse effect: might they be connected? *Science*, 244(4906), 806-811.
- Penland, S., and Ramsey, K.E., 1990. Relative Sea-Level Rise in Louisiana and the Gulf of Mexico: 1908-1988. *Journal of Coastal Research*, 6(2), 323-342.
- Pugh, D.T., 1987. Tides, surges and mean sea level. John Wiley and Sons Inc. OSTI ID(5061261), 472.
- Rendigs, R.R., and Oldale, R.N., 1990. Maps Showing the Results of a Subbottom Acoustic Survey of Boston Harbor, Massachusetts. USGS Miscellaneous Field Studies, 1990.
- Robertson, W., Whitman, D., Zhang, K., and Leatherman, S.P., 2004. Mapping shoreline position using airborne laser altimetry. *Journal of Coastal Research*, 20(3), 884-892.

- Scavia, D. Field, J.C., Bosesch, R.W., Buddemeier, R.W., Burkett, V., Cayan, D.R., Fogarty, M., Harwells, M.A., Howarth, R.W., Mason, C., Reed, D.J., Royer, T.C., Sallenger, A.H., and Titus, J.G., 2002. Climate Change Impacts on U.S. Coastal and Marine Ecosystems. *Estuaries*, 25(2), 149–164.
- Shinkle, K.D., and Dokka, R.K., 2004. Rates of Vertical Displacement at Benchmarks in the Lower Mississippi Valley and the Northern Gulf Coast. NOAA Technical Report, NOS/NGS 50.
- Simon, B.G., 2000. Boston Harbor: The Shape of Things Past and Present: *Bulletin of the Massachusetts Archeological Society*, 63(1,2), 2-10.
- Teh, L., Cabanban, A.S., and Sumaila, U.R., 2005. The reef fisheries of Pulau Banggi, Sabah: A preliminary profile and assessment of ecological and socio-economic sustainability. *Fisheries Research*, 76(3), 359-367.
- Thieler, E.R., Himmelstoss, E.A., Zichichi, J.L., and Ergul, A., 2008. Digital Shoreline Analysis System (DSAS) version 4.0—An ArcGIS extension for calculating shoreline change. USGS Open-File Report, 1278(2008).
- Van den Brink H.W., Konnen G.P., and Opsteegh J.D., 2003. The reliability of extreme surge levels estimated from observational records of order hundred years. *Journal of Coastal Research*, 19(2), 376–388.
- Van Der Meulen, F., Bakker, T.W.M., Houston, J.A., 2004. The costs of our coasts: examples of dynamic dune management from Western Europe. In: Martinez, M.I., Psuty, N. (Eds.), *Coastal Dunes: Ecology and Conservation*, Springer-Verlag, Berlin. 259-278.
- Woodward, R.T., and Wui, Y., 2001. An overview of socio-economic and ecological perspectives of Fiji's inshore reef fisheries. *Ecological Economics*, 37(2), 257-270.
- Yin, J., Schlesinger, M.E., and Stouffer, R.J., 2009. Model projections of rapid sea-level rise on the northeast coast of the United States. *Nature Geoscience*, NGE0(462), 10.1038.
- Zeidler, R.B., 1997. Continental shorelines: climate change and integrated coastal management. *Ocean and Coastal Management*, 37(1), 41–62.
- Zhang, K., Douglas, B., and Leatherman, S.P., 2000. Twentieth-century storm activity along the U.S. East Coast. *Journal of Climate*, 13, 1748–1761.
- Zhang, K., Huang, W., Douglas, B.C., and Leatherman, S.P., 2002. Shoreline position variability and long-term trend analysis. *Shore and Beach*, 70(2i), 31-35.

Zuzek, P.J., Nairn, R.B., and Thieme, S.J., 2003. Spatial and temporal consideration for calculating shoreline change rates in the Great Lakes Basin. *Journal of Coastal Research*, 38(1), 125–146.